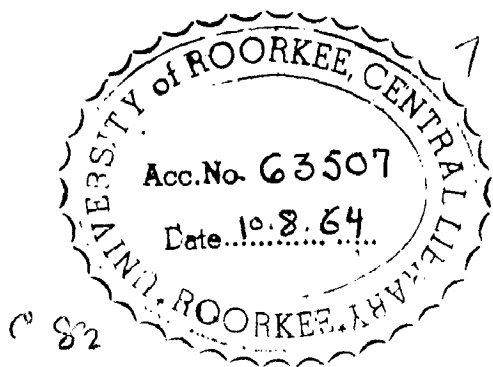


DESIGN AND PERFORMANCE OF PERMANENT MAGNET GENERATORS

D66-64
VED

BY
VED PARKASH



CHECKED
1964

DISSERTATION SUBMITTED IN PARTIAL FULFILMENT
OF REQUIREMENTS FOR THE DEGREE
OF
Master Of Engineering
IN
Electrical Machine Design

DEPARTMENT OF ELECTRICAL ENGINEERING
UNIVERSITY OF ROORKEE,
ROORKEE (INDIA)

1964

...ACKNOWLEDGEMENTS...

The author wishes to acknowledge his deep sense of gratitude to Dr. T.J.M. Rao, Associate Professor in Electrical Engineering, University of Roorkee, Roorkee for his initiating this topic and his valuable advice and suggestions at every stage of the preparation of this dissertation.

Sincere thanks are due to Professor C.J. Ghosh for the various facilities afforded in the department in connection with this work.

The author acknowledges the valuable suggestions by Dr. L.M. Ray, Reader and Mr. K.B. Verma, Lecturer in Electrical Engineering during the experimental work. Thanks are also due to Mr. R.J. Khurana for typing this dissertation.

Roorkee

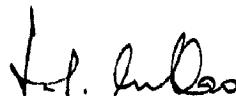
VED PARKASH

May 18, 1964.

...CERTIFICATE...

Certified that the dissertation entitled "Design and performance of permanent magnet generators" which is being submitted by Shri Ved Prakash in partial fulfilment for the award of the degree of Master of Engineering in Electrical Machine Design of University of Roorkee is a record of the student's own work carried out by him under my supervision and guidance. The matter embodied in this dissertation has not been submitted for the award of any other degree or diploma.

This is further to certify that he has worked for a period of eight months from September 10, 1963 to May 10, 1964 for preparing dissertation for Master of Engineering degree at the University.



Dated, May 18, 1964.
Roorkee.

(T.S.M. RAO)
Associate Professor in Elect.Engg.
University of Roorkee,
Roorkee.

...CONTENTS...

| | | | |
|--|-----|-----|---------|
| (i) Synopsis | ... | ... | ... iv |
| (ii) List of Symbols | ... | ... | ... vi |
| (iii) Introduction | ... | ... | ... ix |
| Chapter 1. Permanent magnet materials | ... | ... | ... 1 |
| Chapter 2. Demagnetization curve and stabilization of permanent magnets | ... | ... | ... 11 |
| Chapter 3. Design of generator | ... | ... | ... 29 |
| Chapter 4. Equivalent magnetic circuits and generator reactances | ... | ... | ... 62 |
| Chapter 5. Voltage regulation and control | ... | ... | ... 74 |
| Chapter 6. Performance of the generator | ... | ... | ... 82 |
| Chapter 7. Mechanical considerations | ... | ... | ... 99 |
| Chapter 8. Guide to applications... | ... | ... | ... 106 |
| Chapter 9. Experimental details | ... | ... | ... 129 |
| Chapter 10 Conclusions | ... | ... | ... 129 |
| Appendix I - Equations for λ (defined in Chapter 3) | | | ... 133 |
| Appendix II Comparative values of machines parameters for generators with p.m. field and electro-magnet field. | ... | ... | ... 134 |

20

...SYNOPSIS...

This dissertation presents the design aspects and performance of permanent magnet generators, used in air craft and portable applications. On account of the absence of a separate exciter, permanent magnet generators are free from commutation troubles, and their associated radio interference. Light weight, small size and higher efficiency are additional features of p.m. generators.

Design of the p.m. magnet, including the methods of its stabilization and magnetization, has been considered in detail. Equations for estimating pole leakage which forms a considerable amount of the total flux, have also been derived. Most of the remaining dimensions are calculated in the same way as in synchronous machines with wound-field, and have, therefore, been discussed briefly. In addition, mechanical problems encountered during the manufacturing process have been considered.

Expressions for the machine parameters have been developed with the help of the equivalent magnetic circuit of the p.m. generator. Tensors have been applied to derive the performance equations.

Although a perfect control of the output voltage of the p.m. generator is not possible because of the absence of a separate excitation system, some indirect methods for the voltage control have been suggested, which are in actual use.

Experimental analysis to verify some of the theoretical

consideration has been carried out on a small single phase permanent magnet generator obtained from Electrical Engineering Department, University of Hoorkee, Hoorkee, and the results have been found satisfactory.

...LIST OF SYMBOLS...

Electrical, mechanical and magnetic ...

- A = Cross-section of magnet, general, m^2
Ad = demagnetizing m.m.f.
A_m = Cross-section of magnet, optimum, m^2
a = material constant, defined by equations 3.18 & 2.2
B = magnetic induction, general, Wb/m^2
B_r = magnetic induction, residual, Wb/m^2
B_g = magnetic induction, air gap
 \bar{B} = Specific magnetic loading.
b = material constant defined by equation 2.2.
b_h = width of pole shoe, meter
C = demagnetization factor F_a/F_t
d₁ = slot depth, meter
d₂ = wedge depth, meter
E = generated e.m.f., volts
E₀ = excitation voltage, volts.
ENL = No load voltage, volts.
F = m.m.f., general, amp.turns
F_a = m.m.f., externally applied, amp-turns.
F_c = m.m.f., coercive of magnet M_a, amp. turns.
f = frequency, cycles/sec.
H = magnetizing force, general, AT/m
H_c = magnetizing force, coercive, AT/m
H_d = magnetizing force, demagnetizing, AT/m
h_h = depth of pole shoe, meter
I = armature current, amps.
K = demagnetization factor
K_w = winding factor

- K_g = generated o.m.f. p.u. air gap flux
 K_d = demagnetising armature m.m.f. p.u. d-axis current.
 L = Axial length of core, meters
 l = length of magnet, general, meter
 l_m = length of magnet, optimum, meter
 l_p = axial length of pole shoe, meter
 N = equivalent turns of armature winding
 P = differential operator, $\frac{d}{dt}$
 P = Permeance, general, henry.
 P_g = Permeance, gap, henry
 P_L, P_1, P_2 = Permeance, leakage, henry
 P_1 = Permeance, in-stator leakage, henry
 P_0 = Permeance, out-stator leakage, henry
 $P_m = \frac{b_p l_p}{2h_p}$
 R = Reluctance, general, yrneh
 R_g = reluctance, gap, yrneh
 R_1, R_L, R_2 = reluctance, leakage, yrneh
 S = output in KVA
 S = slope of the permeance line
 S = shape factor, general, per meter.
 V = voltage, terminal, volts.
 v = magnet volume, general, meter³
 μ = magnification factor
 ϕ, θ = load p.f. angle
 δ = load angle
 ϕ_g = magnetic flux, gap, Wb.
 ϕ_r = magnetic flux, residual, Wb.
 ψ = flux linkages, No-turns

μ_0 = permeability of free space = $4\pi \times 10^{-7}$ H/m

μ_R = recoil permeability = $\mu_r \mu_0$ = H/m

μ_a = average slope of minor loops.

μ_{as} = average slope of minor loops (resultant)

μ_d = differential permeability at B_r , H/m

η = Volume correction factor.

I, II, IV, V, VI, XII, alnico grades.

Matrices

e = Voltage matrix

i = current matrix

R = resistance matrix

L = inductance matrix

G = torque matrix

Z = transient impedance matrix

C = connection matrix

t = transpose of a matrix.

Indices and suffixes...

2 ϕ = 2-phase axes

3 ϕ = 3-phase axes

dq = d & q axes

a, b, c = 3-phases axes

β o = 2-phase, and zero axes

d, q, o = direct, quadrature, & zero axes.

d_s = direct-axis stator field (i.e. field)

d_e = d-axis eddy current axis

K_d = axis of p.m. damper

f = field axes

d_r = d-axis armature axis

I N T R O D U C T I O N .

Developments in the field of permanent magnet materials and the methods of processing, have made it possible to construct generators with permanent magnets from small sized units of fractional KVA ratings such as tachometer generators, governor frequency sources, and magnetos upto units rated at many KVA (of the order of 75 KVA to 100 KVA). About 30 years ago Alnico II was used commercially as the permanent magnet material, which has a moderate amount of coercive force but quite poor permeability. It gets easily demagnetized when exposed to high reluctance circuits, such as removing a rotor from a stator. Useful flux per unit area of the magnet material is quite low which meant that the machines with larger cross section could only be possible and hence the means of assembling and using this material in large cross-section had to be found. This material found its use only in fractional KVA sizes. Development of powerful permanent magnets such as Alnico V has raised the capacity of the generators with permanent magnet field system.

Elimination of the d.c. exciter in permanent magnet generators results in elimination of Commutation problems, saving in weight and space, and thus making the overall cost, in some ratings, lower than that for generators with electromagnetic field. Permanent magnet generators thus find their use in portable and aircraft applications.

Design of a permanent magnet machine involves certain problems and factors that are different from those encountered

in machines with Conventional field system, as follows:

- (1) a consideration of the behaviour of magnetic circuits employing permanent-magnet materials,
- (2) the effects of demagnetizing forces,
- (3) the means of magnetizing the machine.
- (4) stabilization of permanent magnet
- (5) the methods of reducing the voltage regulation and means for voltage control.
- (6) the methods of shielding the permanent magnets from transient demagnetizing forces and
- (7) the methods of reducing negative sequence reactance.

Analysis of the behaviour of a synchronous machine with electromagnetic field, under steady state and transient conditions has been done previously by others and the results show a satisfactory conformity between the prediction and actual performance. Most of the equations originating from these investigations are applicable also to machines with permanent magnet fields. There are, however, some basic deviations from the Conventional design procedures and equations. In p.m. generators the same degree of conformity between prediction and actual performance, as in the case of an electromagnetic machine, can not be expected. This discrepancy is due to the following reasons.

1. Difficulties in magnetizing the field magnets of machines with closely spaced poles to the maximum residual flux.

2. Leakage flux can not be calculated precisely.
3. Uncertainty in predicting exactly the position of the minor hysteresis loop when the stabilization has been done by short circuit.

This dissertation deals with the optimum design keeping in view the aforesaid problems and factors associated with p.m. generators, derivation of the equivalent magnetic circuit, the machine reactances, and performance equations of the generator. Experimental results have been obtained on a 300 Watt, 240V, 60~3600 r.p.m., p.m. alternator. Some of the applications of p.m. generators have been discussed in detail.

M.K.S. rationalised system has been used in deriving the various equations. Tensors have been applied to analyse the performance of the p.m. generators.

...CHAPTER -1...PERMANENT MAGNET MATERIALS1.1. INTRODUCTION^{1,8}

Magnets which retain indefinitely a considerable portion of the magnetic flux after the magnetizing force is removed, are termed as permanent Magnets. Such magnets should also be able to retain their magnetism when used in connection with air gaps, soft iron pole pieces, and other parts of magnetic circuits to which they may be required to supply magnetic flux.

When the permanent magnets become magnetized, the domains become oriented with the pole axes parallel to one another and become so closely locked in position that it requires a high demagnetizing force to unlock them and make them assume the random relation to one another which results in the demagnetization of the magnet. Obviously, the domains which are most difficult to turn are most valuable in producing permanent magnets.

The materials for use as permanent magnets should, therefore, have high coercivity and high retentivity. In fact the hysteresis loop for permanent magnet materials should expand to the greatest possible degree.

1.2. MAGNET MATERIALS^{1,3,6,7}

permanent magnet materials may be divided into three classes as follows:

1. those made of carbon steels, known as Martensitic steels, usually modified and improved by the addition of one or more other elements.

2. alloys which are dispersion-hardened by the precipitation of one phase in another or by the formation of a super-structure
3. material formed of Very small particles of the order of 10^{-4} cm or less in one dimension.

Before 1910 hardened carbon steel containing upto 1.5% carbon, was commonly used. Magnese to the extent of 0.8% was often added. Although tungsten and chromium steel had originated as early as in about 1870, it was during world War I that it was found that addition of high cobalt content to tungsten and chromium steel could give a high coercive force as high as three times that of any material existing at that time and thus had replaced other materials at that time. In 1931 the Fe-Co-Mo and Fe-Co-W systems were investigated Remalloy, one of the alloys of this group, has the advantage that it can be hot rolled and machined before the final hardening treatment. The Fe-Co-Mo alloys were the first commercial permanent magnet materials that contained no essential carbon, and since then all of the improvements have been affected with alloys by the precipitation of some other elements than carbon. In the same year alloys containing iron, nickel, and aluminium. were found to have coercive force as high as 56,000 AT/m. Now similar alloys, heat treated in an improved manner, are made commercially and have a coercive force of 38,000 AT/m. Fe-Ni-Al alloys are known as "Alnico" in United States and "Alcomax" in England. These alloys have higher energy product than Remalloy but are mechanically hard and must be ground. Addition of

COMPOSITIONS AND PROPERTIES OF SOME USEFUL PERMANENT MAGNETIC MATERIALS

| Name | When used | Typical composition (%) (Balance is iron) | H_c : AT/M | B_r : Wb/M ² | (BH) _m x 10 ⁻³ |
|---------------------------------|-------------|--|-----------------|------------------------------|--------------------------------------|
| <u>Martensitic steels</u> | | | | | |
| Carbon steel | Before 1885 | 1.2 | 4800 | 0.8 | 1.44 |
| Tungsteel | 1885 | 6W, 0.7C, 0.3Mn | 5200 | 1.05 | 2.4 |
| Chrome steel | 1916 | 6Cr, 1C, 0.4Mn | 5600 | 0.95 | 2.24 |
| KS magnet steel ¹ | 1917 | 36Co, 7W, 3.5Cr, 0.9C | 18400 | 1.0 | 7.20 |
| Cobal chrome steel ² | 1921 | 16Co, 9Cr, 1C, 0.3Mn. | 14400 | 0.8 | 4.80 |
| Remalloy ³ | 1931 | 12Co, 17Mo (or W) | 20000 | 1.05 | 9.60 |
| Mishima alloy ⁴ | 1931 | <u>Dispersion hardened alloys</u> 25 Ni, 12Al | 38000 | 0.7 | 11.20 |
| Alnico 25 | 1934 | 12 Co, 17 Ni, 10Al, 6Cu | 44800 | 0.73 | 13.60 |
| Magneto flux ⁶ | 1935 | 20Ni, 60 Cu | 48000 | 0.58 | 16.0 |
| Platinum Cobalt alloy | 1936 | 77 Pt, 23 Co | 240000 | 0.50 | 20.0 |

Contd....

| Name | When used (Balance in Iron) | Typical composition (%) (Balance in Iron) | H _C AT/M | B _{T2} Wb/M | (BH) × 10 ⁻³ |
|-----------------------|--------------------------------|--|------------------------|-------------------------|-------------------------|
| Vicalloy | Before 1938 | 52 Co, 10V | 14000 | 1.15 | 12.0 |
| Alnico 5 ⁷ | 1940 | 24 Co, 14Ni, 8Al, 3Cu | 46000 | 1.25 | 36.0 |
| Alnico 6 | | 24 Co, 14 Ni, 8Al, 3 Cu, 1.25 Ti | 64000 | 1.05 | 31.2 |
| Alnico 12 | | 35Co, 18 Ni, 8Al 8.0 Ti | 80000 | 0.6 | 13.6 |

1. Called Kocrzit in Germany
- 2 Also alloys containing 3,6,9 Co with variable Cr.
- 3 Also called Comel in U.S.A. and Osstitt in Germany
- 4 Also called Alnico 3. Alnico 1 contains Cobalt
5. Called Alnico in England and Oersht in Germany
- 6 Also called Cunife 1. Cunife 2 & Cunico contains Cobalt
- 7 English Alcomax has a some what different composition.

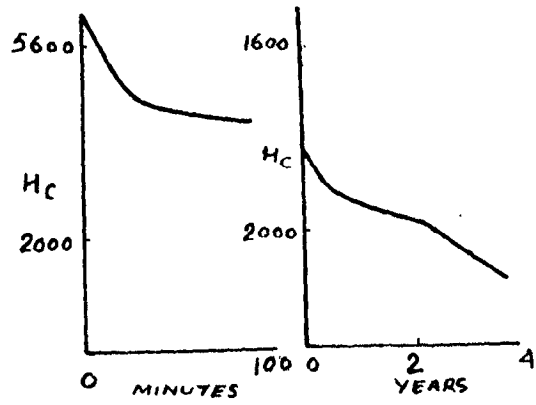


Fig. 1.1
Effect of time on H_c of 0% tungsten steel.

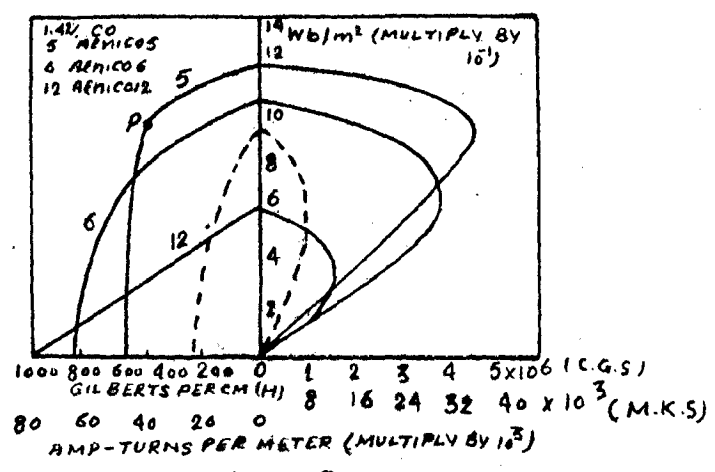


Fig. 1.2

Demagnetization curves for different materials.

cobalt and copper, with approximate heat treatment, results in good properties in many sizes and shapes of magnets.

At present the material having the highest energy product $(BH)_m$ and made in large quantities is Alcomax or Alnico 5. An essential part of the heat treatment of this material is the cooling from a high temperature in a strong magnetic field prior to the final hardening treatment.

The various permanent magnet materials, with their compositions and properties, are listed in table 1.1.

1.3. MARTENSITIC STEELS^{1,3,7}

For a permanent magnet material where the largest possible hysteresis loop is desired, atomic lattice must be put into the highest possible state of strains. Strains introduced due to cold working increase the hysteresis and the coercivity to a certain degree but such strains are insufficient to give the effects desired in permanent magnet. For this the severest lattice distortion throughout the whole of the constituent crystals of the metal is necessary. The earlier permanent magnets, as pointed out previously, were of steel in which high internal strains, and high degree of mechanical and magnetic hardness depended upon the presence of carbon and the formation of a martensitic structure resulting from quenching of the metal from a high temperature in oil or water.

Consider carbon steel with carbon content of 1.2%. At 1000°C such a steel would consist of iron in the face-centered, or F condition, having iron carbide, Fe_3C in solution, a structure known as austenite. When cooled below about 870°C, the iron carbide would begin to precipitate out of the solution

into a second phase called cementite. Further cooling below about 690°C the iron would re-crystallize on to a body-centered lattice, as α iron or ferrite, and with this would be intimately mixed iron carbide to form a structure known as pearlite, having a total carbon content of 0.89%. The remaining carbon is then present in a second phase of iron carbide or cementite. For these changes to occur during cooling sufficient time must be allowed, and if the steel is rapidly cooled by quenching the movement of the iron carbide is partially arrested. Martensite is the structure corresponding to the condition immediately following the decomposition of austenite into pearlite. Its hardness and high internal strains are probably due to the iron carbide in a fine state of division throughout the lattice in the process of separating out, the crystal structure also having just changed from the face centered to the body centered state.

Such simple steels suffer from the following two disadvantages:

1. Structure obtain by quenching is unstable and 'ageing' of the material goes on at room temperature, the effect is further accelerated if the temperature is raised.
2. Vibration and mechanical shock also badly affect the magnetic properties of the steel.

Such changes are highly undesirable in a permanent magnet material.

A good improvement is observed if either tungsten or chromium is added to the Martensite steel. These steels are also affected by ageing Fig.1.1 shows some results due to

"Evershed"³ for the fall in coercivity with time of a sample of tungsten magnet steel immediately after hardening, also after a period of several years. Addition of cobalt upto about 42% to steel containing carbon, tungsten or molybdenum etc. gives quite improved results. The heat treatment of such martensitic steels consists in oil or air quenching from temperatures in the range 800 to 950°C, depending on the composition.

1.4. DISPERSION - HARDENED ALLOYS^{1,3,7,8}

As mentioned above, quench - hardened or Martensitic materials are fundamentally unstable as they consist of super-saturated solid solutions and with passage of time the carbides tend to pass out of solution. Dispersion hardened alloys are stable and have for superior magnetic properties over the martensitic steels. Their specific gravity is 15% less than 35% cobalt steels and are cheaper than this steel. They are relatively free from corrosion and the effects of atmospheric conditions. Various alloys forming this class of alloys is listed in Table 1.1. At the present time there is a large number of Alnico alloys some having similar and others widely varying characteristics; which adapt them to innumerable applications. Alnico V, VI and XII have greater use regarding permanent magnet generators. Alnico V is subjected to a magnetizing force during heat treatment. This increases the magnetic properties in the direction of the grain which is developed during this operation.

From Fig.1.2, it will be noted that with Alnico V, when H reaches the value of -40,000 AT/m the induction density suddenly drops to zero. This drop off is due to the fact that up to the 40,000 AT/m point the domains are firmly

locked in a direction of easy magnetization and it is possible to unlock only a relatively few. Most of the domains are, however, similar in character, and they all become unlocked almost simultaneously, producing a sudden drop off. This material is highly effective with short fixed air-gaps which would cause it to operate above the point P. In Alnico VI the sudden drop-off is eliminated and the domains respond progressively to the demagnetizing force. Alnico XII has the highest coercive force among Alnicos and is an almost perfect example of progressive unlocking of domains. Its characteristic is almost a straight line.

Many of the Alnico magnets can be made by the sintering process. The constituent powders such as iron, nickel, cobalt and copper are pressed in a die. If some slots, holes and grooves etc. are also required, they are made part of the die. The compact powder is then heated in a hydrogen atmosphere furnace at a temperature just below the melting point of the constituent. The resultant product is hard and fine-grained but is non-machinable and is to be finished by grinding. It is not possible to make Alnicos V, VI and XII by this process and are made by the sand or precision casting process. They are also non-machinable and must be ground.

1.5. Other materials^{1,7}

There are some other alloys which though ^{are} of little commercial utility are of great scientific interest. Vectolite, Cunico, Cunife and silmanal and vicalloy fall in this class. Detailed discussion of these materials is outside the scope of the present work. However their compositions and other properties are enlisted in table 1.2.

Table 1.2

| Alloy | Composition (%) | $B_T (Wb/m^2)$ | H_{CAI}/m' | $(BH)_m$ | Remarks |
|-----------|--|----------------|--------------|-----------------------|---------------------------|
| Vectolite | Fe ₂ O ₃ -30, Fe ₃ O ₄ -44, Co ₂ O ₃ -26 | 0.16 | 72000 | 4x10 ³ | Practically non conductor |
| Cunico | Cu-50, Ni-21, Co-29 | 0.34 | 56800 | 6.8x10 ³ | Ductile |
| Cunife | Cu-60, Ni-20, Fe-20 | 0.54 | 44000 | 12.40x10 ³ | " |
| Silmanal | Ag-86.75, Mn-8.8, Al-4.55 | 0.54 | 480000 | 0.680x10 ³ | " |
| Vicalloy | Co-52, Vn-10, Fe-38 | 0.90 | 24000 | 8x10 ³ | " |

...CHAPTER - 2...

DEMAGNETIZATION CURVE AND STABILIZATION
OF PERMANENT MAGNETS.

2.1. DEMAGNETIZATION CURVE...

permanent magnets are required to produce external magnetic fields of sufficient strength and constancy. In all its applications such as loud speakers, meters, motors and generators magnetic circuit containing permanent magnets contains also an air gap and the magnet is to operate under the influence of a demagnetizing field and thus the portion of the hysteresis loop lying in the second quadrant, between residual induction and coercive force, is important in case of permanent magnets. This curve is known as 'Demagnetization Curve'. Magnetization and demagnetization curve shown in Fig.2.1 are for Alnico V, one of the important materials used for permanent magnets.

Attempts have been made to find analytical expression fitting the demagnetization curve. This Curve can be simulated by a rectangular hyperbola passing through the points B_r , the residual flux density for which H is zero and $-H_c$, the Coercive force for which $B = 0$. General expression for a rectangular hyperbola is -

$$(x-x_0) (y-y_0) = C_0^2 \quad \dots \quad \dots 2.1$$

Making the substitutions -

$$y = B, \quad x = H$$

$$y_0 = \frac{1}{b}, \quad x_0 = -H_c - \frac{a}{b} \text{ and}$$

$$C_0^2 = -\frac{a}{b^2} \text{ we can write the relation 2.1. in}$$

the form

$$\frac{H + H_c}{B} = a + b(H + H_c)$$

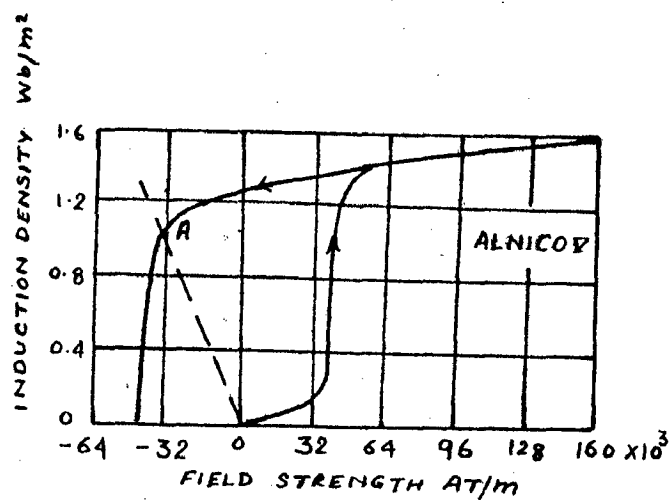


Fig. 2.1

Magnetization and Demagnetization
curve for Alnico V.

$$\text{or } B = \frac{H + H_c}{a + b(H + H_c)} \quad \dots \quad \dots \quad 2.2$$

Relation (2) is similar to the Frilich - Kennelly relation

$$\frac{B}{H} = \mu = \frac{1}{a+bH}$$

and differs from it in that the B, H Curve is displaced horizontally such that when $B = 0$ $H = -H_c$

Now, when $H = 0$, $B = B_r$, we get from equation (2),

$$B_r = \frac{H_c}{a + bH_c}$$

If B_s represents the flux density at saturation, then

$$\frac{1}{b} = B_s$$

Solving for a, we get

$$a = \frac{H_c}{B_r} - \frac{H_c}{B_s}$$

$$\text{and } B = \frac{H + H_c}{\frac{H_c}{B_r} + \frac{H}{B_s}} \quad \dots \quad \dots \quad 2.3$$

The energy product BH is given by

$$BH = \frac{H^2 + HH_c}{a + b(H + H_c)}$$

This is maximum when $\frac{d(BH)}{dH}$ is zero

or when

$$\frac{d(BH)}{dH} = \frac{[a + b(H + H_c)] [2H + H_c] - (H^2 + H_c H)(b)}{(a + b(H + H_c))^2} = 0$$

Solving, we have

$$H_m = \frac{H_c}{bB_r} \left(\sqrt{1 - bB_r} - 1 \right) \quad \dots \quad 2.4$$

$$B_m = \frac{1}{bB_s} \left(\sqrt{1 - bB_r} - 1 \right) \quad \dots \quad 2.5$$

where H_m and B_m are the coordinates of $(BH)_{\max}$

It is to be noted from relations 2.4 and 2.5 that

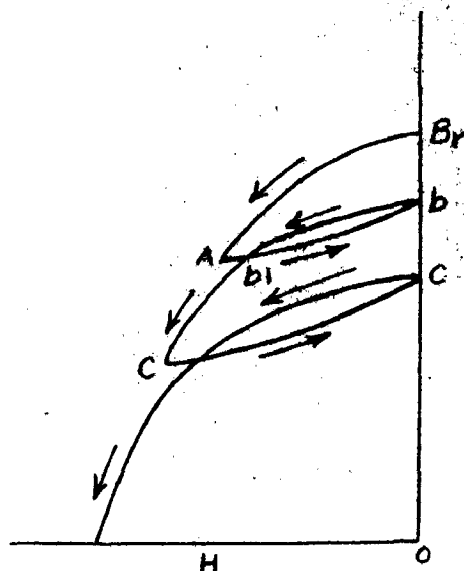


Fig. 2.2
recoil loops of permanent magnets.

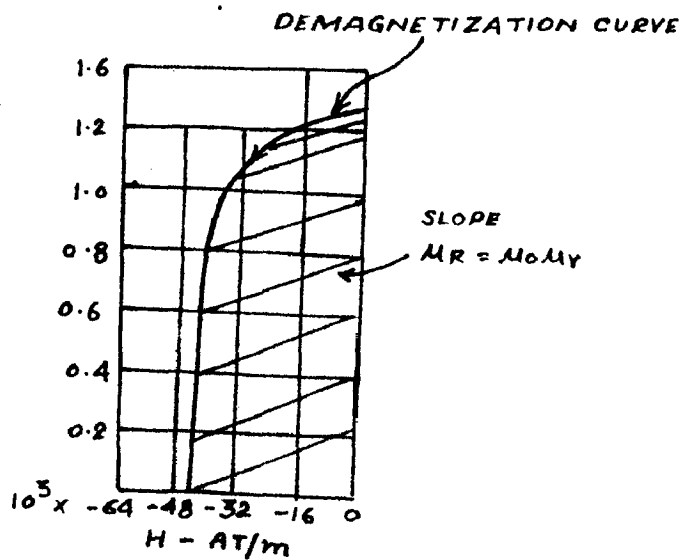


Fig. 2.3
recoil permeability of Alnico V.

$$\frac{B_m}{H_m} = - \frac{B_r}{H_c} \quad \dots \quad \dots \quad 2.6$$

and the diagonal of the rectangle constructed with H_c and B_r as sides, drawn through the origin will intersect the BH curve at the coordinates of $(BH)_{max}$.

The ratio $\frac{B_m H_m}{B_r H_c}$ known as 'fullness factor' of the Curve is denoted by K. For a large number of materials this factor is 0.4 and for Alnico V it is approximately 0.65.

2.2. AIR GAP or LOAD LINE^{6,9}

If a magnet is initially magnetized to a point represented by the tip of the loop and an air gap is introduced in the magnetic circuit, the magnetization will drop to a point A, as shown in Fig.2.1 on the demagnetizing curve. This point will represent the magnetizing force which the magnet is applying to the air gap and the induction existing in the magnet. The line from origin through A is termed the air-gap line or load line. The slope of this line determines the permeance of the air-gap.

2.3. RECOIL LOOPS AND REVERSIBLE PERMEABILITY^{6,1}

The hysteresis loop obtained for a magnetic material by normal method is termed the 'major loop' of the material. Let it be assumed that the major loop for a permanent magnet material is being drawn. When moving down the demagnetizing curve, suppose point A, as shown in Fig.2.2, is reached and the magnetizing force is now increased. It can be seen that the lower branch of the path Ab as marked by an arrow will be traced. On decreasing the magnetizing force again, the upper branch bb₁ will be traced. If now the magnetization force

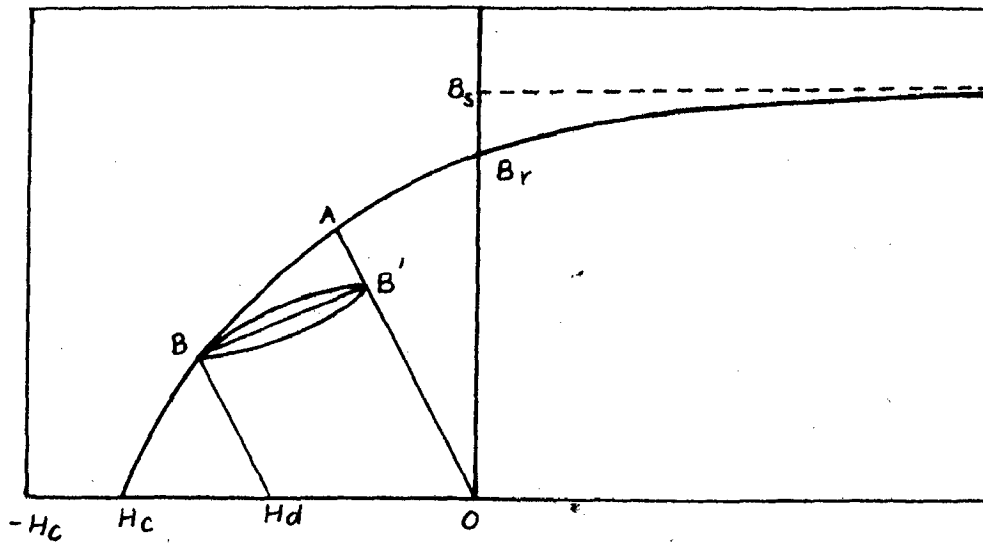


Fig. 2.4

Effect of magnetization force

is alternately increased and decreased, the induction will trace the loop b_1bb_1 . Such a loop is known as a 'Recoil loop'. Now by descending the major demagnetization curve bC , a further similar recoil loop can be obtained and, thus, an infinite number of such minor loops can be drawn. Normally, the area of such minor loops is so small that a straight line can be drawn through the tips of the loop. This line is called the 'Recoil line' and the slope of this line determines the average slope of the loop. The slope of the recoil line is called the recoil or reversible permeability and denoted by the symbol μ_R . Various recoil lines for Alnico V are drawn in Fig.2.3. Recoil permeability is, to a fair approximation, constant over the working point of the major loop.

2.4. EFFECT OF DEMAGNETIZATION FORCE^{9:1}

Consider the demagnetizing curve shown in Fig.2.4. A is the working point on the demagnetizing curve and OA is the air gap line. Let a demagnetizing force H_d be applied. This diminishes the magnetization to the point B , determined by the intersection of the line BH_d drawn parallel to the air-gap line OA . Now, if the demagnetizing force H_d is removed, the magnetization is given by the point $A'B'$ which lies on the load line OA and is the tip of the minor hysteresis loop. The magnetization represented by the point 'B' is stable to any demagnetizing force that is applied temporarily, provided it does not exceed H_d .

2.5. STABILIZATION...^{16,28}

The field of the permanent magnet is not stable and should, therefore, be stabilized in order to avoid any voltage change subsequent to the application of a specified load

condition. Stabilization in case of generators may be effected by either of the following methods:

- a; air stabilization or stabilization out of assembly.
- b; Stabilization by demagnetization with a given m.m.f. after magnetization in-assembly.

The above methods for stabilizing the magnets are fundamentally similar in the sense that partial demagnetization is required to achieve stabilization. The B & H co-ordinates of the operating point after stabilization are fixed by the tip of the minor loop on the closed circuit air gap line Op. The location of this point depends upon the following:

- a: the reversible permeability
- b: the slope of the air-gap line
- c: the degree of demagnetization.

As the slope of the air gap line changes from zero to infinity, the operating point traces another curve which passes through H_c & B_r . This curve is known as 'Secondary demagnetization curve' and, obviously, lies below the major demagnetization curve. The magnet under stabilized conditions will, therefore, operate at a lower energy level.

Air stabilization is desirable when frequent withdrawal of the ^{rotor} armature from the stator is required without special tools or when magnetization can not be easily effected in the machine. In this method the rotor is withdrawn from the stator without a special keeper and replaced in stator. When the rotor is withdrawn from the stator, let the magnetization be represented by M, fig.2.5, given by the intersection of the

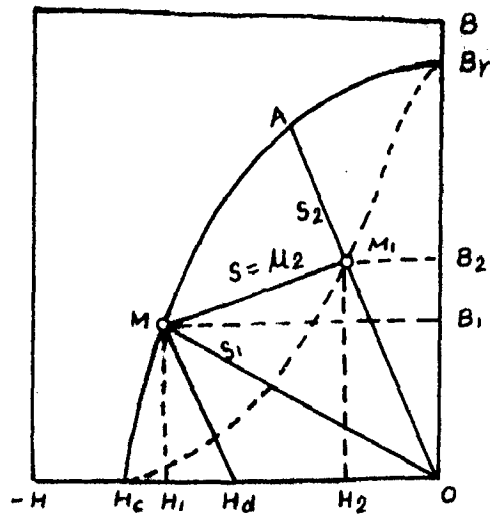


Fig. 2-5

Stabilization by Magnetization before assembly.

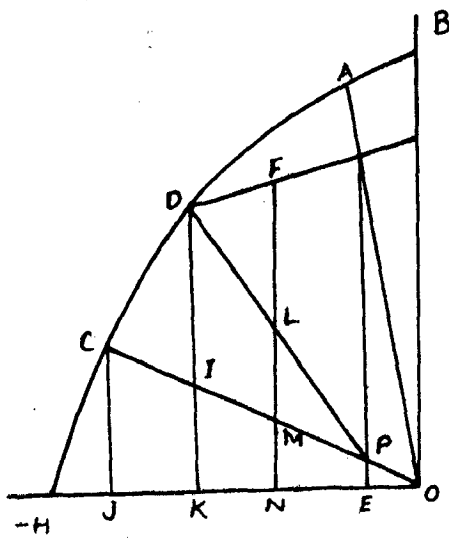


Fig. 2-6.

Short circuit stabilization

out-of-assembly air gap line OM with the demagnetization Curve. Upon assembly in the magnetic circuit the magnetization proceeds to M', the intersection of the minor loop with the closed circuit load line. The maximum demagnetization force for which the magnet is stable is H_d . If at any subsequent period the generator is dismantled and is reassembled without remagnetization, the output voltage should be maintained alright. The disadvantage of this method is that an increase of 20 to 40% can be expected in the size and weight of the rotor and thus a relatively poor use of the permanent magnet material is made.

In case of stabilization by demagnetization with a given m.m.f. after magnetization in-assembly, the demagnetizing m.m.f. may ^{be} corresponding to some specified maximum load of the generator or to the condition of short circuit. The former method is known as 'load stabilization' and the latter 'short circuit stabilization'. Load stabilization is a particular case of short circuit stabilization. Let the machine be assumed to be fully magnetized and running at normal speed on no load. Under these conditions, the flux in the air gaps is maximum and the machine will work at the point A, Fig.2.6, generating an open circuit e.m.f. E_0 . OC represents the leakage line. ~~Now~~ let the ~~machine~~ be short circuited. The working point will now be given by D as the armature reaction will have a demagnetizing effect. D and C can never coincide because at C there is no flux in the gaps and thus no voltage can be generated to drive the short-circuit current in the armature winding. Upon removing the short circuit, the magnetization will be given by the point A'. For any load between no load and short circuit, the magnet shall operate on the recoil line A'D. Considering

unit volume of the magnet, DK represents the magnet flux at short circuit and IK is the leakage. The flux responsible for short circuit is given by DI . Since the flux necessary to circulate the armature current in the winding is proportional to the current, DI is proportional to the short circuit current. The output current at P is zero and hence the perpendicular distance between the lines PI and PD at any load gives the output current and the flux to drive the current in the winding at that load. Thus at F the output emf and useful flux are proportional to FL , the leakage flux to MN , while LM is proportional to the output current and the flux and e.m.f. necessary to drive this current in the armature winding.

Load stabilization finds its use in application where weight is of utmost importance. Maximum generating flux is retained and thus minimum weight is achieved. Short circuit stabilization finds its use in applications where a short circuit may accidentally be applied to the generator. A sudden short circuit causes the greatest possible load demagnetization and thus no further decrease in the operating voltage is possible unless the alternator ^{rotor} armature is withdrawn from the stator.

2.6. SECONDARY DEMAGNETIZATION CURVE...

..Stabilization By Magnetization Before Assembly..

In fig.2.7, M represents the open circuit magnetization and M' , the closed circuit magnetization after assembly in the circuit. The coordinates of M are B_1, H_1 , and those of M' are B_2, H_2 . The in-and the out-of-assembly air gap lines are represented by OA and OM .

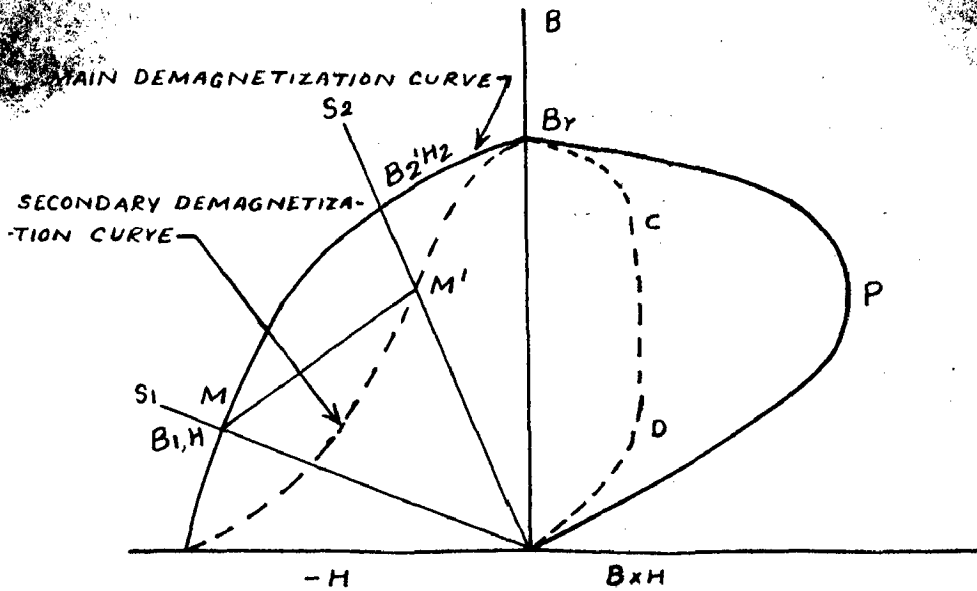


Fig. 7.

Secondary demagnetization curve and corresponding energy product curve for stabilization by magnetization before assembly.

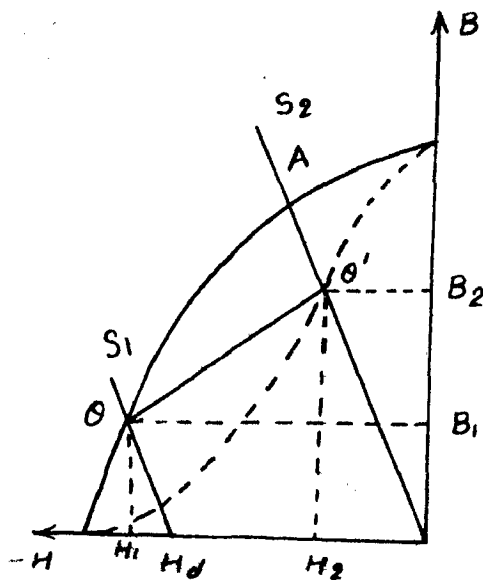


Fig. 8.

Stabilization by demagnetization with a given c.m.f.

Let l = length of magnet in meters.

A = area of cross section of the magnet in meter².

R_1 = open circuit reluctance of the air gap in Yrneh

R_2 = closed circuit reluctance of the air gap in Yrneh

μ_R = reversible permeability = $\mu_r \mu_0$

The the slope of the line OM is

$$s_1 = \frac{B_1}{H_1} = \frac{\phi_1}{A} \cdot \frac{1}{\frac{NI}{\mu l}} = \frac{1}{A} \cdot \frac{\phi_1}{NI} = \frac{1}{A} \cdot \frac{1}{R_1} \quad \dots 2.7$$

The slope of the line OA is

$$s_2 = \frac{B_2}{H_2} = \frac{1}{AR_2} \quad \dots \quad \dots 2.8$$

From (1) & (2)

$$s_2 = \frac{R_1}{R_2} s_1 = K s_1 \quad \dots \quad \dots 2.9$$

Where $K = \frac{R_1}{R_2}$

R_1 and R_2 are determined from magnetic circuit analysis.

Slope of the line MM' = reversible permeability = μ_R and from Fig.2.7

$$\mu_R = \frac{B_2 - B_1}{H_1 - H_2} \quad \dots \quad \dots 2.10$$

Solving equations 2.7, 2.8, 2.9 and 2.10 together, we get

$$H_2 = \frac{H_1 (\mu_R H_1 + B_1)}{\mu_R H_1 + K B_1} \quad \dots \quad \dots 2.11$$

$$\text{and } B_2 = \mu_R (H_1 - H_2) + B_1 \quad \dots \quad \dots 2.12$$

The secondary demagnetization curve can now be drawn by taking successive values of B_1 and H_1 on the major demagnetization curve and calculating the corresponding values of B_2 and H_2 from equations (5) and (6). Having drawn the secondary demagnetization curve, the corresponding energy product

curve may be drawn.

Referring to fig. 2.7 once again, it can be seen that

$$S_2 = \frac{B_1}{H_1 - H_d} \quad \dots \quad \dots \quad 2.13$$

Solving equations (1), (3) and (7) together we get,

$$H_d = \frac{H_1(K-1)}{K} \quad \dots \quad \dots \quad 2.14$$

The m.m.f. to which the magnet is stable is

$$F_d = H_d \cdot l \quad \dots \quad \dots \quad 2.15$$

Let B_2, H_2 be the co-ordinates of the point on the secondary demagnetization curve for which the magnet assembly is just stable for a given stabilizing m.m.f. F_d .

$$\text{The m.m.f. } F = H_2 \cdot l \quad \dots \quad \dots \quad 2.16$$

$$\frac{F_d}{F} = \frac{H_d}{H_2} = C \quad \dots \quad \dots \quad 2.17$$

$$\text{where } C = \frac{F_d}{F} = \frac{\text{Demagnetizing field}}{\text{operating field}} \quad \dots \quad 2.18$$

which is fixed

$$\text{and } S_2 = \frac{\mu_r [K(C-1) + 1]}{K-C-1} \quad \dots \quad 2.19$$

The intersection of the air-gap line of slope S_2 with the secondary demagnetization curve gives the desired operating point.

2.7. STABILIZATION BY DEMAGNETIZATION WITH A GIVEN M.M.F. AFTER MAGNETIZATION IN ASSEMBLY...

As mentioned earlier, in this method, the magnet is magnetized after assembly and is then stabilized by applying a demagnetizing m.m.f. for which the magnet is to be stabilized.

Referring to Fig.2.8,

B_2, H_2 are the co-ordinates of Q' , a point on the secondary demagnetization curve B_r, Q', H_c .

$$\frac{B_2 - B_1}{H_1 - H_2} = \mu_R \quad \dots \quad \dots \quad 2.20$$

$$S_2 = \frac{B_2}{H_2} \quad \dots \quad \dots \quad 2.21$$

and equations 2.15, 2.16, 2.17 and 2.18 apply in this case also and are written once again.

$$F_d = H_d l \quad \dots \quad \dots \quad 2.15$$

$$F = H_2 l \quad \dots \quad \dots \quad 2.16$$

$$\frac{F_d}{F} = \frac{H_d}{H_2} = C \quad \dots \quad \dots \quad 2.17$$

$$C = \frac{F_d}{F} \quad \dots \quad \dots \quad 2.18$$

Solving equations 2.17, 2.18, 2.20 and 2.21

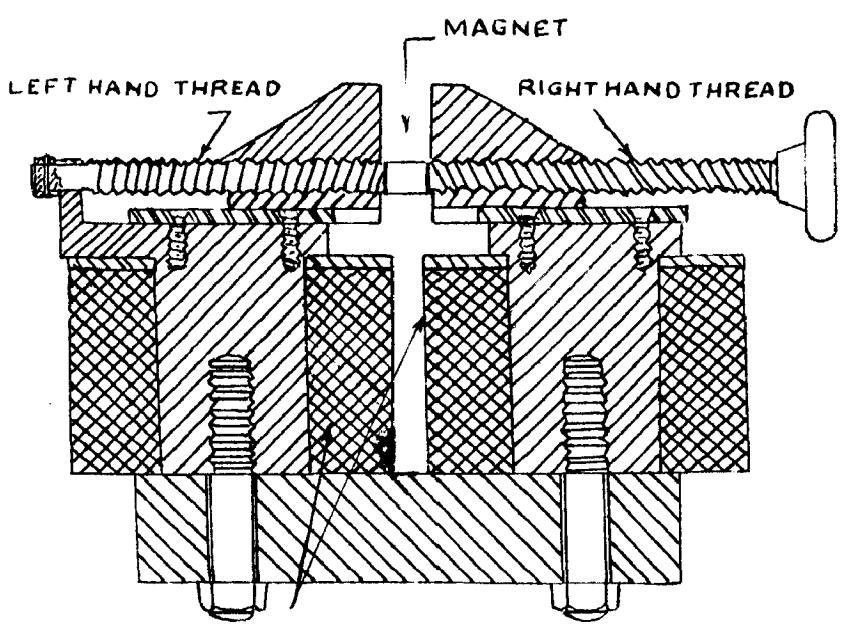
$$H_2 = \frac{(B_1 + \mu_R H_1) \left[(C+1) - \sqrt{(C+1)^2 - \frac{4 \mu_R C H_1}{H_1 + \mu_R H_1}} \right]}{2 \mu_R C} \quad \dots \quad 2.22$$

$$\text{and } B_2 = \mu_R (H_1 - H_2) + B_1 \quad \dots \quad \dots \quad 2.23$$

The secondary demagnetizing curve can then be drawn from equations ^{2.22}(17) & ^{2.23}(18)

2.8. OPTIMUM MAGNET DIMENSIONS FROM SECONDARY DEMAGNETIZATION CURVE...

If H_2, B_2 are the co-ordinates of the operating point on the secondary demagnetization curve, then l and A can be determined as follows:



COILS CONNECTED
IN SERIES

Fig. 1
Magnet

$$l = \frac{F}{H_2} \quad \dots \quad \dots 2.24$$

$$\text{and } A = \frac{F}{RB_2} \quad \dots \quad \dots 2.25$$

Volume of the magnet = $V = l.A$

$$= \frac{F^2}{RB_2^2} \quad \dots \quad \dots 2.26$$

This volume is minimum if the energy product B_2H_2 is maximum.

17

2.9. METHODS OF MAGNETIZATION...

The rotor may be magnetized by any of the following methods;

- (1) Coils around the poles
- (2) direct current in the armature
- (3) leading power leads on the generator
- (4) magnetizing fig. if the rotor is to be magnetized outside the machine.

Method (1) requires a special winding around the poles. Method (3) involves the principle that leading power factor currents produce magnetic field that aids the main field. This method is limited to small machines as for large machines the capacitors needed may be prohibitively large. Method (2) is more suitable. In this case the field is oriented with respect to the armature before energizing the armature. This can be done by passing first a small value of the current and then a relatively larger current. Method 4 utilises a particular type of magnetizer. One magnetizer is the 'Contact Magnetizer', shown in Fig.2.9. It consists of a low reluctance Yoke upon

which a magnetizing winding is wound. At the top of the Yoke and above the winding, a fixture is attached which can be adjusted to receive various forms and sizes of magnets.

To ensure the magnetization to saturation, the maximum magnetizing m.m.f. equal to five times the coercive m.m.f. has been found satisfactory.

...CHAPTER - 3...

DESIGN OF GENERATOR.

3.1. In the design of the generator with permanent magnet fields, the design of the field system is of great importance. This problem can be tackled in many ways and all the methods involve in some form or the other the same basic principles. One approach to the optimum design of the magnet has been given in Chapter 2 and two more are discussed in this Chapter. Other dimensions are determined in the same way as those in synchronous machines with electromagnetic fields.

3.2. DESIGN OF PERMANENT MAGNET¹...

Permanent magnets may be required to perform either

- (1) a static function or
- (2) a dynamic function

If the permeance of the circuit to which the magnet is connected is constant, the magnet is fulfilling a static function and if the permeance is variable, the magnet is fulfilling a dynamic function. Obviously in a generator, the permanent magnets are performing a dynamic function and thus, in this work the design for dynamic function only is considered. Consider a magnet, initially fully magnetized, and connected to a circuit of which OA, figure 3.1, represents the maximum unit permeance. Unit permeance refers to the $\frac{B}{H}$ conditions for 1 m³ of magnet material. Now if the circuit reluctance is increased and the flux exists in leakage paths only, let the unit permeance be given by OC. During the

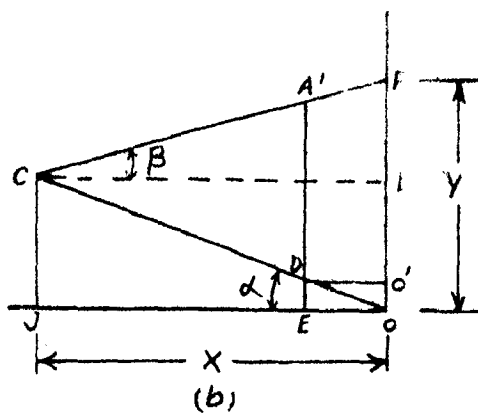
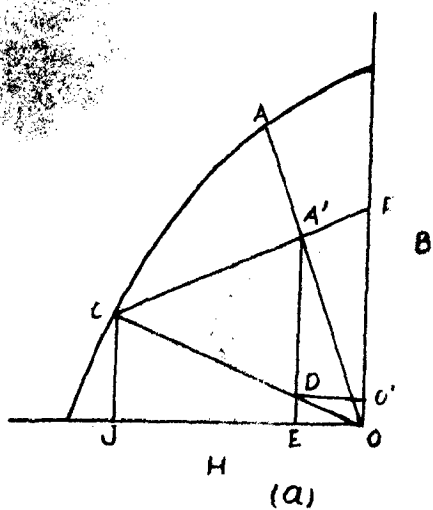


Diagram
Permanent (steady) operation-dynamic conditions.

increase in reluctance, the working point moves down the demagnetization curve from A to C. Now if the circuit reluctance is decreased until the unit permeance is again OA, the magnet operates, during this process, along the recoil line CF and the working point corresponding to maximum permeance is now OA' instead of OA. Under this condition, the total flux per unit volume of the magnet is given by A'E and of this DE is the leakage flux. The useful flux per unit volume is, thus, A'D.

The slope of the useful permeance line is

$$\begin{aligned} \frac{1}{A} P_g &= \frac{1}{A} \frac{(A'E - DE)A}{Hl} \\ &= \frac{A'E - DE}{H} \quad \dots 3.1 \end{aligned}$$

where l = length of the magnet and

A = X-sectional area.

Obviously from relation 3.1 slope of the useful permeance line is equal to the slope of the line O'A'.

Leakage coefficient is

$$\frac{A'E}{A'D} = \frac{P}{P_g} \quad , \quad P \rightsquigarrow P_g + P_l \quad \dots 3.2$$

and also

$$\frac{\text{Total energy}}{\text{Useful energy}} = \frac{A'E \times OE}{A'D \times OE} = \frac{P}{P_g} \quad \dots 3.2(a)$$

For the magnet material to be minimum, the area A'DxOE should be maximum.

Referring fig.3.1(b) which shows a part of fig.3.1(a) in details-

Both S_1 and S can be varied by variation of $1/A$. If the optimum value of S_1 can be determined, S can then be fixed for maximum economy.

From fig. 3.1

$$XY = OJ \times OF = H(B + \sqrt{u_R}H) \quad \dots 3.10$$

where B and H are the coordinates of C .

XY is a maximum when $H (B + \sqrt{u_R}H)$ is also maximum

$$\text{or } \frac{d(BH)}{dH} + 2\sqrt{u_R}H = 0$$

It is to be noted that at $(BH)_{\max}$ point $\frac{d(BH)}{dH} = 0$ and thus C must be below the $(BH)_{\max}$ point.

$$\frac{d(BH)}{dH} = B + H \frac{dB}{dH}$$

$$\text{or } \frac{H + H_c}{a+b(H+H_c)} + \frac{aH}{[a+b(H+H_c)]^2} + 2\sqrt{u_R}H = 0$$

$$\text{or } 2\sqrt{u_R}b^2H^3 + (b+4\sqrt{u_R}ab + 4\sqrt{u_R}b^2H_c)H^2 + (2a + 2bH_c + 2\sqrt{u_R}a^2 + 4\sqrt{u_R}abH_c + 2\sqrt{u_R}b^2H_c^2)H + aH_c + bH_c^2 = 0 \quad \dots 3.11$$

Solve equation 3.11 for H . Let the corresponding values be H_1 and B_1 . We must have

$$\frac{1}{A} P_1 = \frac{B_1}{H_1} \quad \dots \quad \dots 3.12$$

At the working point $H = \frac{H_1}{2}$

$$\frac{1}{A} P = \frac{B_1 + \sqrt{u_R} \frac{H_1}{2}}{H_1/2} = S \quad \dots 3.13$$

$$\text{But } P = P_g + P_1^S$$

$$P_g = \frac{A}{1} (S_1 + \sqrt{u_R}) \quad \dots 3.14$$

P_g is settled by the m/c into which the magnet must work and not by consideration of economy of material. Having

$$\begin{aligned} A'D &= OF - OE \tan \alpha - OE \tan \beta \\ &= OF - OE (\tan \alpha + \tan \beta) \end{aligned}$$

$$\begin{aligned} \text{Area } A' &= A'D \times OE \\ &= OF \times OE - (OE)^2 (\tan \alpha + \tan \beta) = 0 \end{aligned}$$

For this area to be maximum

$$\frac{dA'}{d(OE)} = OF - 2 OE (\tan \alpha + \tan \beta) = 0$$

$$\text{and } OE = \frac{OF}{2(\tan \alpha + \tan \beta)} \quad \dots 3.3.$$

$$\text{From fig. 3.1 } \tan \alpha = \frac{CJ}{OJ} = \frac{1}{A} P_1 \quad \dots 3.4$$

where P_1 = Permeance of the leakage path

$$\text{and } \tan \beta = \frac{FJ}{OJ} = \mu_R, \text{ recoil permeability. } \quad 3.5$$

$$OE = \frac{OF}{2\left(\frac{CJ}{OJ} + \frac{FJ}{OJ}\right)} = \frac{OJ}{2} \quad \dots 3.6$$

From relation 3.6, it is obvious that, for maximum economy of material, the point A' should ^{be} located midway along FC .

$$\begin{aligned} \text{Area } A &= A'D \times OE \\ &= \frac{OF}{2} \times \frac{OJ}{2} = \frac{YX}{4} \end{aligned}$$

where $Y = OF$ and $OJ = X$.

For maximum economy for material, the recoil line should be such that XY is a maximum.

Let S and S_1 be the slopes of the load and leakage lines respectively. Then

$$S_1 = \frac{1}{A} P_1 \quad \dots \quad \dots 3.7$$

$$S = \frac{1}{A} P \quad \dots \quad \dots 3.8$$

$$\text{where } P = P_g + P_1 \quad \dots \quad \dots 3.9$$

fixed P_g , P_1 is also determined.

$$\frac{1}{A} = \frac{1}{P_1} \frac{B_1}{H_1} \quad \dots \quad \dots \quad 3.15$$

Volume of the magnet material

$$V = \frac{K_1 \phi_g M}{B'H'} \quad \dots \quad \dots \quad 3.16$$

where B' , H' are the coordinate of A' ,

ϕ_g = flux in the gap

M = Potential drop across it

$K_1 = P/P_g$.

$$\begin{aligned} B'H' &= \frac{H_1}{2} \frac{1}{\phi A} P \cdot \frac{H_1}{2} \\ &= \frac{H_1^2}{4} \frac{1}{\phi A} P \quad \dots \quad \dots \quad 3.17 \end{aligned}$$

For a given flux ϕ_g , the dimensions of the magnet are determined from equations 3.15, 3.16 and 3.17.

3.2.1. A new approach to the optimum design of magnet has been given by Hans. K. Ziegler²² and the method has been utilized since 1947 with very satisfactory practical results by the Signal Corps. Engineering Laboratories. The elementary assumptions made in this method are the same as those in any of the methods developed earlier. They are:

1. The magnet has uniform cross section and is uniform in properties and magnetic state.
2. The magnet has initially been magnetized to saturation.
3. The minor hysteresis loops originating from the main demagnetization curve are of so small an area that they can be replaced for practical purposes by a straight line connecting their tips.
4. All leakage flux is assumed to come from the ends or the pole shoes of the magnets. Leakage is therefore

regarded as a terminal factor and the optimum design is achieved for the required total magnetic flux ϕ_1 including leakage. Where excessive leakage originating from the lateral magnet faces invalidates such simplification, this part of the leakage is assumed to be replaced by an equivalent fictitious terminal leakage.

The form of the equation chosen is not that of Lamonts', but that as given by Underhill²³ and is given by

$$B = \frac{H_c - H}{H_c - aH} B_r \quad \dots \quad \dots \quad 3.18$$

where a is a material constant given by

$$a = 2 \sqrt{\frac{B_r H_c}{B_0 H_0}} - \frac{B_r H_c}{B_0 H_0} \quad \dots \quad 3.19$$

All the quantities involved in these equations being in c.g.s. system. In M.K.S. rationalised system, the equations remain same and the various quantities involved are defined as under:

B_0 & H_0 = the magnetic induction and the magnetizing force corresponding to the point of max. energy product.

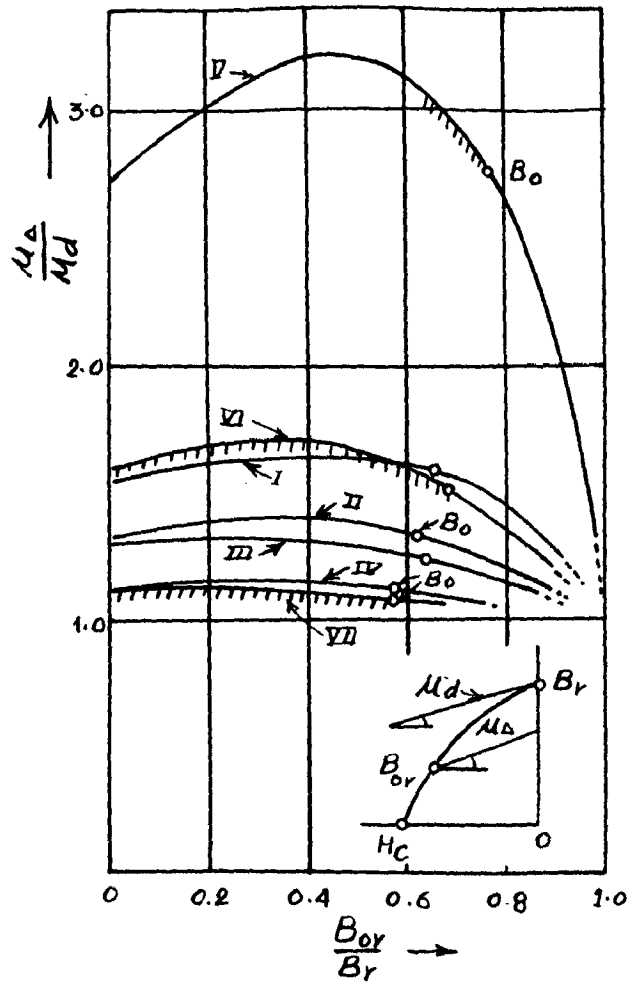
B_r = residual induction

H_c = Coercive force

B & H = the magnetic induction & magnetizing force points on demagnetization curve.

The units for magnetic induction and magnetizing force are Wb/m^2 and amp-turns per meter respectively.

In the previous design methods it has been assumed and



Variation of dynamic pressure ratio for sonic flows.

that the slope of the minor loops is constant. That is not quite true and in fact, it may vary considerably with the point of their origin at the main demagnetization curve. Fig. 3.2. shows how the slope of minor loops ^{varies} varies for various alnico alloys. μ_{Δ} represents the slope of straight line replacement for minor loop and μ_d is the differential permeability at the point B_r . B_{or} is the magnetic induction at the point of origin of minor loops.

It has been found that optimum operating conditions for all practical demagnetizing conditions are confined to minor loops originating from a portion of the main demagnetization curve between the point of max. energy product and a point below, which is different for various materials, and is as shown by the shaded portions in Fig. 3.2, for alnico V, VI & XII. The average slope of these portions which is designated by μ_a , can be used in all design calculations.

The design principle involves the introduction of hypothetical ideal magnet of the magnet material having the same values of B_r and H_c and having the main demagnetization curve as perfect rectangle as shown in Fig. 3.3. The net dimensions of this hypothetical magnet are subsequently corrected for by factors to take into account the deviations in actual and hypothetical ideal magnet. The optimum design is signified by the minimum of volume correction factor.

Two cases are considered viz.

Case A: Demagnetization by varying external reluctance

Case B: Demagnetization by externally applied m.m.f.

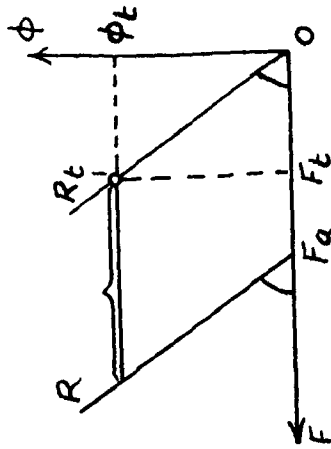


Fig. 2.8
Problem simplification
for Case B.

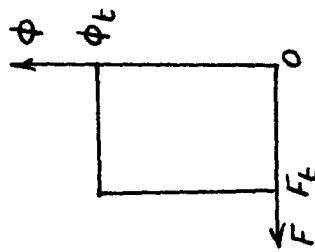


Fig. 2.3
Main demagnetization
curve for hypothetical
local magnet.

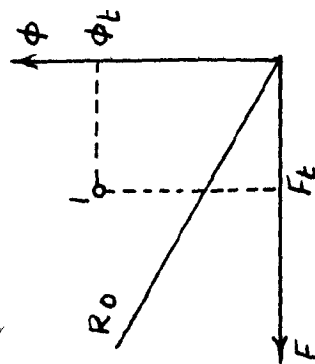


Fig. 2.1
Problem simplifications
for case A.

CASE A-

Fig.3.4 defines the problem specifications ϕ_t , F_t , R_t represent the total magnetic flux, total magnetomotive force and total magnetic reluctance corresponding to the normal operating point, 1, respectively. Demagnetizing condition caused by open circuit reluctance is represented by R_0 . Let

A = cross sectional area of magnet

l = length of magnet

$V = Al$ = volume of magnet

$S = \frac{l}{A}$ = shape factor

A_m, l_m, V_m, S_m , the corresponding values for the optimum magnet

A_0, l_0, V_0, S_0 the corresponding values for the ideal magnet.

$K = R_0/R_t$ = degree of demagnetization

μ_a = the average slope of the minor loops for a standard unit of volume 1 and shape factor 1.

$\mu_{as} = \frac{\mu_a}{S}$ = resultant average slope of minor loops for defined zone and shape factor S .

The ideal magnet does not require a consideration of the demagnetization caused by the open circuit reluctance as no minor loops exist in this case, the dimensions of the ideal magnet are given as

$$A_0 = \phi_t / B_r \quad \dots \quad \dots \quad 3.20$$

$$l_0 = F_t / H_c \quad \dots \quad \dots \quad 3.21$$

$$V_D = \frac{\phi_t F_t}{B_r H_c} \quad \text{and} \quad S_0 = l_0 / A_0 \quad \dots \quad 3.22$$

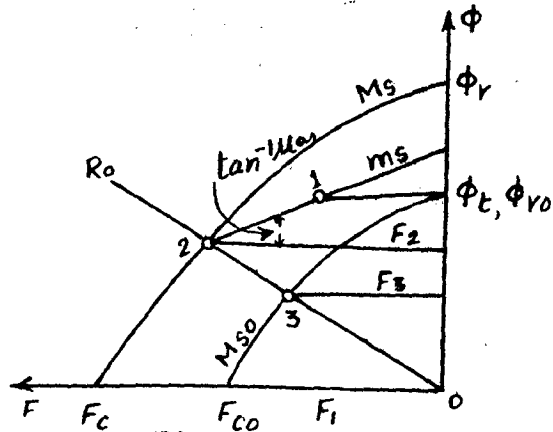


Fig. 3.5.

Basic geometrical relations for magnetization by varying external reluctance.

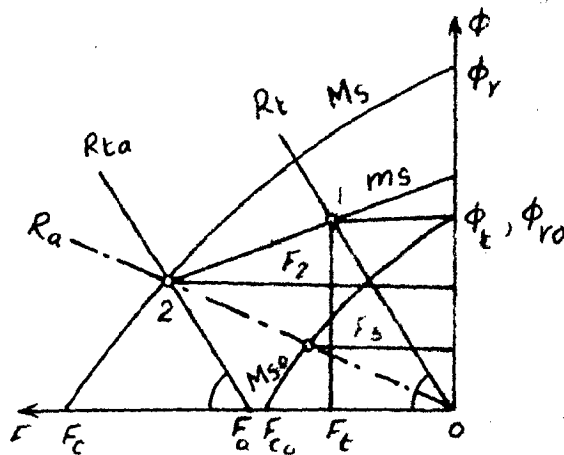


Fig. 3.7

Basic geometrical relations for demagnetization by externally applied magnetomotive force.

The following procedure is employed to derive the correction factors. Point 1, Fig.3.5 must lie on the minor hysteresis loop m_s . For any chosen value of μ_{as} , a main demagnetization curve M_{so} of the given material for the corresponding shape factor can be placed into the diagram, with residual flux ϕ_{r0} equal to ϕ_t . The curve M_s which has the same shape factors and passes through 2, point of intersection of the minor loop m_s and open circuit reluctance R_0 can be obtained by magnifying the curve M_{so} by λ , where

$$\lambda = \frac{0-2}{0-3} = \frac{F_2}{F_3} \dots \dots 3.23$$

Then, ϕ_r = residual flux of the main demagnetization curve.

$$= \lambda \phi_t \dots \dots 3.24$$

$$\text{and } A = \frac{\phi_r}{B_r} = \frac{\lambda \phi_t}{B_r} = \lambda A_0 \dots \dots 3.25$$

As the ideal magnet and M_{so} have the same residual flux and hence the same cross-sectional area, F_{c0} , the coercive force of the magnet M_{so} is given as

$$F_{c0} = S/S_0 F_t \dots \dots 3.26$$

$$F_c = \text{Coercive m.m.f. of the magnet } M_s \dots$$

$$= \lambda F_{c0} = \lambda (S/S_0) F_t \dots \dots 3.27$$

$$l = \frac{F_c}{H_c} = \lambda \left(\frac{S}{S_0} \right) l_0 \dots \dots 3.28$$

$$\text{and volume } V = Al = \lambda^2 \left(\frac{S}{S_0} \right) l_0 A_0 = \lambda^2 \left(\frac{S}{S_0} \right) V_0 \dots \dots 3.29$$

$$= \eta V_0 \text{ where } \dots \dots 3.30$$

$$\eta = \text{correction factor} = \lambda^2 \left(\frac{S}{S_0} \right) \dots \dots 3.31$$

The optimum design is obtained for minimum value of the correction factor.

$$\lambda_m^2 = \left[\lambda \left(\frac{S}{S_0} \right) \right]_{\min} = \lambda_m^2 \left(\frac{S_m}{S_0} \right) \quad \dots 3.32$$

The optimum magnet dimensions are then

$$\begin{aligned} A_m &= \lambda_m A_0 \\ l_m &= \lambda_m \left(\frac{S_m}{S_0} \right) l_0 \\ V_m &= \lambda_m^2 \left(\frac{S_m}{S_0} \right) V_0 = \lambda_m V_0 \end{aligned} \quad \dots 3.33$$

Equations for λ is given in Appendix I

Physically λ_m is the ratio between residual induction B_r and optimum operating induction B_{op}

$$\lambda_m = \frac{B_r}{B_{op}} \quad \dots \quad \dots 3.34$$

It has been found advantageous for the convenience of calculations and best readability of diagrams to use a term Z , where

$$\begin{aligned} Z &= (S/S_0)K \\ \text{For optimum conditions} \\ Z_m &= (S_m/S_0)/K \quad \dots 3.35 \\ \text{and } l_m &= \lambda_m Z_m K l_0 \\ V_m &= \lambda_m^2 Z_m K V_0 \end{aligned}$$

For the final evaluation of results, optimum per unit values for the magnet dimensions can be defined as,

$$\begin{aligned} a_{op} &= \lambda_m / B_r = \frac{1}{B_{op}} \quad (\text{meter}^2 \text{ per Wb}) \\ l_{op} &= \lambda_m^2 Z_m K / H_c = \frac{1}{H_{op}} = (\text{meter/amp-turns}) \\ V_{op} &= \lambda_m^2 Z_m K / B_r H_c = \frac{1}{B_{op} H_{op}} \quad (\text{meter}^3 \text{ /Wb-amp-turns}) \end{aligned} \quad \dots 3.36$$

With these definitions,

$$\begin{aligned} \Lambda_m &= \mu_t a_{op} \\ l_m &= F_t l_{op} \\ V_m &= \mu_t F_t V_{op} \end{aligned} \quad \dots 3.37$$

Case B

Fig.3.6 defines the problem specifications. As in case A, μ_t , F_t , R_t represent the total magnetic flux, total m.m.f., and total magnetic reluctance respectively corresponding to the operating point 1. F_a is the externally applied demagnetizing m.m.f. F_a . The degree of demagnetization in this case is defined as

$$C = \frac{F_a}{F_t} \quad \dots 3.38$$

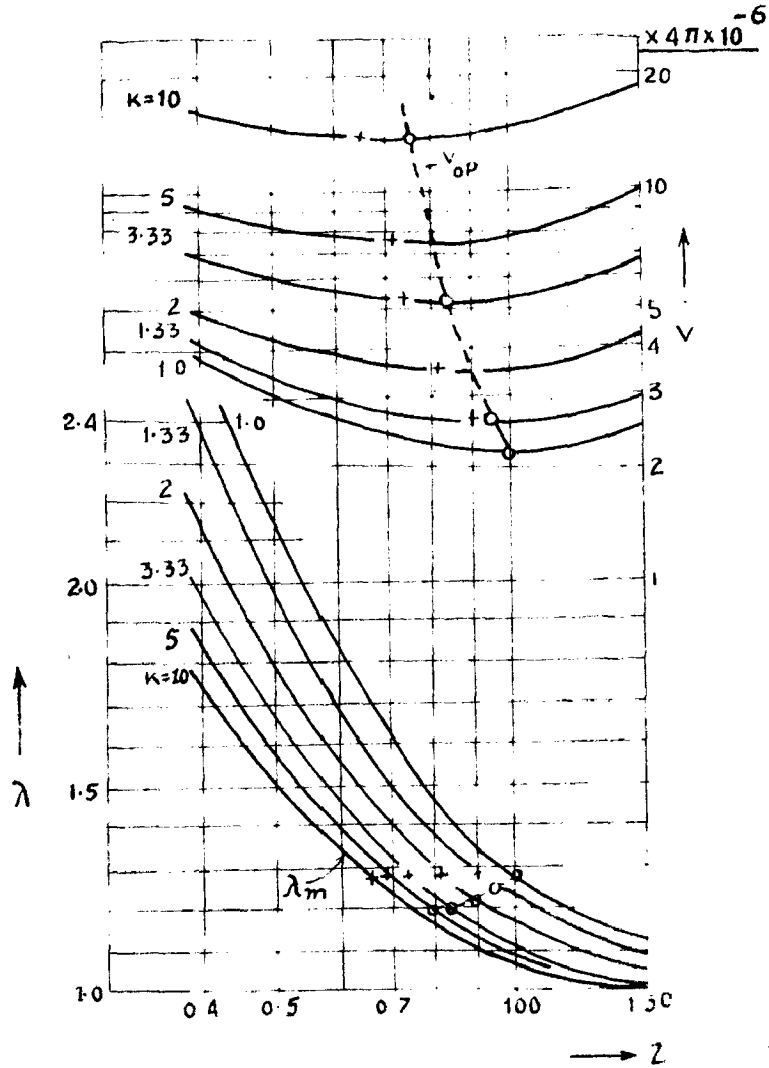
The design relations are similar to those obtained in case A. A shifting auxiliary line R_a is drawn passing through the point 2 and origin. The procedure is explained by Fig.3.7.

The per unit optimum dimensions are given as follows:

$$\begin{aligned} a_{op} &= \frac{m}{B_r} = \frac{1}{B_{op}} \\ l_{op} &= m \left(\frac{S_m}{S_0} \right) / H_c \\ V_{op} &= \frac{2}{m} \left(\frac{S_m}{S_0} \right) / B_r H_c \end{aligned} \quad \dots 3.39$$

and final optimum magnet dimensions are given by

$$\begin{aligned} \Lambda_m &= \mu_t a_{op} \\ l_m &= F_t l_{op} \\ V_m &= \mu_t F_t V_{op} \end{aligned} \quad \dots 3.40$$



λ

1

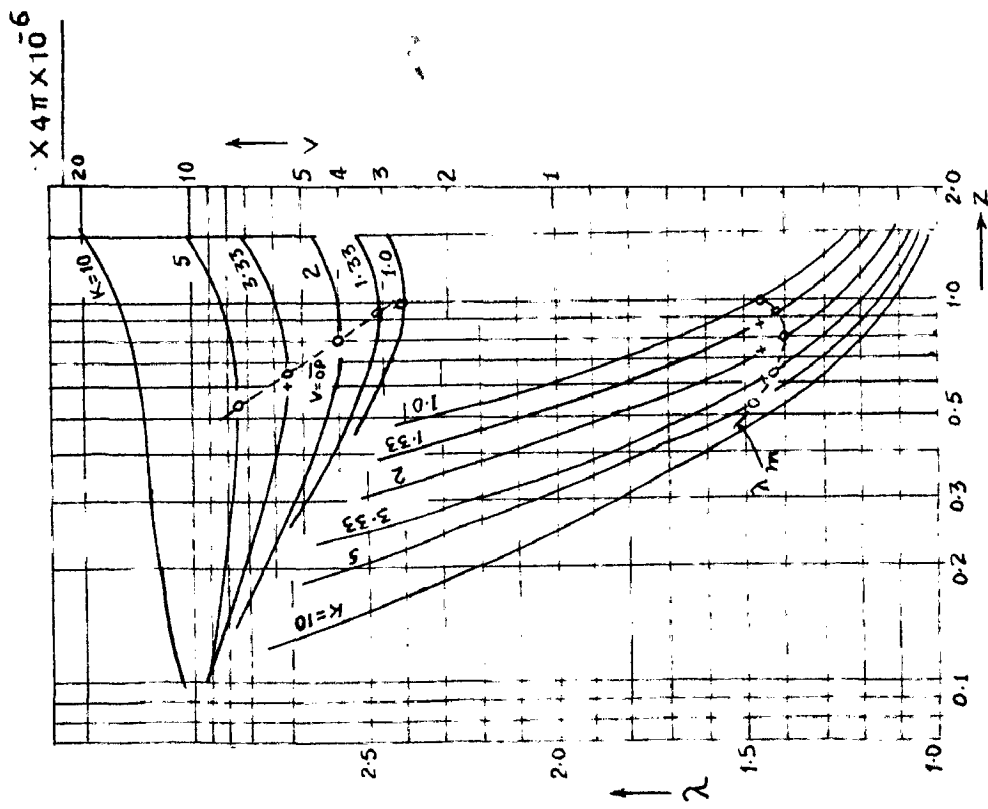


Fig. 1. λ vs z for various K values.

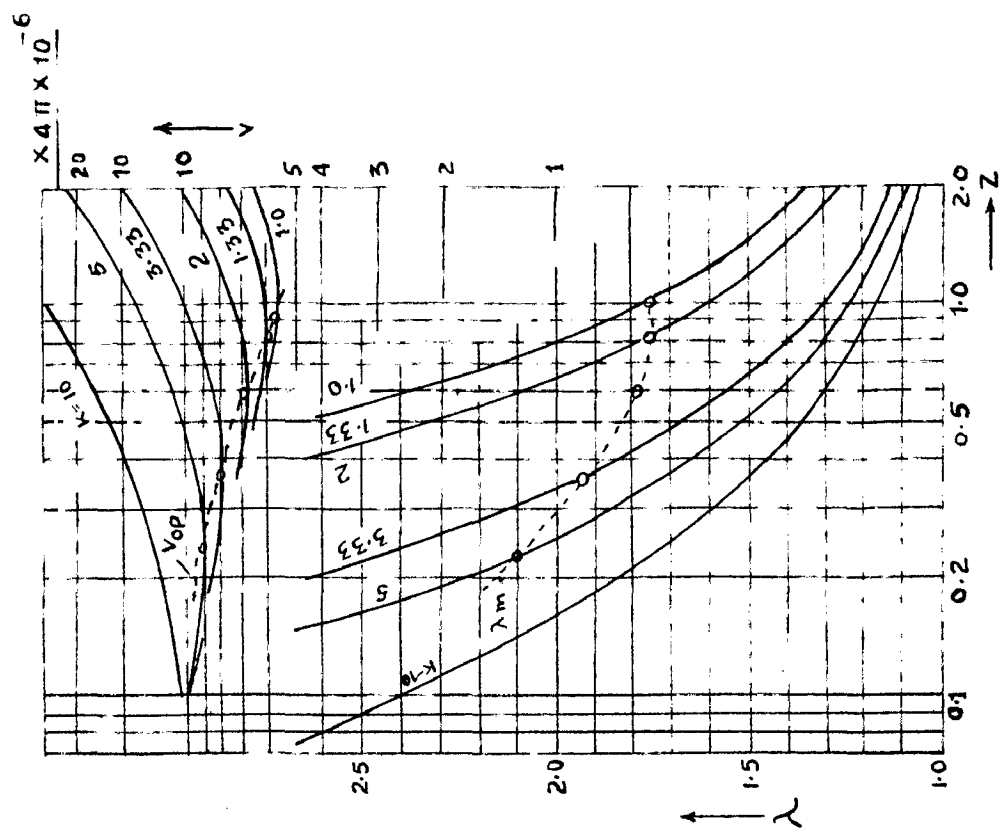


Fig. 2. λ vs z for various K values.

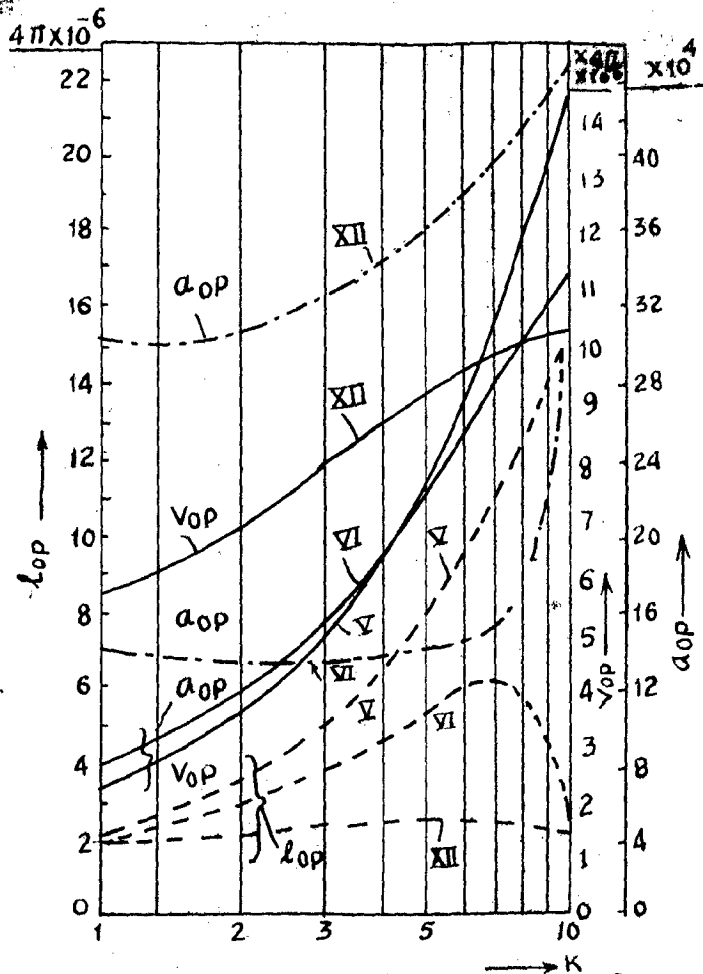
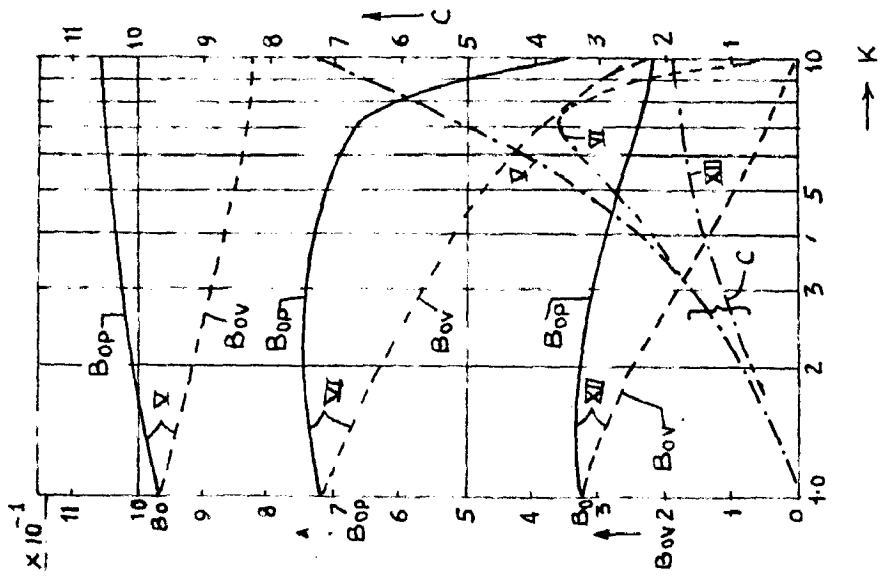
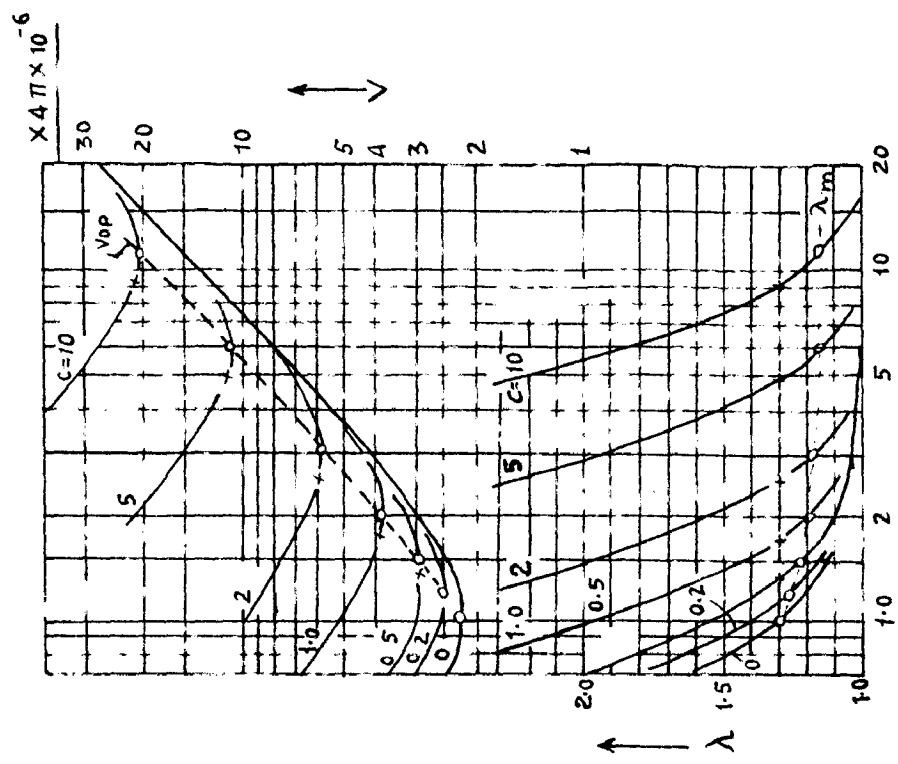


Fig. 3.11

Design chart containing optimum per unit magnet dimensions depending upon degree K of magnetization. Case A, for alloys V, VI, & XII.



$\lambda = \lambda_m$

K

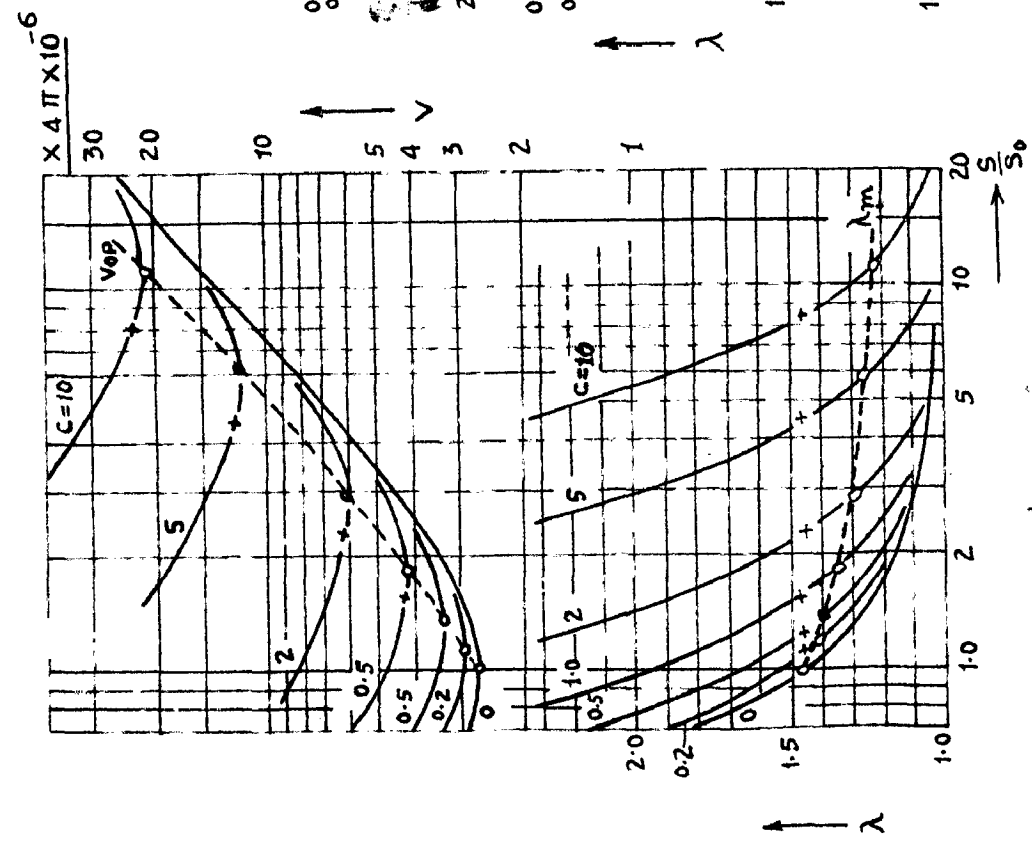
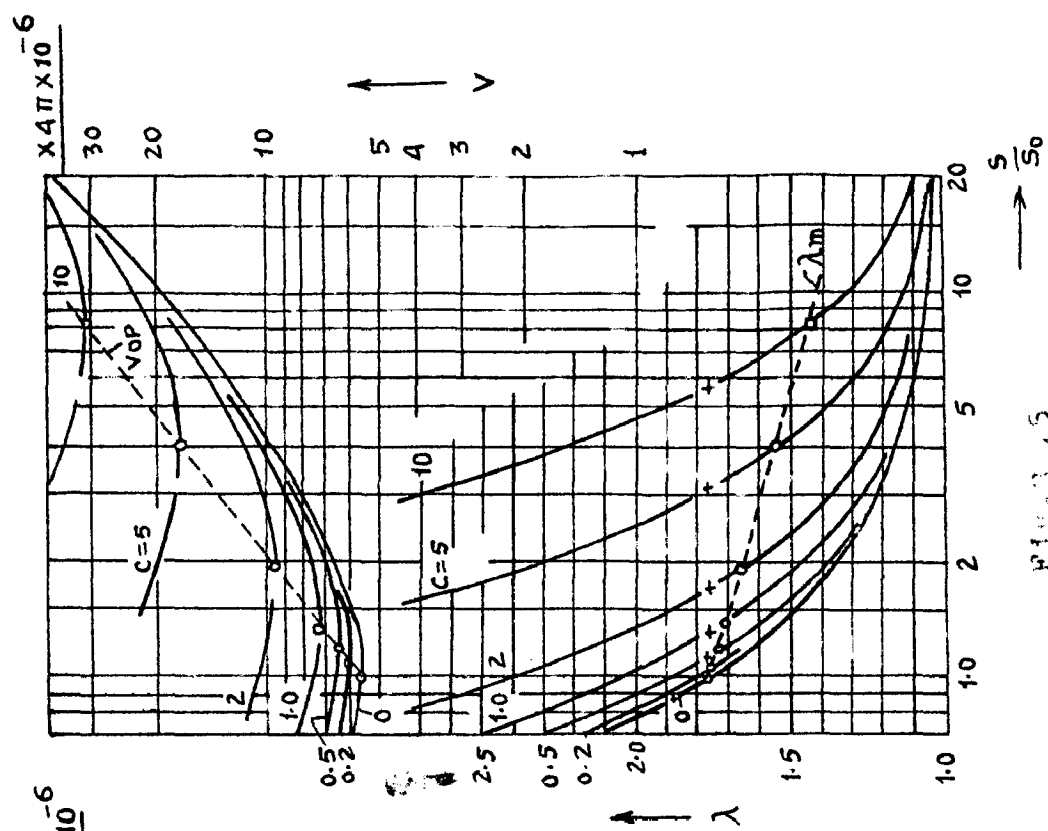
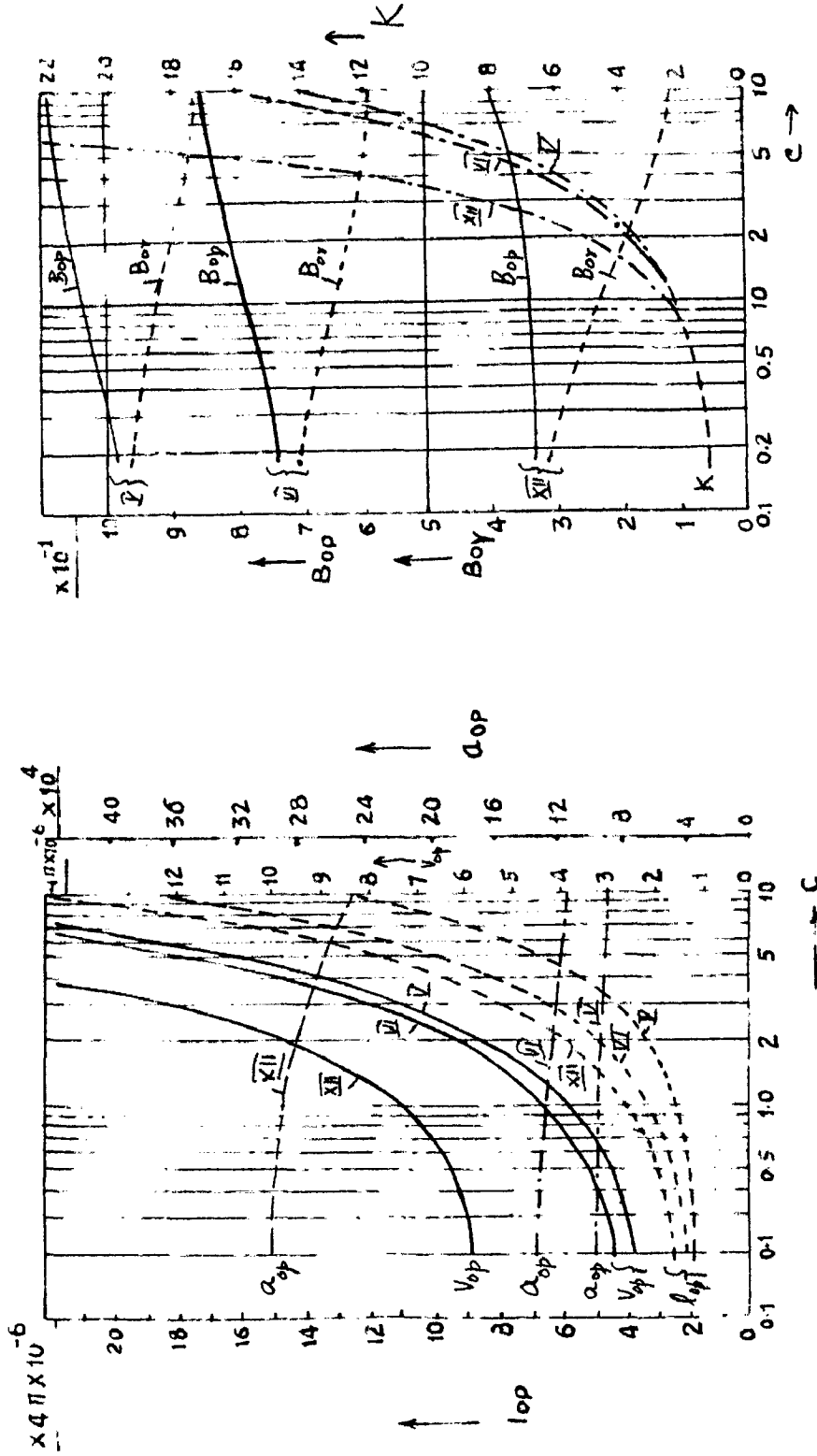


PLATE 15
 Design chart for λ and S/S_0 for $C = 0.5, 1.0, 2, 5, 10$

PLATE 16
 Design chart for λ and S/S_0 for $C = 0.5, 1.0, 2, 5, 10$



Handwritten notes in Russian, partially illegible due to blurriness. Visible words include "расчет", "показатели", "зависимость".

Handwritten notes in Russian, partially illegible due to blurriness. Visible words include "расчет", "показатели", "зависимость".

DESIGN CHARTS...

Figs. 3.8, 3.9 and 3.10 represent the values of V & λ as functions of the variable Z for demagnetization factors K between 1 and 10 for the case A. V is the volume of magnet per-unit external magnetic energy and is given by

$$V = \lambda^2 \frac{ZK}{B_r H_c} \quad \dots \quad \dots \quad 3.41$$

The minimum per unit volume V_{op} and corresponding value λ_m is marked on the curves. Design charts shown in figs. 3.11 and 3.12 give optimum per unit volume V_{op} , cross section a_{op} and length l_{op} , plotted $V_s K$, and help in determining the magnet dimensions for a given degree of demagnetization K and a chosen given material.

Figs. 3.13 - 3.17 are the various design charts to be used for calculating magnet dimensions for case B.

3.2.2. INTERRELATIONS BETWEEN TWO CASES OF DEMAGNETIZATION...

It is obvious that demagnetization of the magnet by varying external reluctance permits also the application of a certain maximum external demagnetizing m.m.f. to the circuit, when operating at its normal reluctance. R_t , without causing further demagnetization. Similarly, demagnetization by applying external demagnetizing force, permits a certain maximum open circuit reluctance. In permanent magnet generator design it is important to know how much short-circuit armature reaction will be permissible if the rotor is designed for a certain value of K , corresponding to the "rotor out of its stator" condition.

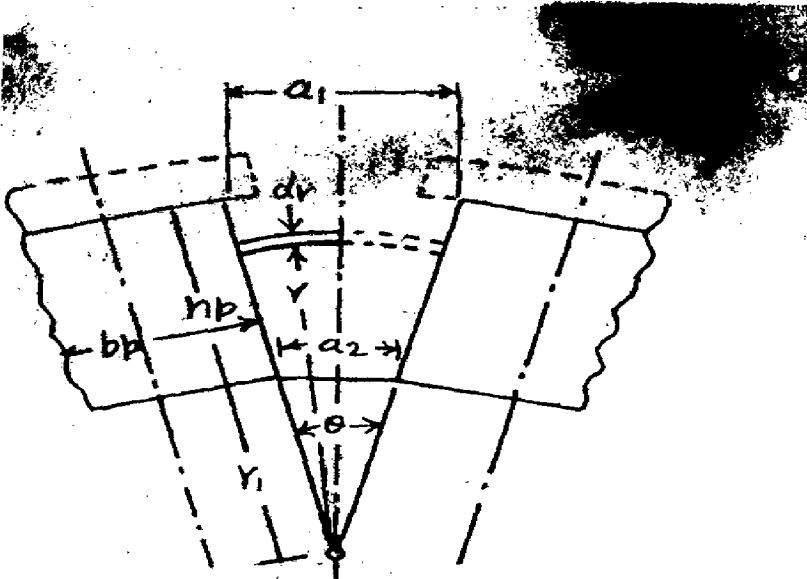
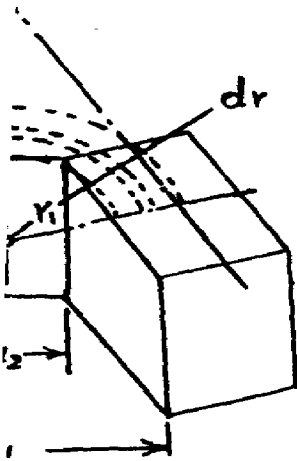


Fig. 3.18
 assumed path of the leakage flux between magnet sides facing each other.



3.20
 the leakage flux peripheral

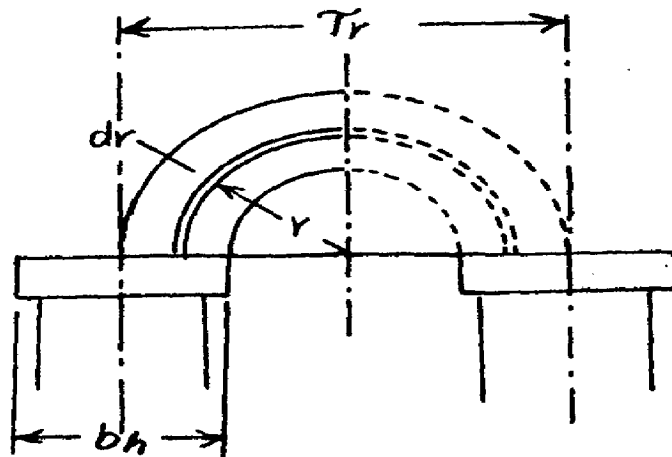


Fig. 3.19
 assumed path of the out-stair leakage flux.

POLE LEAKAGE 5,12

The permeability of the modern permanent magnet material is very small as compared with that of soft iron parts and the leakage exhibited by the permanent magnet is so small that it can not be neglected. Exact leakage calculations require graphical field mapping but good convenient methods to the problem can be made by "estimating permeances of probable flux paths"¹².

The following assumptions are made⁵:

1. The magnetic circuit is not saturated.
2. The actual field lines are replaced by lines which are of simple shape, such as circles and straight lines.
3. All permeances are estimated between one half of a pole and the equipotential plane between this pole and the adjacent one. The permeances of the various paths are calculated as follows:

Permeance P_1 of the Surface Leakage Between Pole Magnets...

Ref. fig. 3-18 Leakage flux between magnet sides facing each other can be expressed by

$$\phi_1 = V_m P_1 \text{ where} \quad \dots 3.42$$

V_m = maximum potential of the magnet

$$\text{or by } d\phi_1 = V_r dp_1 \text{ where} \quad \dots 3.43$$

V_r = magnetic potential of the magnet at a distance

from O . The leakage permeance between the surface element and neutral plane is

$$dp_1 = \frac{\mu_0}{r(\theta/2)} l_p dr \text{ where} \quad \dots 3.44$$

θ = mechanical angle between two poles axes.

$$= \frac{2 \pi}{p}, \quad p = \text{no. of poles}$$

and l_p = axial length of the pole shoes.

Combining equations 3.42, 3.43 and 3.44 and integrating within r_1 and $r_1 + h_p$ as limits for r , specific leakage permeance per unit length

$$\frac{P_1}{l_p} = \frac{\mu_0 \pi}{h} \left[1 - \frac{a_2}{a_1 - a_2} \times \log_e \left(1 + \frac{a_1 - a_2}{a_2^2} \right) \right] \quad 3.45$$

where $a_2 = r, \theta$ and $a_1 - a_2 \simeq h_p \theta$

Permeance P_2 of the Additional out-stator Leakage...

Assume path of leakage lines on the top of the pole shoes is as shown in figure 3.19. The leakage permeance between surface element $dr - l_p$ and neutral plane is

$$dP_s = \mu_0 \frac{l_p dr}{\pi r/2} \quad \dots \quad 3.46$$

Integrating between limits $\frac{\tau_r - bh}{2}$ and $\tau_r/2$,

$$\frac{P_s}{l_p} = \frac{2\mu_0}{\pi} \log_e \frac{\tau_r}{\tau_r - bh} \quad \text{where} \quad \dots \quad 3.47$$

τ_r = pole pitch.

Specific permeance of the fringing flux between the pole shoe edges

$$\begin{aligned} \frac{P_f}{l_p} &= \mu_0 \frac{0.322 (\tau_r - bh)}{1.220 (\tau_r - bh)/2} \quad \dots \quad 3.48 \\ &= 0.534 \mu_0 \end{aligned}$$

So P_2 is given by

$$P_2/l_p = \frac{2 \mu_0}{\pi} \log_e \frac{r_r}{r_r - bh} + 0.534 \mu_0$$

$$= \frac{2 \mu_0}{\pi} \log_e \frac{1}{1-l} + 0.534 \mu_0 \quad \dots 3.49$$

where $l \approx bh/r_r$

Permeance P_3 of the Magnets' Peripheral Leakage...

Fig.3.20 represents the leakage paths. Magnetic potential varies from zero at the neutral section to maximum at magnet terminals and the average value is estimated as one half of the maximum potential. In its effect on the calculated result, it is equivalent to one half of the permeance.

$$dp_s = 2 \mu_0 \frac{h_p \cdot dr}{2r\pi/2} \quad \dots \quad \dots 3.50$$

Integration limits are taken midway between the poles i.e. between

$$\frac{a_1 + a_2}{4} \text{ and } \frac{a_1 + a_2}{4} + \frac{b_p}{2}$$

$$P_3/h_p = \frac{2 \mu_0}{\pi} \log_e \left(1 + \frac{2}{\frac{a_1}{b_p} + \frac{a_2}{b_p}} \right) \quad \dots 3.51$$

The average fringing flux between the pole edges on both sides is

$$P_0 = \mu_0 2 \times 1/2 \times 2 \times 0.26 h_p = 0.52 \mu_0 h_p \quad \dots 3.52$$

$$P_3/h_p = 0.52 \mu_0 h_p + \frac{2 \mu_0}{\pi} \log_e \left(1 + \frac{2}{\frac{a_1}{b_p} + \frac{a_2}{b_p}} \right) \quad \dots 3.53$$

Permeance of Pole-Shoe Leakage...

The leakage permeance between the sides of pole shoes facing each other is

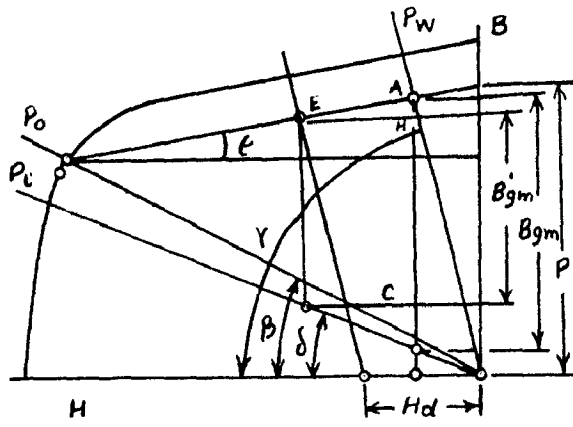


Fig. 2.2.1

Working lines on air gap
and condition.

$$P_{s1} = 2/\mu_0 \frac{h_p l_p}{dr^n - p b_h} \dots \dots 3.54$$

and on one peripheral side

$$\frac{P_{s2}}{2h_h} = \frac{2\mu_0}{\pi} \log_2 \frac{J_r}{J_r - b_h} + 0.534 \mu_0 \dots 3.55$$

or $= P_2/l_p$

where d_r = dia. of the rotor

h_h = depth of pole shoe

b_h = width of pole shoe

Total Leakage Permeance...

The in-stator leakage permeance can be written as

$$P_i = P_{s1} + P_{s2} + P_1 + P_2 \dots 3.56$$

and the out-stator leakage permeance

$$P_o = P_1 + P_2 \dots 3.57$$

It should be noted that

a_1 = maximum arc length between pole magnets

$$= (d_r - 2h_h) \frac{\pi}{p} - b_p \dots 3.58$$

a_2 = minimum arc length between pole magnets

$$= (d_r - 2h_h - 2h_p) \frac{\pi}{p} - b_p \dots 3.59$$

4.3.4. FLUX DENSITY IN THE AIR GAP.5.

Ref. figure 3.2 P_o , P_i , and P_w represent out-stator leakage permeance line, in-stator permeance line and actual working line. Inter-section of P_w line with h^{re} coil line, gives the working point A. δ , β , and γ are the angles that P_i , P_o and P_w make with the H-axis. Let $P_m = \frac{b_p l_p}{2h_p} \dots 3.60$

$$\left. \begin{array}{l} \text{then } \tan \beta = \frac{P_o}{P_m} \\ \text{and } \tan \delta = \frac{P_i}{P_m} \end{array} \right\} \dots 3.61$$

The minor loop is determined by the inter-section of the shearing line P_0 with the demagnetization curve and P_1 is 'leakage line'.

$$\tan r = \frac{P_1}{P_m} + \frac{P_g}{P_m} \quad \dots \quad \dots \quad 3.62$$

where

$$P_g = \mu_0 \frac{n}{2} \frac{L C_p d r}{g e p} \quad \text{where}$$

C_p = pole constant ratio of average to maximum field form

L = Axial length of core

Air gap flux density is given by

$$B_g = B_{gm} \frac{b_p l_p p}{C_p d r \bar{L}} \quad \dots \quad \dots \quad 3.63$$

where $B_{gm} \propto AB$

= Flux in the air gap/magnet X-section

From trigonometrical relations, it can be shown

$$B_{gm} = P \frac{\cos \epsilon \sin r (\tan r - \tan \delta)}{\tan r \sin (r + \epsilon)} \quad \dots \quad \dots \quad 3.64$$

$$\text{Also } \mu_R = \tan \epsilon \quad \dots \quad \dots \quad 3.65$$

Combining the above relations, we get

$$B_{gm} = B_{st} \frac{P_g}{P_0} \frac{P_0 + \mu_R P_m}{P_g + P_1 + \mu_R P_m} \quad \dots \quad \dots \quad 3.66$$

where

B_{st} = flux density of the magnet at the point of stabilization.

For air stabilization, it is given by the point of inter-section of P_0 & demagnetization curve.

The application of the load decrease B_{gm} due to the

demagnetizing force A_d by an amount

$$EC + AH = H_d \left[\frac{\sin r}{\sin(\epsilon+r)} \times \tan \epsilon + \frac{\tan^2 \delta}{\tan \epsilon + \tan^2 \delta} \tan \delta \right] \dots 3.67$$

The angle ϵ is quite small and the above equation is reduced to $EC + AH = H_d (\tan \epsilon + \tan \delta)$... 3.68

Hence

$$B_{gm}' = B_{gm} - \frac{H_d}{P_m} (P_1 + \mu_R P_m) \dots 3.69$$

These equations for B_{gm} and B_{gm}' have been derived on the assumption that the rotor has been stabilized in air. If the m/c is exposed to ideal steady-state short circuit, the lines OP_1 and OP_0 will coincide and B_{gm} and B_{gm}' , then, are given by

$$B_{gm} = \frac{P_g}{P_1} \frac{P_1 + \mu_R P_m}{P_0 + P_1 + \mu_R P_m} \dots 3.70$$

$$\text{and } B_{gm}' = B_{st} \frac{P_g}{P_1} \frac{1}{P_1 + P_g + \mu_R P_m} - \frac{H_d}{P_m} \times (P_1 + \mu_R P_m) \dots 3.71$$

3.6. SHORT CIRCUIT RATIO⁵...

Short circuit ratio in case of permanent magnet generators is defined by

$$SCR = \frac{A_0}{A_d + x_1 A_g} \dots 3.72$$

where

A_0 = exciting total ampere turns at no load

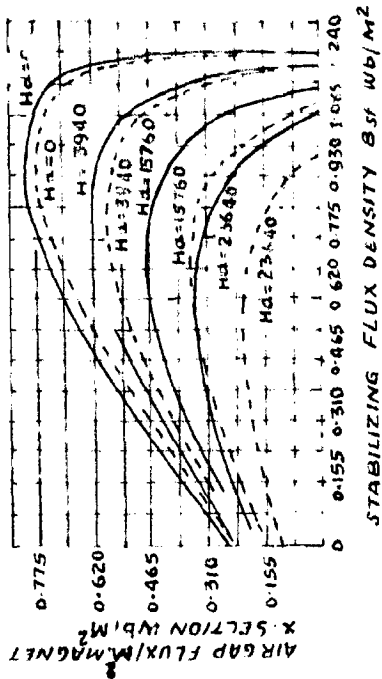
A_g = exciting ampere turns for the air gap only.

$$\frac{A_0}{A_g} = 1+K \text{ where}$$

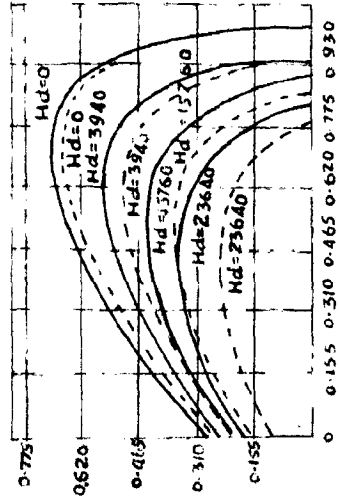
$$K = \frac{H_1 l_1}{H_g g_e'} \text{ where } g_e' = \text{effective air gap length}$$

From figure 3.21

$$A_0 = B_{gm} \frac{P_m}{P_g} h_p$$



AIR GAP FLUX / M² MAGNET



STABILIZING FLUX DENSITY Bst Wb/M²

SECTION 505. 10. 11. 12. 13. 14. 15. 16. 17. 18. 19. 20. 21. 22. 23. 24. 25. 26. 27. 28. 29. 30. 31. 32. 33. 34. 35. 36. 37. 38. 39. 40. 41. 42. 43. 44. 45. 46. 47. 48. 49. 50. 51. 52. 53. 54. 55. 56. 57. 58. 59. 60. 61. 62. 63. 64. 65. 66. 67. 68. 69. 70. 71. 72. 73. 74. 75. 76. 77. 78. 79. 80. 81. 82. 83. 84. 85. 86. 87. 88. 89. 90. 91. 92. 93. 94. 95. 96. 97. 98. 99. 100.

Combining these equations,

$$CR = \frac{B_{gm}}{(H_d)_{rated} P_g / P_m + H_l B_{gm} / l + K} \quad \dots 3.73$$

3.5. ~~BORE~~, AXIAL LENGTH AND AIR GAP...^{5,11,13}

The output of a synchronous machine can be written as ¹³ S .

$$S = 1.1 K_w \bar{B} ac L n^2 D^2 \times 10^{-3} \text{ KVA} \quad \dots 3.74$$

where S = output in KVA

K_w = winding factor

\bar{B} = specific magnetic loading

ac = amp. conductors p.u. length

D = stator bore

L = Core length and n = speed r.p.s.

Equation 3.74 is also applicable to permanent magnet machine.

\bar{B} can be estimated from figures 3.22(A) or 3.22(B) and equation 3.74. Ampere loading ac can be chosen between 5800 and 9750. Ratio bore to axial length is determined more by mechanical than by electrical considerations, such as space requirements of the pole magnets on the circumference and other limitations which are the same as for conventional machines.

Reactance of the armature reaction in the d-axis is lesser than that for synchronous machine with wound field and the air gap is, thus, to be chosen as small as possible. Its minimum size depends mainly on the possibility of formation of an unsymmetrical magnetic field. This dissymmetry may be caused by the eccentricity in rotor position or by unequal

magnetization of the magnets. It has been found that a concentric air gap is quite good both electrically and mechanically. Winding distribution and slot skew have to be so designed, of course, as to produce an electromotive force with low harmonic content.

...CHAPTER - 4...

EQUIVALENT MAGNETIC CIRCUIT AND MACHINE REACTANCES4.1 EQUIVALENT MAGNETIC CIRCUIT ON NO LOAD¹⁰

Figure 4.1 shows the demagnetization curve for a permanent magnet material, with the abscissas reversed. F_c and ϕ_r represent the coercive mmf and residual flux respectively. Let the magnet be demagnetised to the point (F_s, ϕ_s) for stabilization. If the magnet is not subjected to a demagnetizing force greater than that of stabilization, the operation will occur on the recoil line originating at (F_s, ϕ_s) and having a slope equal to that of the major loop at ϕ_r . This recoil line also represents the volt-ampere characteristics of the generator. The inter-section of the recoil line with the ϕ -axis determines the short circuit magnetic flux ϕ_0 and that with the F-axis gives the open-circuit potential (F_0) , although operation outside the major loop is impossible.

Figure 4.2(A) shows developed view of the machine where the air gaps are such that the shaded portions of the circuit represent soft-iron parts of negligible reluctance. Fig.4.2(B) shows the magnetic circuit per pole. Neutral planes are represented by a magnetic ground. Figs. 4.2 (D) and 4.2(E) show the equivalent circuit with potential and flux sources respectively. R_0 and P_0 represent respectively the internal reluctance and permeance of the equivalent magnetic sources. R_1 and P_1 are the reluctance and permeance of the pole leakage paths respectively whereas R_g and P_g respectively are the reluctance and permeance of the gap.

When the generator is working under no load conditions,

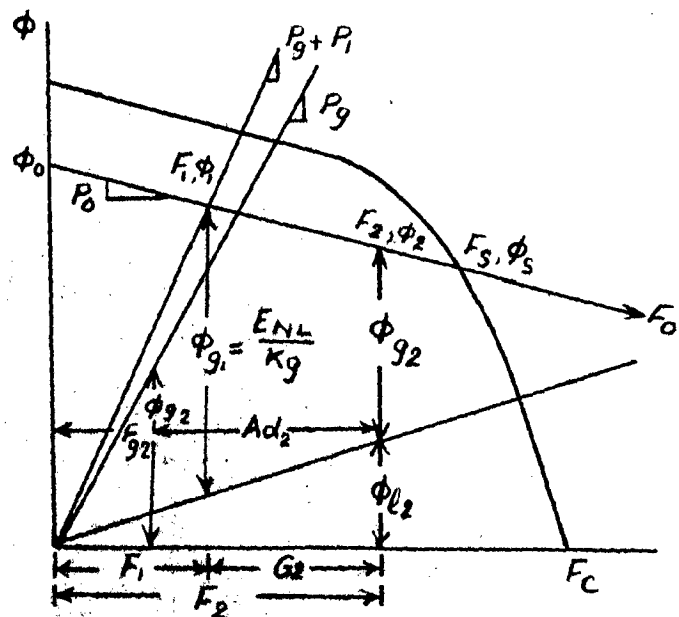
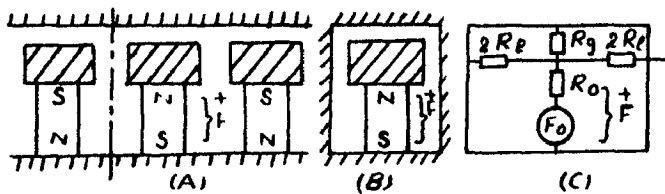
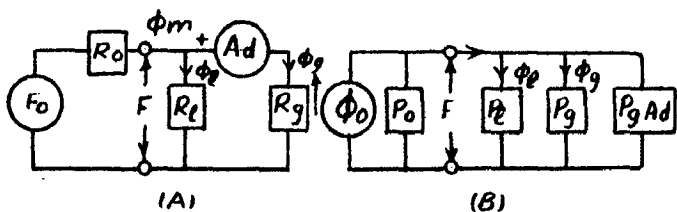
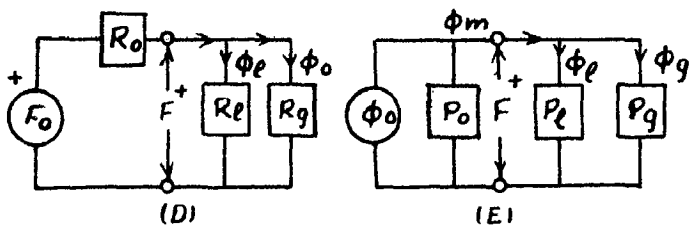


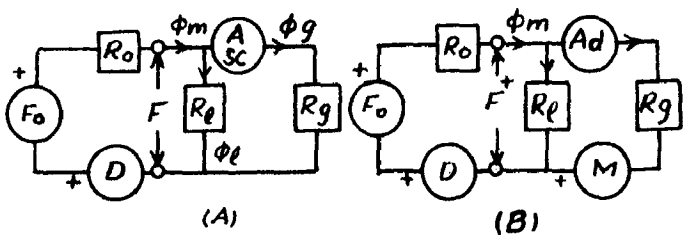
Fig. 4.1
Magnetic characteristics



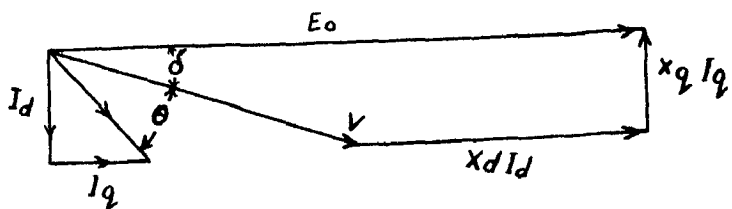
Equivalent circuit for a generator on a per pole basis.



Equivalent circuit for a demagnetizing load.



Equivalent circuit for a generator (a) during normal operation (b) during short-circuit



Phasor diagram for a generator during normal operation.

the operating point is given by (F_1, ϕ_1) , the point of intersection of the $P_g + P_l$ line and the recoil line. The generated voltage at no load is

$$E_{NL} = K_g \phi_g = K_g \frac{P_g}{P_T} \phi_0 = K_g \frac{R_1}{\Delta} F_0 \quad \dots \quad \dots \quad .. 4.1$$

where K_g = generated e.m.f. p.u. air gap flux.

$$P_T = P_0 + P_1 + P_g \quad \text{and} \quad \Delta = R_0 R_1 + R_1 R_g + R_g R_0 \quad \dots \quad \dots \quad .. 4.1(a)$$

4.2. EQUIVALENT MAGNETIC CIRCUIT ON DEMAGNETIZING LOAD¹⁰.

A lagging load produces a demagnetizing effect and can be introduced in the equivalent circuit as shown in Fig.4.3(A) and 4.3(B). The demagnetizing m.m.f. is given by

$$A_d = K_d I_d \quad \dots \quad \dots \quad .. 4.2$$

where K_d = demagnetizing armature m.m.f. p.u. d-axis current
and I_d = d-axis component of armature current I.

Alternatively the same no load equivalent magnetic circuit (Fig.4.2) can be used with a new value of gap permeance P_g' which is a function of d-axis current, and is related to P_g as

$$P_g' = P_g \frac{\phi_0 - (P_0 + P_1)A_d}{\phi_0 + P_g A_d} \quad \dots \quad \dots \quad .. 4.3$$

This relation can be proved as follows:

From fig. 4.2(D)-

$$\phi_g = R_1 F_0 \quad \text{and} \quad \phi_1 \Delta = R_g F_0 \quad \dots \quad \dots \quad .. 4.3(a)$$

From fig.4.3(a)

$$\phi_g \Delta = R_g F_0 - (R_0 + R_1)A_d$$

and $\phi_1 \Delta = R_g F_0 + R_0 A_d \quad \dots \quad \dots \quad .. 4.3(b)$

$$\text{Also } \phi_m = \phi_g + \phi_1 \quad \dots \quad \dots 4.3(c)$$

Let R_g' be such that, replacing R_g in Fig. 4.2, equation 4.3(a) and 4.3(b) yield the same fluxes. Substituting R_g' for R_g in the expression for ϕ_1 from equation 4.3(a) and equating this ϕ_1 to that given by 4.3(b), we get

$$R_g' [R_1 F_0 - (R_0 + R_1) A_d] = R_1 (R_g F_0 + R_0 A_d)$$

$$\text{and } P_g' = P_g \frac{\phi_0 - (P_0 + P_1) A_d}{\phi_0 + P_g A_d} \quad \dots 4.3$$

When the generator is supplying a demagnetizing load, it will be working at the point (F_2, ϕ_2) $\phi_{g2} (= \phi_2 - \phi_{12})$ is the gap flux that requires an m.m.f. drop across gap, $F_{g2} = R_g \phi_{g2}$. The demagnetizing m.m.f. causing operating at (F_2, ϕ_2) in accordance with fig. 4.3(A) is given by $F_2 - F_{g2}$. The point F_2 can be located by adding $G = \frac{P_g}{P_T} A_d$ to F_1 ... 4.4

4.3. EQUIVALENT MAGNETIC CIRCUITS FOR TRANSIENT AND SUBTRANSIENT CONDITIONS...

Fig. 4.4 shows the equivalent magnetic circuits for transient and subtransient conditions. D represents the m.m.f. of the damper winding around the magnet and M represents the d-axis m.m.f. of the pole face winding.

4.4. RELATION BETWEEN TERMINAL VOLTAGE AND DRIVING VOLTAGE¹⁰...

When operating at the point (F_2, ϕ_2) , figure 4.1, the driving voltage or the excitation voltage E_0 is given by the ordinate to the P_g line at F_2 .

$$E_0 = K_g P_g F_2 = K_g P_g \left(F_1 + \frac{P_g}{P_T} A_d \right)$$

$$= E_{NL} + K_g \frac{P_g^2}{P_T} A_d \quad \dots \quad \dots 4.5$$

Thus it is seen that in case of permanent magnet generator supplying an inductive load, there is an increase in excitation voltage over that of the no load voltage by

$$K_g \frac{P_T^2}{P_T} A_d$$

Figure 4.5 shows that Blandel's two-reaction vector diagram of the permanent magnet generator with resistance neglected. V is the terminal voltage and I the load current lagging V by an angle θ . I_d , X_d and I_q , X_q are the d-axis and q-axis quantities as in wound field synchronous generator. It is readily seen from the Vector diagram that

$$\sin \delta = \frac{\cos \theta}{\sqrt{1 + 2 \frac{Z}{X_q} \sin \theta + \frac{Z^2}{X_q^2}}} \quad \dots \quad \dots 4.6$$

$$\text{and } \cos \delta = \frac{\frac{Z}{X_q} + \sin \theta}{\sqrt{1 + 2 \frac{Z}{X_q} \sin \theta + \frac{Z^2}{X_q^2}}} \quad \dots \quad \dots 4.7$$

where Z = load impedance

The terminal voltage is given by

$$V = E_o \frac{Z / \sqrt{Z^2 + 2X_q Z \sin \theta + X_q^2}}{Z^2 + Z(X_d + X_q) \sin \theta + X_d X_q} \quad \dots 4.8$$

Using equation 4.5 and noting that

$$A_d = K_d I_d = K_d I \sin(\theta + \delta) = K_d \frac{V}{Z} \sin(\theta + \delta)$$

$$V = \frac{Z P_T E_{NL} / \sqrt{Z^2 + 2X_q Z \sin \theta + X_q^2}}{Z^2 + Z(X_d + X_q) \sin \theta + X_d X_q P_T - K_g K_d X_q P_T^2 \left(1 + \frac{Z}{X_q} \sin \theta\right)} \quad \dots 4.9$$

4.5. D-AXIS REACTANCE OF ARMATURE REACTION^{10,5,14}

Let subscript s_c stand for short circuit. ... 4.10

$$I_{sc} = \frac{(E_g)_{sc}}{X_d} = \frac{K_g (\phi_g)_{sc}}{X_d} \quad \dots 4.10$$

From equation 4.3(b)

$$(\phi_g)_{sc} = \frac{R_1 F_o - (R_o + R_1) A_{sc}}{\Delta} \dots \dots 4.11$$

Also $A_{sc} = K_d I_{sc}$.. \dots .. 4.12

Solving equations 4.10, 4.11 and 4.12

$$I_{sc} = \frac{K_g R_1 F_o}{X_1 \Delta + K_g K_d (R_o + R_1)} \dots \dots 4.13$$

Also, in the voltage equation 4.9, substituting ZI for V and then setting $Z = 0$

$$I_{sc} = \frac{E_{NL}}{X_d - K_g K_d \frac{P_g'^2}{P_T}} \dots \dots 4.14$$

Combining equation 4.13 and 4.14

$$X_d = X_1 + K_g K_d P_g \dots \dots 4.15$$

from which

$$\begin{aligned} X_{ad} &= D - \text{Axis reactance of Armature reaction} \\ &= K_g K_d P_g \dots \dots 4.16 \end{aligned}$$

X_{ad} can also be calculated as in conventional way i.e.

$$X_{ad} = X C_m C_1 \lambda_a \dots \dots 4.17$$

where X = reactance factor

C_m = ratio of field to armature ampere turns for the same fundamental flux.

C_1 = ratio of the maximum fundamental to the actual maximum value of the fundamental.

λ_a = Specific permeance of the direct axis.

X_{ad} , in case of electromagnet machines, is determined by the gap permeance but for machines with permanent magnet, the combined permeance of the air gap, the magnet and the pole leakage is to be considered. In that case,

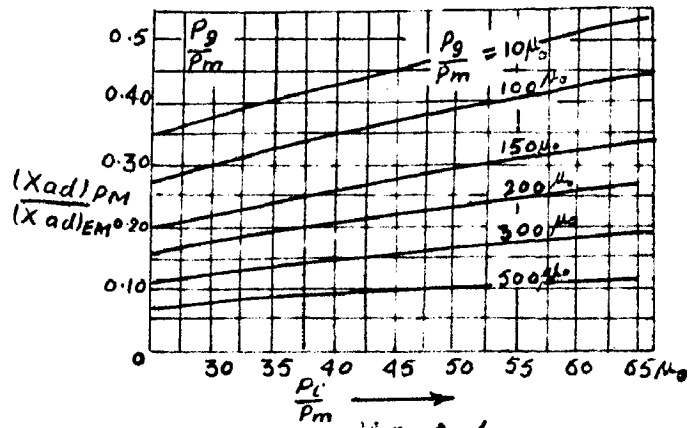


FIG. A-6

Ratio of the reactances of the d-axis armature reaction in synchronous machine with 2-pole and wound rotor.

$$\frac{(x_{ad})_{PM}}{(x_{ad})_{EM}} = \frac{P_1 + \mu_R P_m}{P_g + P_1 + \mu_R P_m} \quad \dots \quad \dots \quad 4.18$$

Variations of this ratio are plotted in figure 4.6

It is seen that d-axis reactance in generators with permanent magnet field is smaller than that in electromagnet machines.

4.6 Q-AXIS REACTANCE^{5,15}

The reactance of armature reaction in q-axis can be calculated on the same basis as that in case of conventional synchronous machine. In most of the designs it is found that X_d is smaller than X_q . X_d is low because the permanent magnet has a very low recoil permeability (the range of values of relative permeability for modern materials is 2.5 to 3.5), and because the steel sleeve is normally completely saturated, and its incremental permeability approaches unity.

4.7. D-AXIS TRANSIENT REACTANCE¹⁰

The following assumptions are made:

1. The machine is subjected to a sudden 3-phase short circuit at no load and, is such that only rotor circuits are loops around the magnet.

2. In accordance with constant flux linkage theorem, the magnet flux can not change immediately.

3. d.c. transient is neglected.

D is the m.m.f. of the winding around the magnet by which the magnet flux ϕ'_m is sustained.

From equation 4.3

$$\phi_m = \frac{(R_1 + R_g) F_0}{\Delta}$$

and from figure 4.4

$$\phi_m = \frac{(R_1 + R_g)(F_0 + D) - R_1 A_{sc}'}{\Delta} \dots \dots 4.19$$

$$\phi_g' = \frac{R_g(F_0 + D) - (R_0 + R_g) A_{sc}'}{\Delta} \dots \dots 4.20$$

$$= \frac{E_g'}{K_g} = \frac{X_1 I_{sc}'}{K_g} \dots \dots 4.21$$

where

$$A_{sc}' = K_d I_{sc}'$$

From these relations, as proved in the last section

$$X_d' = X_1 + K_g X_d \left[\frac{R_0 R_g}{R_g} + \frac{1}{R_1 + R_g} \right] \dots \dots 4.22$$

$$= X_1 + X_{ad}'$$

where

$$X_{ad}' = K_g K_d \left[\frac{R_0 R_1}{R_g} + \frac{1}{R_1 + R_g} \right] \dots \dots 4.23$$

4.8. D-AXIS SUBTRANSIENT REACTANCE¹⁰.

The machine is assumed to have a pole face winding and the airgap flux ϕ_g is prevented from changing immediately by the m.m.f. M of the amortisseur winding.

E_g'' is then equal to E_{NL}

$$I_{sc}'' = \frac{E_{NL}}{X_1} = \frac{K_g F_0}{X_1} \times \frac{R_1}{\Delta} = \frac{E_0''}{X_d''} \dots \dots 4.24$$

$$= \frac{E_{NL} + K_g K_d \left(\frac{R_g^2}{R_1} \right) I_{sc}''}{X_d''}$$

from which

$$X_d'' = X_1 + K_g K_d \frac{R_0 R_1}{R_g \Delta}$$

$$\text{and } X_{ad}'' = K_g K_d \frac{R_0 R_1}{R_g \Delta} \dots \dots 4.25$$

Comparing equation 4.23 and 4.25, it is seen that

$$X_{ad}' = X_{ad}'' + \frac{K_g K_d}{R_1 + R_g} \dots \dots 4.26$$

4.9. LEAKAGE REACTANCE^{11,18}

The armature leakage flux is divided into four parts

1. Slot leakage flux
2. The end connection leakage flux
3. The Zig-zag leakage flux
4. The belt leakage flux.

The largest portion of leakage reactance is slot and zig-zag reactance and can be expressed as follows¹¹

$$X_1 = X_s + X_z = 24 \frac{\pi}{n_s} \frac{\mu_0 f L N^2}{n_s} \left[K_s \left(\frac{d_1}{3w_s} + \frac{d_2}{w_s} \right) + \frac{0.266 DK_w^2}{n_s g} \right]$$

where N = no. of series armature turns per phase

n_s = no. of armature slots

K_s = slot leakage factor

K_w = winding factor

D = Dia of rotor

w_s = slot opening

d₁ = slot depth and d₂ = wedge depth.

4.10. SHIELDING THE MAGNET FROM TRANSIENT DEMAGNETIZING EFFECTS¹⁷.

Under short circuit, the armature m.m.f. is quite large, which has to be balanced by an equal and opposite m.m.f. by the poles if no Cage winding is present in the poles. Consequently, a serious demagnetization of the magnets occurs. A heavy Cage winding in the poles establishes a Counter m.m.f. to oppose the transient armature m.m.f. and if this Cage winding is

sufficiently large and well coupled, the net demagnetizing m.m.f. to which the poles will be subjected may be well below the stabilizing m.m.f. and no net reduction of pole strength will be there. This objective can be achieved by -

- (1) Casting the rotor in aluminium
- or (2) using a copper plated pole.

Casting the rotor in aluminium places an infinite bar Gage winding on the rotor. Too much of aluminium thickness over the pole shoe will increase the effective air gap and too ^{thin} ~~thick~~ will be mechanically weak. Copper plating the pole is superior to the former and involves plating all the surfaces of pole except the one in contact with the spider. In this method copper can be made thinner over the pole face thus retaining the optimum air gap.

4.11 DECREASING THE NEGATIVE SEQUENCE¹⁷

A large negative sequence reactance adversely affects the regulation of single phase machines, as under 1-phase conditions the negative sequence reactance is ⁱⁿ ~~the~~ series with the positive sequence reactance. It has been found that the methods adopted to shield the magnets from transient demagnetizing effects, also reduce the negative sequence reactance. For a 3-phase machine, a series capacitor may be added which will resonate both the positive and negative sequence reactances thus making the single phase regulation quite small even though the machine reactances may be large.

...CHAPTER 5...

VOLTAGE REGULATION AND CONTROL5.1. INHERENT REGULATION^{10,4}

In figure 4.2(A) the m.m.f. F at the magnet terminals represents the excitation of the generator. For synchronous machines with wound fields, F gives the effective ampere-turns of the field winding and is constant for a given field current. Such a machine therefore has a large inherent regulation and the voltage has to be kept within specified limits by a voltage Regulator. When a permanent magnet generator is loaded with a demagnetizing load, fig.4.1, the operating point moves downward on the recoil line and the magnet terminal mmf F increases i.e. there is an increase in excitation as a demagnetizing load is put on the p.m. generator. The permanent-magnet generator, thus, behaves as though it had a "built-in-voltage regulator". The variable-excitation characteristic of a permanent magnet generator has three features.

1. Small inherent voltage regulation.
2. Rapid Voltage recovery during sudden load changes
3. High Current capability for starting induction motors.

The inherent voltage regulation of the permanent magnet generator varies from fairly close regulation for unity power factors to poor regulation for highly lagging power-factor loads. Leading power factor loads increase the voltage and, thus, quite a close regulation can be obtained if the demagnetizing load is power-factor corrected by adding a parallel capacitor. Figure 5.1 shows the regulation curves.

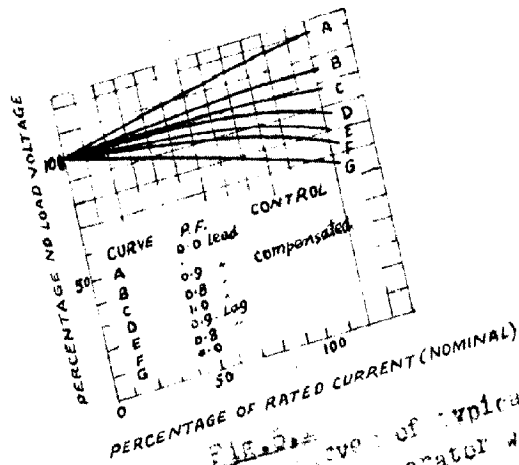


FIG. 2
Voltage load curves of typical
magnet magnet generator with
various power factor loads.

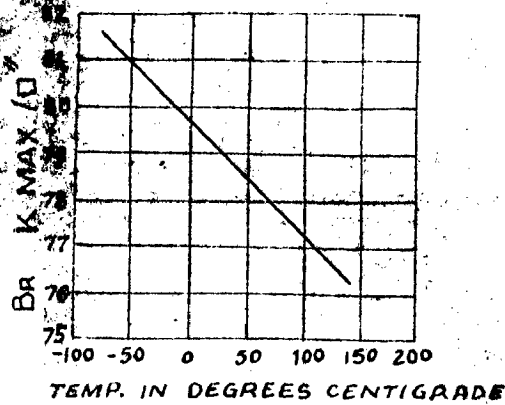


Fig. 5.2

Variations with temperature in residual inductance of slice V.

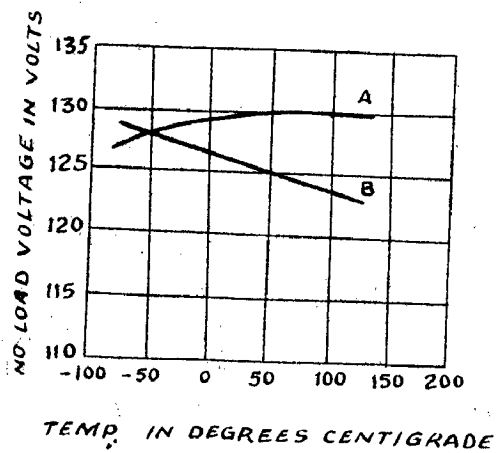


Fig. 5.3

Magnetic temperature compensation
No load voltage over temperature
range of -

A-over compensated rotor

B-Non compensated rotor

5.2. EXTERNAL VOLTAGE CONTROL^{16,4}

If the inherent voltage regulation is not sufficient enough to be within close limits, external controls are necessary. External control may be obtained by using any of the following:

1. a series capacitor device, called a compensator
2. temperature compensation
3. toroidal back winding.

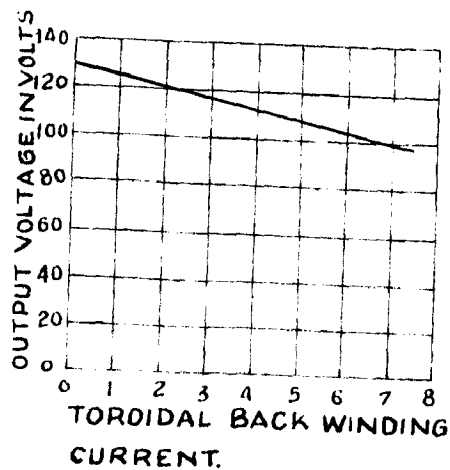
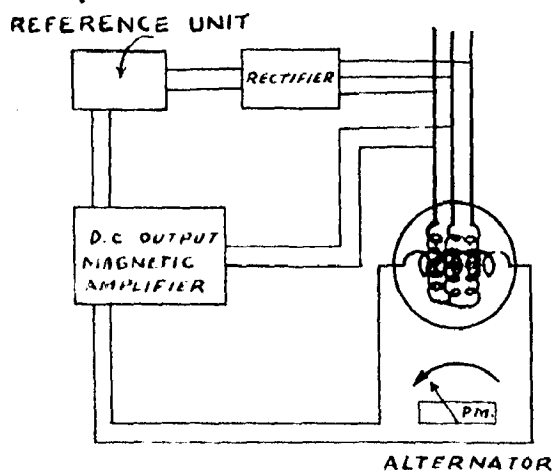
COMPENSATOR⁴

It consists of a series transformer in each phase lead with a capacitor connected across each secondary. "By inter-connection between the capacitor circuit and the phase windings, a bucking or boosting action may be obtained in addition to the usual voltage stability at low power factors". This compensator is suitable for a low voltage generator.

TEMPERATURE COMPENSATION¹⁶

Figure 5.2 shows the variations in residual flux densities with temperature for alnico V permanent magnet. It is obvious that the output voltage of a permanent magnet alternator using alnico V magnets increases as the temperature decreases. Thus, if the inherent voltage regulation of a permanent magnet generator is to be kept within close limits, the generator must be temperature compensated.

A temperature sensitive ("thermomagnetic") alloy is used for a portion of the stainless-steel (non-magnetic) plates used in the rotor-cage structure. This alloy shunts a given amount of the usable generating flux. The foregoing temperature



The graph shows the relationship between the output voltage and the toroidal back winding current. The output voltage decreases linearly as the current increases. This is a characteristic of a magnetic amplifier where the output voltage is controlled by the current in the control winding.

effects can be fully compensated by choosing a suitable thermo-magnetic shunt and the generator can, thus, be made to deliver voltages independent of temperature. In practice it is preferable to over compensate the generator. Figure 5.3 shows the voltage-temperature characteristics for a p.m. generator with and without compensation for the temperature.

TOROIDAL BACK WINDING^{16,4}

This control winding consists of a series helical winding in the bottom of the slots around the armature core and over the back of the toroidal winding. If the winding is uniform around the entire circumference, no appreciable alternating voltage will appear at the terminals of the winding. A typical automatic static control system is shown in figure 5.4. Direct Current is given to this winding, which superposes an unidirectional flux on the alternating flux in the stator core. This increases the reluctance of core and decreases the generated voltage as the control current is increased. The change in generated voltage is practically linear with the control current. This fact can be seen from figure 5.4. Under no load conditions, maximum control excitation is required. The use of the control winding, results in no increase of the armature heating, and, thus, no decrease of efficiency, when working under full load conditions. The air gap flux density with control winding can be obtained as follows:

For an air stabilized machine, it has been shown that the air gap flux density reduced to magnet area (*chapter 3*)

$$B_{gm} = B_{st} \frac{P_g}{P_o} \frac{P_o + \mu R P_m}{P_g + P_1 + \mu R P_m} \quad \text{---} \quad \text{---} \quad \text{---} \quad \text{---} \quad 3.66$$

where the air gap permeance = $\mu_0 \frac{NLI}{2} \frac{C_p dr}{g_e p}$

The value of g_e includes the effects of the air gap and the equivalent path of all soft iron components of the magnetic circuit.

$$\text{Let } \tau = \frac{P_g}{P_b} \quad \dots \quad \dots 5.1$$

where P_b = permeance of the stator core

$$= \frac{2 \mu_0}{\pi} \mu_e \frac{h \sigma L p}{D-h} \quad \dots 5.2$$

where μ_e = effective relative permeability of the stator core.

h = width of stator core

L = axial length of stator iron

D = stator outside diameter

σ = stacking factor of stator laminations

$$\text{Thus } \tau = 2.45 \frac{C_p d_r (D-h)}{\mu_e g_e h \sigma p^2} \quad \dots 5.3$$

In equation 3.66 replace P_{ge} by the equivalent air gap permeance

$$P_{ge} = P_g \frac{1}{1+\tau} \quad \dots 5.4$$

The air gap flux density at no load is then given by.

$$B_{gm} = B_{at} \frac{P_g}{P_0} \frac{P_0 + \mu_{R1} P_m}{P_g + (1+\tau)(P_1 + \mu_{R1} P_m)} \quad 5.5$$

Similar calculations can be made for short circuit stabilization.

An explanation for μ_0 is given as under:

When the rotor flux enters the core, ^{it} the subdivides itself into two opposite directions. The control winding superposes an unidirectional field. This means that the total flux must be either the sum or the difference of the two, as the core may be. Magnetic characteristics of the soft iron are non-linear and, thus, one half-wave of the resultant flux is peaked and the other half wave is flat topped. Moreover, the rotating air gap field is far from sinusoidal. μ_0 should thus be determined from tests on a typical machine and can be used with other machines of the same material and identical configuration.

...CHAPTER-6...

PERFORMANCE OF THE P.M. GENERATOR.6.1. PERMANENT MAGNET OPERATION...

Fig. 6.1 represents the demagnetization Curve of the magnet. D is the point at which the magnet has been stabilized and DE represents the recoil line. The magnet flux ϕ can be divided into leakage flux ϕ_e and useful gap flux ϕ_g . Neglecting the leakage, except the one that occurs across the terminals, the leakage path is in parallel with the useful path. The conditions can be represented as in figure 6.2. Let i^{dr} and i^{kd} be the instantaneous currents in the armature and damper slug in the direct axis. Working under no load conditions,

$$i^{dr} = i^{kd} = 0 \quad \dots \quad \dots 6.1$$

and from figure 6.2 it can be seen that

$$H_2 + H_g l_g = 0 \quad \dots 6.2$$

$$H_1 + H_{l1} l_1 = 0 \quad \dots 6.3$$

$$\text{Also } \phi = BA = \phi_g + \phi_l$$

$$= H_g l_g P_g + H_{l1} l_1 P_l$$

$$= -H_l (P_g + P_l)$$

$$\therefore B = -\frac{1}{A} (P_g + P_l) H \quad \dots 6.4$$

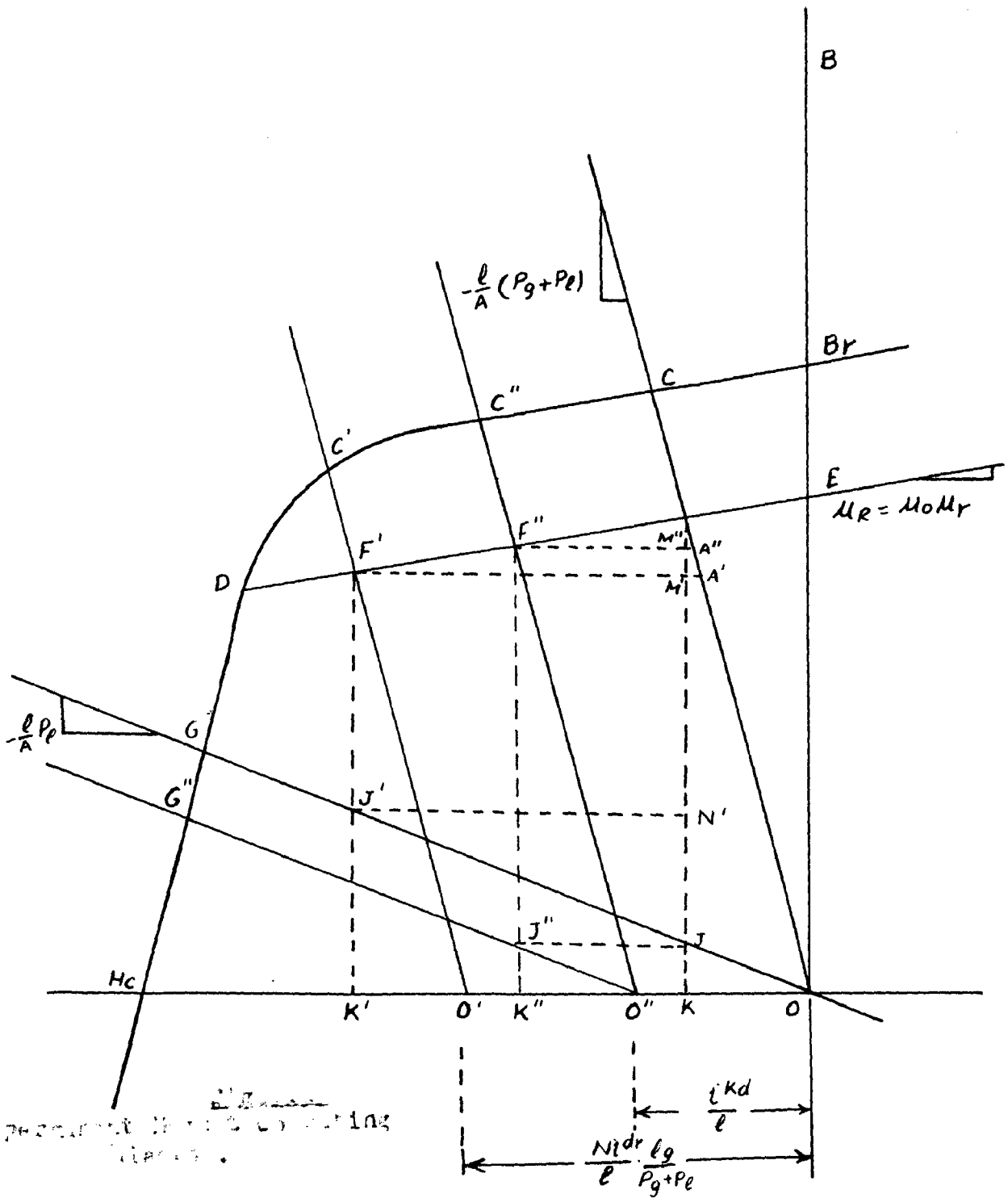
$$\text{and } B_l = \frac{\phi_l}{A} = H_l \frac{l_l}{A} P_l = -\frac{1}{A} P_l H \quad \dots 6.5$$

Equation 6.4 gives the straight line OC, so that its inter-section with the recoil line DE at F gives the no load operating point.

Equation 6.5 represents the leakage line OG.

When the d-axis current i^{dr} is flowing, from figure 6.2,

$$H_l + H_g l_g = -N i^{dr} \quad \dots 6.6$$



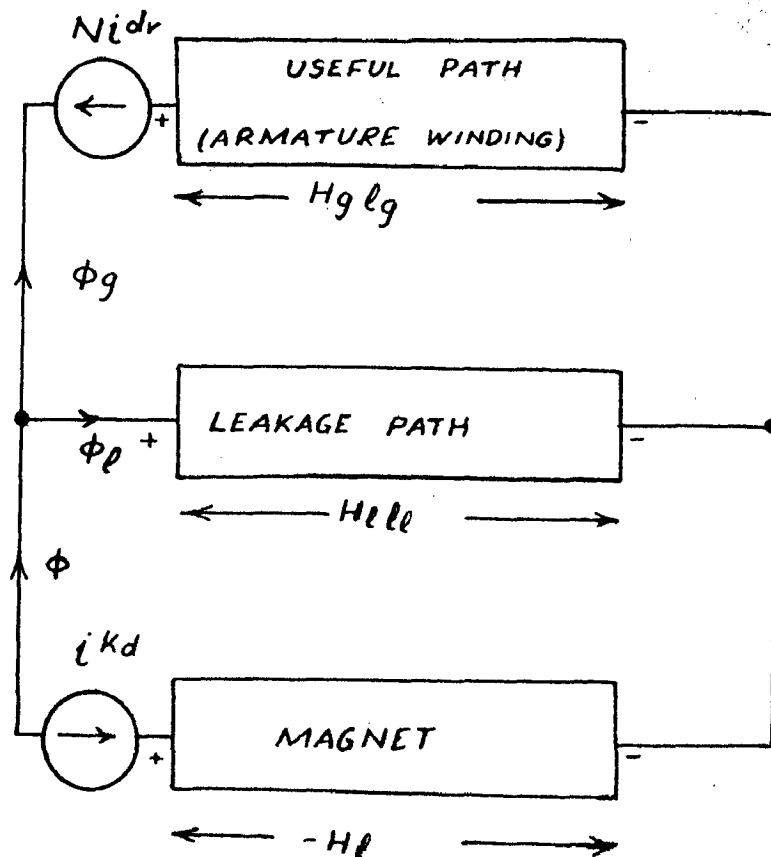


Fig. 2.2
 shows the circuit of the p.m. generator, showing a.e.f.'s magnetic potential drops, and fluxes.

$$H_1 + H_1 l_1 = 0 \quad \dots \quad \dots \quad 6.6(a)$$

So that $\phi = \phi_g + \phi_1$

$$= - (N_1 i^{dr} + H_1) P_g + H_1 P_1$$

$$B = - \frac{1}{A} (P_g + P_1) \left(H + \frac{N_1 i^{dr}}{l} \cdot \frac{P_g}{(P_g + P_1)} \right) \quad \dots \quad 6.7$$

$$\text{and } \frac{\phi_1}{A} = - \frac{1}{A} P_1 H$$

Comparing equations 6.4 and 6.7, it can be seen that the effect of flow of current i^{dr} is to shift the load line OC to a new position O'C' such that $OO' = N_1 i^{dr} \frac{P_g}{l(P_g + P_1)}$ and O'C' is parallel to OC. The working point is now given by F' and the leakage line remains unchanged. The reduction in the useful flux density is given by Fig.6.1.

$$\begin{aligned} \Delta B'_0 &= FJ - F'J' \\ &= FM + JN' \\ &= \mu_R F'M + F'M \frac{1}{A} P_1 \\ &= \frac{F'M}{F'A} \cdot O'O \left(\mu_R + \frac{1}{A} P_1 \right) \\ &= K \frac{N_1 i^{dr}}{l} \frac{P_g}{P_g + P_1} \left(\mu_0 \mu_R + \frac{1}{A} P_1 \right) \quad \dots \quad 6.8 \end{aligned}$$

$$\text{where } K = \frac{F'M}{F'A} \text{ and } \mu_R = \mu_0 \mu_r$$

Now consider that the damper current i^{kd} is flowing from Fig.6.2

$$H_1 + H_g l_g = - i^{kd}$$

$$H_1 l_1 + H_1 l_1 = - i^{kd}$$

$$\text{So that } B = - \frac{1}{A} (P_g + P_1) \left(H + \frac{i^{kd}}{l} \right) \quad \dots \quad \dots \quad 6.9$$

$$\text{and } \frac{\phi_1}{A} = - \frac{1}{A} P_1 \left(H + \frac{i^{kd}}{l} \right) \quad \dots \quad \dots \quad 6.10$$

Equations 6.9 and 6.10 are represented by the lines O''C'

and $O'G''$. It can be seen that both lines are shifted to the left by an amount $\frac{1 \text{ kd}}{1}$

The reduction in flux density in this case, figure 6.1, is given by

$$\begin{aligned} \Delta B''_O &= (FK - JK) - (F''K'' - J''K'') \\ &= FM'' - JN'' \\ &= A''M'' \frac{1}{A} (P_g + P_1) - A''M'' \frac{1}{A} P_1 \\ &= A''M'' \frac{1}{A} P_g \quad \dots \quad \dots \quad 6.11 \end{aligned}$$

Let $K = \frac{F''M''}{F''A''}$

$$\begin{aligned} FM &= F''A''K \frac{\mu_0}{\mu_r} = A''M'' \frac{1}{A} (P_g + P_1) \\ \therefore A''M'' \frac{1}{A} &= F''A'' \frac{K \mu_0 / \mu_r}{P_g + P_1} \quad \dots \quad 6.12 \end{aligned}$$

From 6.11 and 6.12

$$\Delta B''_O = K \frac{1 \text{ kd}}{1} \frac{\mu_0 / \mu_r P_g}{P_g + P_1} \quad \dots \quad 6.13$$

6.2. FLUX LINKAGE AND VOLTAGE EQUATIONS...

Let the flux density under no load conditions be $B_0 = FJ$. On load i^{dr} and i^{kd} are flowing and useful flux density in the magnet is

$$B_g = B_0 - \frac{KNP_g}{1(P_g + P_1)} (\mu_0 / \mu_r + \frac{1}{A} P_g) i^{dr} - \frac{K \mu_0 / \mu_r P_g i^{kd}}{1(P_g + P_1)} \quad \dots \quad 6.14$$

Flux linkages with the d-axis coil are given by

$$\begin{aligned} \Psi_{dr} &= -B_g AN + (\text{armature leakage flux-linkages}) \\ &= -B_0 AN + \frac{KAN^2 P_g}{1(P_g + P_1)} (\mu_0 / \mu_r + \frac{1}{A} P_1) i^{dr} + \frac{KAN \mu_0 / \mu_r P_g}{1(P_g + P_1)} i^{kd} \\ &\quad + L_{dr} i^{dr} \quad \dots \quad 6.15 \end{aligned}$$

Where L_{dr1} = leakage inductance in direct axis armature axis
 Equation 6.15 can be written as

$$\psi_{dr} = - B_0 AN + M_d i^{kd} + L_{dr} i^{dr} \quad \dots \quad \dots \quad 6.16$$

where M_d = Mutual inductance in the d-axis = $\frac{KAN \mu_0 \mu_r P_g}{l (P_g + P_l)}$

and L_{dr} = total self inductance in the direct axis armature axis
 $= \mu_0 \mu_r + \frac{l}{a} P_l + L_{dr1}$

Proceeding the same way, it can be seen that the flux-linkages with the damper coil are

$$\begin{aligned} \psi_{kd} &= - BA = - B_1 A + \frac{KAN \mu_0 \mu_r P_y i^{dr}}{l(l_g + P_l)} + \frac{KA \mu_0 \mu_r i^{kd}}{l} \\ &= - B_1 A + M_d i^{dr} + L_{kd} i^{kd} \quad \dots \quad 6.17 \end{aligned}$$

where B_1 = no load magnet flux density = FK

L_{kd} = Self inductance of the damper in the d-axis

Let L_{qr} = Self inductance of the q-axis armature coil, the flux linkages equations can be written as

$$\psi_{kd} = - B_1 A + L_{kd} i^{kd} + M_d i^{dr} \quad \dots \quad 6.17$$

$$\psi_{dr} = - B_0 AN + M_d i^{kd} + L_{dr} i^{dr} \quad \dots \quad 6.16 \quad \Big| \quad 6.18$$

$$\psi_{qr} = L_{qr} i^{qr} \quad \Big| \quad \Big| \quad \Big|$$

Assuming sinusoidal flux distribution, the voltage equations can be written as

$$\begin{aligned} V_{kd} &= (r_{kd} + L_{kd} p) i^{kd} + M_d p i^{dr} = 0 \\ V_{dr} &= M_d p i^{kd} + (r_r + L_{dr} p) i^{dr} + L_{qr} p i^{qr} \\ V_{qr} &= B_0 AN p \theta - M_d p \theta i^{kd} - L_{dr} p \theta i^{dr} + (r_r + L_{qr}) i^{qr} \quad \Big| \quad 6.19 \end{aligned}$$

where p = differential operator $\frac{d}{dt}$

$p\theta$ = electrical rotor speed, radians/sec.

Voltage equations for a synchronous generator with wound field can be written as

$$\begin{array}{r}
 d_s \\
 dr \\
 qr \\
 qs
 \end{array}
 \begin{array}{l}
 V_{ds} \\
 V_{dr} \\
 V_{qr} \\
 V_{qs}
 \end{array}
 \begin{array}{l}
 ds \\
 dr \\
 qr \\
 qs
 \end{array}
 \begin{array}{cccc}
 r_{ds} + L_{dsp} & M_{dp} & L_{dp} p \\
 M_{dp} & r_r + L_{drp} & L_{qr} p \\
 -M_{dp} & -L_{drp} & r_r + L_{qrp} \\
 M_{qp} & M_{qp} & r_{qs} + L_{qsp}
 \end{array}
 \begin{array}{l}
 i_{ds} \\
 i_{dr} \\
 i_{qr} \\
 i_{qs}
 \end{array}
 \quad \dots 6.20$$

The various axes are defined in the Nomenclature.

Comparison of equations 6.19 and 6.20 shows that equations of the two machines are similar except that V_{ds} , the voltage applied to the damper K_d , is zero and in V_{qr} there is an additional term E , which is the open circuit generated e.m.f. E . It can be inferred that the permanent magnet field system is equivalent to a conventional field coil ds , having a resistance r_{kd} and inductance L_{kd} , to which a battery with zero internal impedance is connected, that circulates a constant current i^f which generates E , given by

$$E = M_{dp} \theta i^f \quad \dots \quad \dots 6.21$$

Let the battery e.m.f. be V_g , given by $r_{kd} i^f$, and i_{ds} , the instantaneous current in the fictitious field coil

$$i_{ds} = \frac{V_g}{r_{kd}} = i^f \quad \text{and} \quad p i_{ds} = p i^f$$

Add $-V_f = -i^f r_{kd}$ to both sides of first equation in 6.19, the equations can be rewritten as

$$\begin{aligned}
 -V_f &= (r_{kd} + L_{kd} p) i_{ds} + M_{dp} i_{dr} \\
 V_{dr} &= M_{dp} i^f + (r_r + L_{drp}) i_{dr} + L_{qrp} p i_{qr} \\
 V_{qr} &= -M_{dp} i^f - L_{drp} p i_{dr} + (r_r + L_{qrp}) i_{qr}
 \end{aligned}
 \quad \dots 6.22$$

Eddy currents are flowing in the steel sleeve of the rotor, the pole pieces, and the copper damper segments, which can be represented through short-circuited coil de & qe in the two axes. The voltage equations can then be written as

| | | de | ds | dr | qr | qe | | |
|------|----------|--------|----------------------|----------------------|---------------------|--------------------|----------------------|------|
| de | 0 | de | $r_{de} + L_{dep} p$ | M_{kdp} | M_{dep} | de | i_{de} | |
| ds | $-V_f$ | ds | M_{kdp} | $r_{kd} + L_{kdp} p$ | M_{dp} | ds | i_{ds} | |
| dr | V_{dr} | $= dr$ | M_{dep} | M_{dp} | $r_r + L_{drp} p$ | $L_{qrp} p \theta$ | $M_{qp} p \theta$ | dr |
| qr | V_{qr} | qr | $-M_{dep} p \theta$ | $-M_{dp} p \theta$ | $-L_{drp} p \theta$ | $r_r + L_{qrp} p$ | M_{qp} | qr |
| qe | 0 | qe | | | | M_{qp} | $r_{qe} + L_{qep} p$ | qe |

....6.23

Eliminating i_{de} , i_{ds} , and i_{qe} and referring all quantities to the armature,

$$\begin{matrix} d \\ q \end{matrix} \begin{matrix} V_d \\ V_q - E \end{matrix} = \begin{matrix} r + L_d(p) p & L_q(p) p \theta \\ -L_d(p) p \theta & r + L_q(p) p \end{matrix} \begin{matrix} i^d \\ i^q \end{matrix} \quad \dots 6.24$$

where

$$L_d(p) = L_d \frac{p^2(L_{de} M_d^2 - 2M_d M_{ks} M_{de} + L_{kd} M_{de}^2) + p(r_{de} M_d^2 + r_{kd} M_{de}^2)}{p^2(L_{de} L_{kd} - M_{ks}^2) + p(r_{kd} L_{de} + r_{de} L_{kd}) + r_{de} r_{kd}} \quad \dots 6.25$$

and $L_q(p) = L_q - \frac{M_q^2 p}{r_{qe} + L_{qep}}$

Under steady state balanced conditions, $p=0$ and $L_d(p)$ and $L_q(p)$ are respectively equal to synchronous inductances L_d & L_q

6.3. PERFORMANCE EQUATIONS

Under steady state conditions ($p=0$), equations 6.20 yield the following equations:

$$\begin{aligned}
 V_f &= -r_{kd}i^{ds} = r_{kd}i^f \\
 V_{dr} &= r_r i^{dr} + X_{qr} i^{qr} \\
 V_{qr} &= E - X_{dr} i^{dr} + r_r i^{qr}
 \end{aligned}
 \quad \dots 6.26$$

These equations are the same as that would be obtained in case of synchronous generator and help in drawing the two-reaction diagram of the generator.

The applied voltage is equal to the sum of the resistance voltage drops, the voltages induced by changing currents, and the voltages generated by the motion of conductors. Equations 6.20 can be written as

$$e = Ri + Lp i + G i p \theta = Zi \quad \dots \quad \dots 6.27$$

where

Z = transient impedance of the machine

R = diagonal matrix containing the resistances r in Z ,

L = matrix of the coefficients of p

and G = matrix of the co-efficients of $p\theta$

The electrical input power can be expressed as

$$P = e_t i = i_t e = i_t R i + i_t L p i + i_t G i p \theta \quad \dots 6.28$$

$i_t R i = i^2 R$ power loss in the whole machine

$i_t L p i =$ rate of increase of stored magnetic energy

$i_t G i p \theta =$ mechanical power developed at a mechanical speed

$p\theta_m$

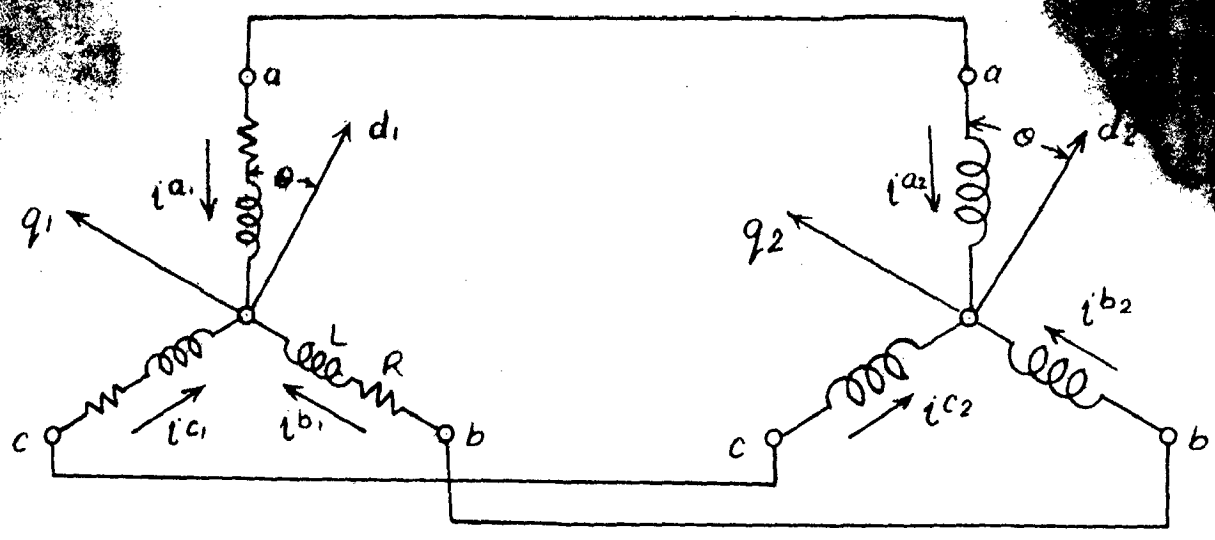
The torque applied to the shaft is given by

$$T_{app} = I_p^2 \theta_m - n i_t G i \quad Nw - \text{meters} \quad \dots 6.29$$

where-

I_p = moment of inertia

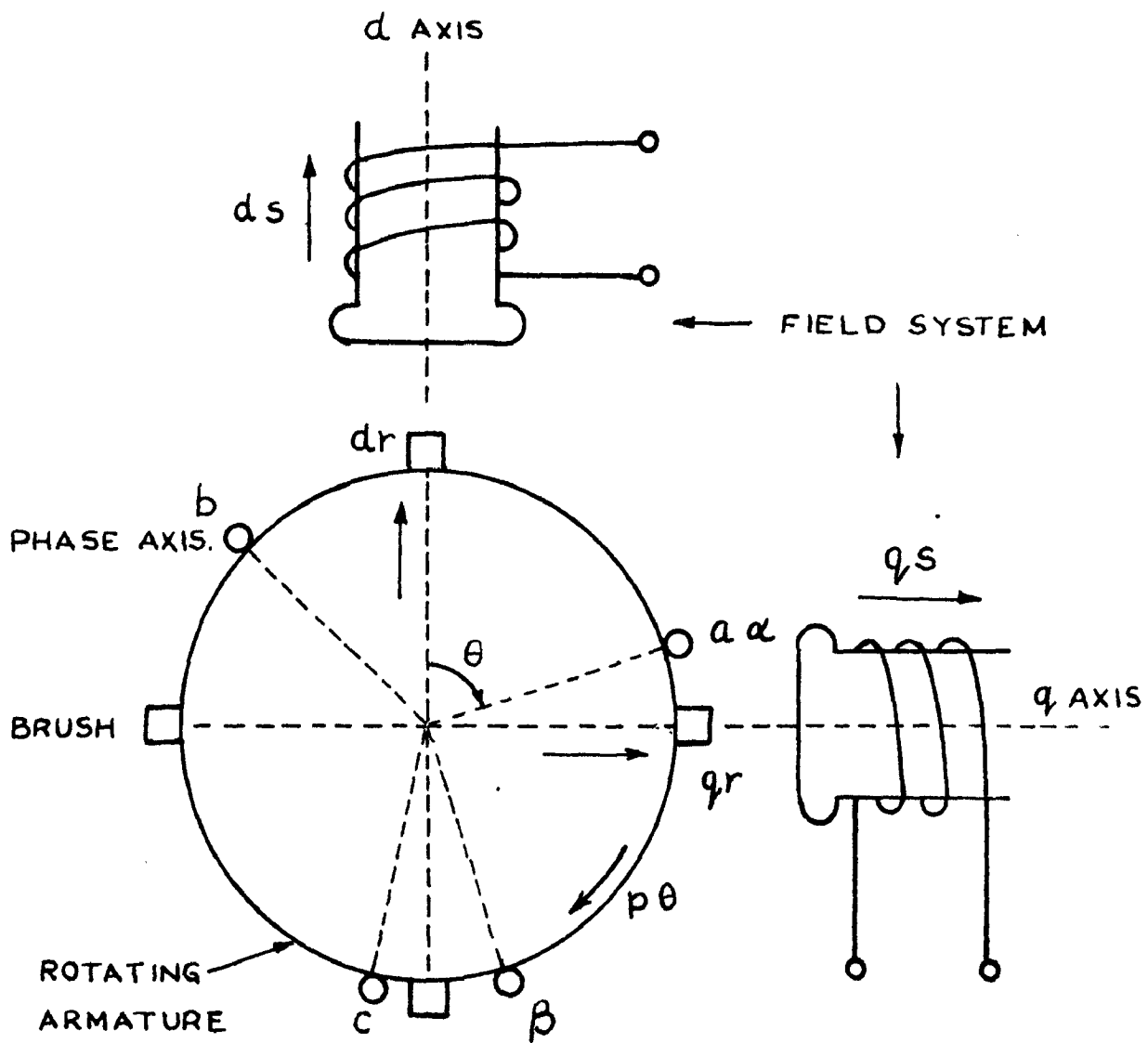
n = no. of pairs of poles



LOAD

ALTERNATOR

FIG. 1.1
Alternator & simple load.



The diagram shows the electrical connections and the relationship between the d and q axes and the phase axis.

Under steady state conditions

$$T_{app} = -n i_t G_1$$

$$T_{app} = -n \begin{bmatrix} ds & dr & qr \\ -i^f & i^{dr} & i^{qr} \end{bmatrix} \begin{bmatrix} ds & dr & qr \\ ds' & & \\ dr' & & L_{qr} \\ qr' & -M_d & -L_{dr} \end{bmatrix} \begin{bmatrix} ds' & -i^f \\ dr' & i^{dr} \\ qr' & i^{qr} \end{bmatrix}$$

$$= -n M_d i^f i^{qr} + n (L_{dr} - L_{qr}) i^{dr} i^{qr}$$

$$= -n \frac{E}{\omega} i^q + n(L_d - L_q) i^d i^q \quad \dots \quad \dots 6.30$$

Mechanical power input to the alternator is

$$P_m = p \theta_m T_{app}$$

$$= \frac{\omega}{n} T_{app}$$

$$= -E i^q + (X_d - X_q) i^d i^q \text{ watts} \quad \dots \quad \dots 6.31$$

6.4. BALANCED 3-PHASE LOAD ON THE P.M. GENERATOR.

The connection diagram is shown in figure 6.3 Indices 1 and 2 denote the load and the generator respectively.

Three phase voltage and currents have to be transferred to the d-q axis, which can be carried out in two steps i.e. first transform to the 2-phase (α, β) and zero sequence and then d-q axis. Let i^a, i^b, i^c be the phase currents (Sequence a-b-c) and i^α, i^β, i^0 , the 2-phase and sequence currents (sequence $\beta - \alpha$), as shown in figure 6.4.

Then

$$\begin{matrix} 2\phi \\ \alpha \\ \beta \\ 0 \end{matrix} \begin{matrix} | \\ | \\ | \\ | \\ | \\ | \\ | \\ | \\ | \\ | \\ | \\ | \end{matrix} = \begin{matrix} 2\phi \\ \alpha \\ \beta \\ 0 \end{matrix} \begin{matrix} | \\ | \\ | \\ | \\ | \\ | \\ | \\ | \\ | \\ | \\ | \\ | \end{matrix} \begin{matrix} a \\ b \\ c \end{matrix} \begin{matrix} | \\ | \\ | \\ | \\ | \\ | \\ | \\ | \\ | \\ | \\ | \\ | \end{matrix} \begin{matrix} 3\phi \\ a \\ b \\ c \end{matrix} \begin{matrix} | \\ | \\ | \\ | \\ | \\ | \\ | \\ | \\ | \\ | \\ | \\ | \end{matrix} \dots 6.32$$

Transformation from 2-phase to d-q axis is given by

$$i^{dq} = c^{dq} i^{2\phi}$$

$$\begin{matrix} dq \\ d \\ q \\ 0 \end{matrix} \begin{matrix} | \\ | \\ | \\ | \\ | \\ | \\ | \\ | \\ | \\ | \\ | \\ | \end{matrix} = \begin{matrix} dq \\ \alpha \\ \beta \\ 0 \end{matrix} \begin{matrix} | \\ | \\ | \\ | \\ | \\ | \\ | \\ | \\ | \\ | \\ | \\ | \end{matrix} \begin{matrix} a \\ b \\ c \end{matrix} \begin{matrix} | \\ | \\ | \\ | \\ | \\ | \\ | \\ | \\ | \\ | \\ | \\ | \end{matrix} \begin{matrix} 2\phi \\ \alpha \\ \beta \\ 0 \end{matrix} \begin{matrix} | \\ | \\ | \\ | \\ | \\ | \\ | \\ | \\ | \\ | \\ | \\ | \end{matrix} \dots 6.33$$

The overall transformation from 3-phase to d-q axes is given by multiplication of the connection matrices of (6.32) and (6.33).

$$i^{dq} = c_{3\phi}^{dq} i^{3\phi}$$

$$\begin{matrix} dq \\ d \\ q \\ 0 \end{matrix} \begin{matrix} | \\ | \\ | \\ | \\ | \\ | \\ | \\ | \\ | \\ | \\ | \\ | \end{matrix} = \begin{matrix} dq \\ \alpha \\ \beta \\ 0 \end{matrix} \begin{matrix} | \\ | \\ | \\ | \\ | \\ | \\ | \\ | \\ | \\ | \\ | \\ | \end{matrix} \begin{matrix} a \\ b \\ c \end{matrix} \begin{matrix} | \\ | \\ | \\ | \\ | \\ | \\ | \\ | \\ | \\ | \\ | \\ | \end{matrix} \begin{matrix} 3\phi \\ a \\ b \\ c \end{matrix} \begin{matrix} | \\ | \\ | \\ | \\ | \\ | \\ | \\ | \\ | \\ | \\ | \\ | \end{matrix} \dots 6.34$$

Transformation from d & q components to 3-phase components is obtained by transposing the connection matrix.

$$i_{3\phi} = C_{dq}^{3\phi} i_{dq}$$

| | | | | | | |
|----------|------|---|---|----------------------|------|-------|
| 3ϕ | | d | q | 0 | dq | |
| $a' i^a$ | a' | $\frac{1}{\sqrt{3}} \cos \theta$ | $\frac{1}{\sqrt{3}} \sin \theta$ | $\frac{1}{\sqrt{3}}$ | d' | i^d |
| $b' i^b$ | b' | $\frac{1}{\sqrt{3}} \cos(\theta - 120^\circ)$ | $\frac{1}{\sqrt{3}} \sin(\theta - 120^\circ)$ | $\frac{1}{\sqrt{3}}$ | q' | i^q |
| $c' i^c$ | c' | $\frac{1}{\sqrt{3}} \cos(\theta + 120^\circ)$ | $\frac{1}{\sqrt{3}} \sin(\theta + 120^\circ)$ | $\frac{1}{\sqrt{3}}$ | o' | i^o |

...6.35

The voltage equations of the load along the phase axes are expressed as

$$e = Zi = (R + L_p)i$$

| | | | | | | |
|-----------------|--------|-----------|-----------|-----------|---------|------------|
| 3ϕ | | a_1 | b_1 | c_1 | 3ϕ | |
| $a_1' V_{a_1'}$ | a_1' | $R + L_p$ | | | a_1' | $i^{a_1'}$ |
| $b_1' V_{b_1'}$ | b_1' | | $R + L_p$ | | b_1' | $i^{b_1'}$ |
| $c_1' V_{c_1'}$ | c_1' | | | $R + L_p$ | c_1' | $i^{c_1'}$ |

...6.36

R and L refer to the load resistance and inductance respectively. Equations 6.36 can be transformed to d-q axes by the connection matrix 6.35.

$$\begin{aligned}
 e' &= Z'i' = C_t Z C i' \\
 &= C_t (R + L_p) C i' \\
 &= C_t (R + L_p) C i' + C_t L (p_c) i' \quad \dots \quad \dots 6.37
 \end{aligned}$$

So that the new impedance matrix is,

$$\begin{aligned}
 Z' &= C_t (R + L_p) C + C_t L p_c \\
 &= C_t (R + L_p) C + C_t L \cdot \frac{\partial C}{\partial \theta} p_\theta \quad \dots \quad \dots 6.38
 \end{aligned}$$

Thus

$$\begin{array}{c}
 d_q \begin{array}{|c|c|c|c|} \hline d_q & d_l & q_l & 0 \\ \hline d_l & R + Lp & & \\ \hline q_l & & R + Lp & \\ \hline 0 & & & R + Lp \\ \hline \end{array} + \\
 Z_l = q_l \begin{array}{|c|c|c|c|} \hline d_q & d_l & q_l & 0 \\ \hline d_l & & Lp & \\ \hline q_l & -Lp & & \\ \hline 0 & & & \\ \hline \end{array}
 \end{array}$$

Or

$$Z_l = \begin{array}{|c|c|c|c|} \hline d_q & d_l & & \\ \hline d_l & R + Lp & & Lp \\ \hline q_l & -Lp & & R + Lp \\ \hline & & & \\ \hline \end{array} \dots \dots \dots 6.39$$

Zero sequence quantities are dropped on the assumptions that there is no connection to the star point.

Now the load is to be connected to the alternator. Let the axes of the connected system, d and q, be the same as those of alternator, d₂, q₂. The old and new currents are given by

Contd...

$$1 = c i'$$

| | | | | | | | | | | | | | |
|---------|--|------------|--------|--------|-----|-----|--|----|--|----|--------|--|------------|
| or dq \ | | dq | ds_2 | d | q | d | | | | | | | |
| ds_2 | | 1^{ds_2} | | ds_2 | | 1 | | | | | ds_2 | | 1^{ds_2} |
| d_2 | | 1^{d_2} | | d_2 | | | | 1 | | | d | | 1^d |
| q_2 | | 1^{q_2} | | q_2 | | | | | | 1 | q | | 1^q |
| d_1 | | 1^{d_1} | | d_1 | | | | -1 | | | | | |
| q_1 | | 1^{q_1} | | q_1 | | | | | | -1 | | | |

..6.40

From equations (6.23) and (6.40), the impedance matrix of the unconnected system is

| | | | | | | | | | | | | | |
|-------|--------|--------------------|---------------------|----------|---------------------|-------|--------------------|--|------------------|--|--|--|--|
| $Z =$ | dq | ds_2 | d_2 | q_2 | d_1 | q_1 | | | | | | | |
| | | $r_{kd} + L_{kd}p$ | | M_{dp} | | | | | | | | | |
| | ds_2 | | M_{dp} | | $r + L_{dp}$ | | $L_{qp}e^{\theta}$ | | | | | | |
| | d_2 | | | | $r + L_{dp}$ | | $L_{qp}e^{\theta}$ | | | | | | |
| | q_2 | | $-M_{dp}e^{\theta}$ | | $-L_{dp}e^{\theta}$ | | $r + L_{qp}$ | | | | | | |
| | d_1 | | | | | | $r + L_p$ | | $L_p e^{\theta}$ | | | | |
| | q_1 | | | | | | $-L_p e^{\theta}$ | | $r + L_p$ | | | | |

..6.41

The voltage equation of the connected system is

$$e' = Z' i' \text{ or } e'_t e = C'_t Z C i'$$

| | | | | | | | | | | | | | |
|-----|--------|--------|--|--------|--------------------|----------------|--|--------|------------|--|--------------|------------------|--|
| d | ds_2 | $-V_f$ | | ds_2 | $r_{kd} + L_{kd}p$ | M_{dp} | | ds_2 | 1^{ds_2} | | | | |
| d | | 0 | | d | M_{dp} | $(r + R_+)$ | | d | 1^d | | $(L_q + L)p$ | $L_p e^{\theta}$ | |
| q | | 0 | | q | $-M_{dp}$ | $-(L_d + L)$ | | q | 1^q | | $r + R_+$ | $(L_q + L)p$ | |
| | | | | | | $p e^{\theta}$ | | | | | | | |

..6.42

In steady state, $p = 0$, $p\theta = w$, $i^{ds2} = -i^f$ and $M_{dp} i^{ds2} = -E$, so that 6.42 reduces to

$$\begin{array}{c} \begin{array}{|c|} \hline d \\ \hline \end{array} \begin{array}{|c|} \hline 0 \\ \hline \end{array} = \begin{array}{c} \begin{array}{|c|c|} \hline d & q \\ \hline \end{array} \begin{array}{|c|c|} \hline r+R & X_q+X \\ \hline \end{array} \begin{array}{|c|} \hline d \\ \hline \end{array} \begin{array}{|c|} \hline i^d \\ \hline \end{array} \\ \begin{array}{|c|} \hline q \\ \hline \end{array} \begin{array}{|c|} \hline -E \\ \hline \end{array} = \begin{array}{c} \begin{array}{|c|c|} \hline d & q \\ \hline \end{array} \begin{array}{|c|c|} \hline -(X_d+X) & r+R \\ \hline \end{array} \begin{array}{|c|} \hline q \\ \hline \end{array} \begin{array}{|c|} \hline i^q \\ \hline \end{array} \end{array} \dots 6.43$$

Solving for i^d and i^q ,

$$i^d = \frac{E(X_q + X)}{D} \text{ and } i^q = -\frac{E(r+R)}{D}$$

where $D = \begin{vmatrix} r+R & X_q + X \\ -(X_d+X) & r+R \end{vmatrix} = (r+R)^2 + (X_q + X)(X_d+X) \dots 6.44$

Alternator terminal voltage and load terminal voltage are equal.

$$\begin{array}{c} \begin{array}{|c|} \hline d_1 \\ \hline \end{array} \begin{array}{|c|} \hline V_{d1} \\ \hline \end{array} = \begin{array}{c} \begin{array}{|c|c|} \hline d_1 & q_1 \\ \hline \end{array} \begin{array}{|c|c|} \hline R & X \\ \hline \end{array} \begin{array}{|c|} \hline d_1 \\ \hline \end{array} \begin{array}{|c|} \hline -i^d \\ \hline \end{array} \\ \begin{array}{|c|} \hline q_1 \\ \hline \end{array} \begin{array}{|c|} \hline V_{q1} \\ \hline \end{array} = \begin{array}{c} \begin{array}{|c|c|} \hline d_1 & q_1 \\ \hline \end{array} \begin{array}{|c|c|} \hline -X & R \\ \hline \end{array} \begin{array}{|c|} \hline q_1 \\ \hline \end{array} \begin{array}{|c|} \hline -i^q \\ \hline \end{array} \end{array} \dots 6.45$$

From equation 6.45

$$\begin{aligned} V_{d1} &= E (Xr - X_q R) / D \\ \text{and } V_{q1} &= \frac{E \{X(X_q + X) + R(r + R)\}}{D} \end{aligned} \dots 6.46$$

For a given load impedance, the r.m.s. phase current and line voltage are

$$\begin{aligned} I &= \frac{1}{\sqrt{3}} \frac{E}{D} \sqrt{(X_q+X)^2 + (r+R)^2} \\ V &= \frac{E}{D} \sqrt{(Xr - X_q R)^2 + \{X(X_q+X) + R(r+R)\}^2} \end{aligned} \dots 6.47$$

...CHAPTER - 7...MECHANICAL CONSIDERATIONS^{4,16}

The rotor structure in a permanent magnet generator has to be such that it is sound mechanically, efficient magnetically, and is simple to manufacture. Maximum reliability under extreme storage and operating environmental conditions and minimum weight and space for a maximum output are the objectives for the design of a permanent magnet generator. From the magnetic point of view, the optimum design has been discussed earlier. Developments of the new permanent magnet materials involve some mechanical problems. In the early stages of the use of alnico for permanent magnets, the smaller pole structures were of a single shaped casting and the larger units were made with blocks of magnet materials bolted to the central hub or shaft. This simple construction is still used in most ^{of the} magnetos and some medium capacity generators.

There have been gradual improvements in mechanical designs to get the aforesaid objectives and the latest design is shown in figures 7.1, 7.2, & 7.3^{4,16}, which give the details of the magnet assembly for a 75 KVA, 28 pole 400 cycle p.m. generator. The pole shoe is laminated and the inner magnet ties locating the rectangular blocks of Alnico 5 are in exact alignment between annular discs of non-magnetic steel. This is all cast centrifugally with an aluminium alloy. Centrifugal casting, besides the usual advantages of giving a dense and true casting, "allows the parts to be made with adequate clearance for easy assembly yet have no clearance after casting". The inner magnet ties are loosely riveted so that both the

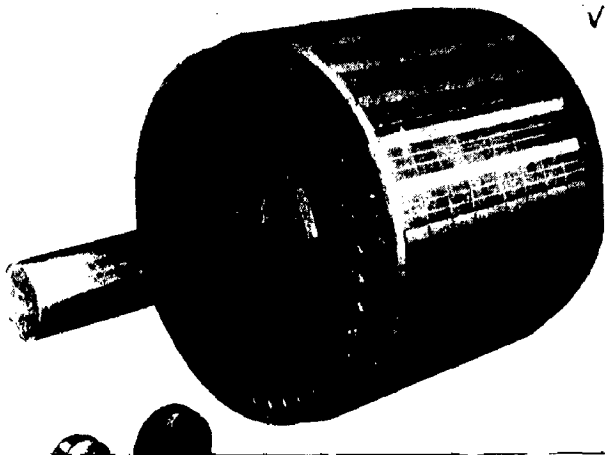


Fig.7.1 (top-left)

A 75 KVA, 28 pole, 1714 r.p.m., 400 cycle rotor with drive shaft for use as a 2-bearing generator. The small rotor is a 0.1 KW 8-pole, 12,000 r.p.m. 800 cycle generator and the uncast magnet assembly for a 0.1 KW, 8 pole, 6,000 r.p.m., 400 cycle unit.

Fig.7.2 (top-right)

75 KVA, 28-pole, 400 cycle rotor magnet assembly, partially stacked, showing main drive tube with casting openings, inner magnet ties with loose fit on rivets, magnets in place, and pole shoes tight on the rivets. The non-magnetic steel retaining discs hold all parts against centrifugal force.

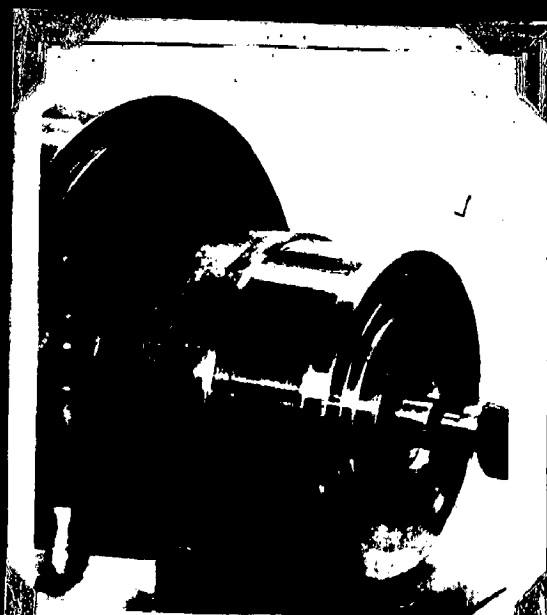


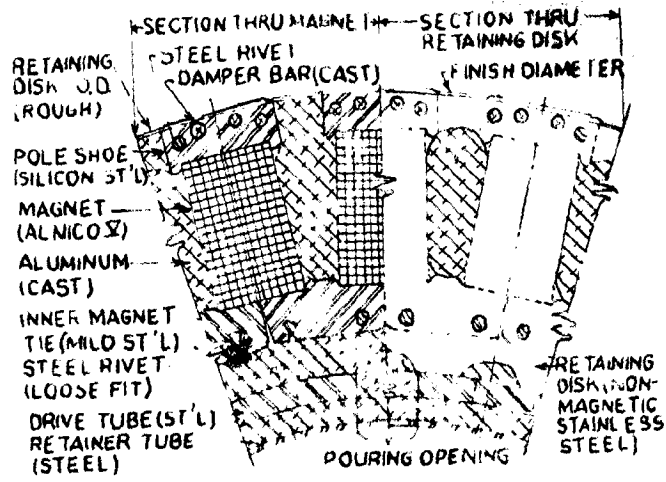
Fig.7.4

rotor of 6.3 KVA, 60 cycle, generator mounted on lathe to remove excess aluminium.

magnets and inner magnet ties are free to move radially outward under the centrifugal force of the casting machine, thereby maintaining a tight internal magnetic circuit during the casting. In centrifugal casting a special type of cast iron mould secures the magnet assembly, which is preheated to a specified temperature. The hot mould is mounted on a vertical axis and rotated at high speed while the molten aluminium is poured slowly into the central opening. The mould is filled from the outside toward the centre under pressure by centrifugal force. If the mould is correctly designed, there shall be no blow holes in the casting. The 0.1 KW rotor illustrated in figure 7.1 is too small to cast centrifugally and other means are used to obtain the desired tight assembly. The air gap in permanent magnet generators is usually small, compared with that of conventional alternators. Rotors of the p.m. generators should be turned on lathe after casting to remove the excess aluminium and finish to a definite diameter. See figure 7.4.

The nonmagnetic stainless steel retainer discs shown in figure 7.3 restrain all centrifugal forces so that there is no stress in brittle magnets due either to tension or shear.

Die casting can also be used¹⁶. Rotor assembly is preheated and die casting performed using a special casting die into which molten aluminium is forced from one end of the die to the other. High die casting pressure ensures the absence of all internal voids or blow holes. Fig. 7.5 shows a typical rotor construction, designed in a basic cage-type



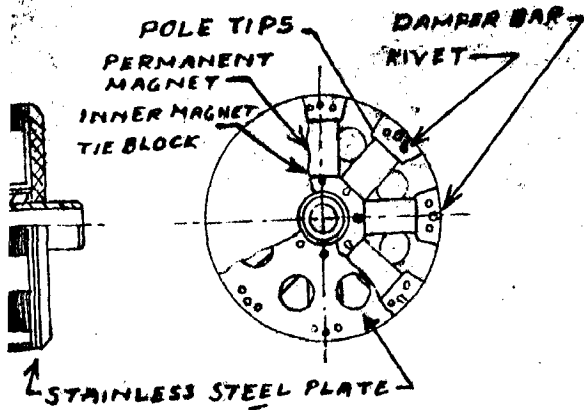


Fig. 7.5

pole rotor, sectioned to show of typical cage structure with shaft.

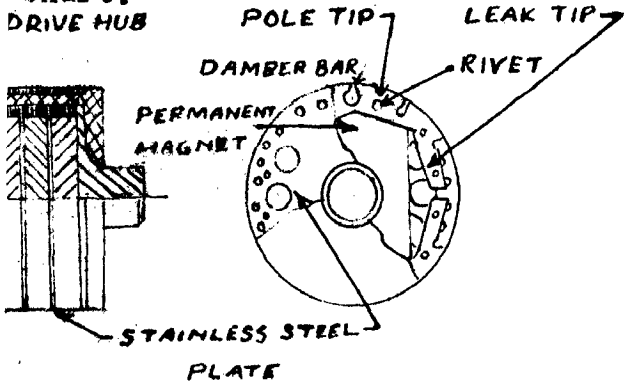


Fig. 7.6

pole rotor, sectioned to show drive hub and other parts of cage structure.

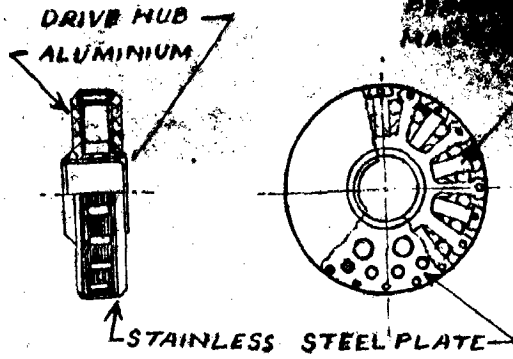


Fig. 7.7

Twenty-pole rotor construction with alternate permanent magnet and soft-steel poles.

structure, which is die cast with an aluminium alloy. In a 2-pole structure, flanged drive hubs are used instead of inner magnet tie block and through shaft, as shown in Fig.7.6.

Aluminium is used because of the following reasons:

1. It is readily cast within the required temperature range.
2. It has good mechanical strength properties.
3. It is a good electric conductor, and thus serves as a closed turn, surrounding each magnet so that permanent magnet is shielded against the transient demagnetizing forces.

The various critical parts used in the rotor structure are made from dies, in a punch press operation, as it results in economy in production quantities. To provide maximum magnetic properties, the alnico 5 magnets are cast in blocks and the desired dimensions obtained by gridding. Since all parts are identical for a given rotor diameter and number of poles a wide range of output ratings can be met with by adjusting stack height.

For P.m. generators operating at high speeds of the order of 24,000 r.p.m., the output frequency is limited in a small rotor by the impossibility of magnetizing the poles of opposite polarity, that are very closely spaced. This is overcome by the unique rotor construction¹⁶ shown in figure 7.57. The permanent magnet and soft steel poles are placed alternately around the circumference. Entire rotor is

magnetized by a unidirectional radial field and the permanent magnets are of the same polarity. During the magnetizing impulse, the soft steel poles are saturated but become poles of a normally fully magnetized rotor.

...CHAPTER 8...

GUIDE TO APPLICATIONS.

8.1. To make a choice between permanent-magnet or a conventional wound field generator, it is essential to consider the relative merits and demerits of each type for a particular application. The various aspects that should be considered are as under⁽⁴⁾

1. SIZE AND WEIGHT.

The permanent magnet generators are inherently smaller and lighter than the conventional wound field generators, due to the absence of the exciter and slip rings in the former. This fact is especially marked in very small high speed units and in high frequency multipole designs where the diameter is large compared to the axial length. In many engine-generator applications a 'no-bearing' design can be adopted since the rotor simply replaces the engine flywheel.

2. COST.

Relatively high cost of Alnico V, used for magnets, makes the permanent-magnet expensive. However, by laminating the structure and using punch press instead of machined parts, the overall cost is greatly reduced. In these designs Alnico is used only as magnet material and not as any connecting or structural part. Smaller permanent magnet generators are much cheaper than the conventional units complete with exciter.

3. LOSSES AND EFFICIENCY.

Many electromagnetic machines are limited in ratings largely by the ability of the field to dissipate the heat loss associated with the windings. Because of the absence of

the field winding, the limiting factor in permanent magnet generators will be the armature. Absence of a field winding reduces the losses associated with a given machine thus increasing the efficiency. A 15KVA 220Volts, 3-phase, 60 cycle, 1200 r.p.m. machine has an efficiency of 82.5% with the electro-magnet field while the efficiency is 90.9% in case of a corresponding permanent magnet generators under the same load conditions. Usually efficiencies range from 75% for 0.1 KW, 12,000 R.p.m. generator with high windage and friction losses upto approximately 93% for 1800 r.p.m. units rated at 10 KW or larger. Apart from the elimination of the actual field power loss, the entire exciter losses are also eliminated and, thus, a higher overall efficiency is obtained. This makes the operating cost of a permanent magnet machine less.

4. MAINTENANCE:

Maintenance cost of the permanent magnet generators is highly reduced because of the elimination of field windings and the associated slip-rings, commutator and brushes. The rotor itself is a solid mass with no insulation material and is, thus, practically indestructible. Alnico V is not demagnetized by time or by any normal vibration or heat. The only remaining wearing parts for which maintenance is necessary, are the bearings, and that, too, when practicable, can be heavy duty "sealed for life" bearings.

5. RATING - HEATING.

If the permanent-magnet generators are correctly the designed, almost no heat is generated in the rotor and usually stator losses are less. The very small high speed units

are operated completely sealed without exceeding class A temperatures but larger units require reasonable cooling and when operated with compensators, or on high power factor loads, heating may become the limiting factor. Generally the maximum capacity of a given unit usually ^{is} determined by inherent voltage regulation limitation rather than by heating.

APPLICATIONS^{4,16}

A permanent magnet generator is simple and rugged in construction and finds applications in rockets and guided missiles where the small size, light weight, high efficiency, positive excitation, and absence of external excitation with moving contacts and associated radio interference are all of vital importance and the cost of the generator and difficulty of voltage control can be sacrificed. Better voltage control will permit the use of the p.m. generators in large air craft applications. The p.m. generators are also used as ground-support power supplies, emergency power supplies, and electric conversion units.

Some of the interesting applications that are in actual operation are detailed as under:

A 15 KVA, 400 cycle, p.m. generator was being used on a military application and it was required to have an additional $2\frac{1}{2}$ KW, 28 Volt d.c. generator with no radio interference. The d.c. generator was eliminated by a low voltage 3-phase winding to the regulator stator winding and the d.c. was obtained through rectifier.

A permanent magnet generator coupled to a liquid -

monopropellant fuel-hot gas-turbine forms a unit that provides electric and mechanical power completely independent of the missile's main power plant and fuel system. Temperature compensation of the generator rotor, gives the generator output voltage relatively constant over the extreme temperature conditions imposed by high-speed and high-attitude flight.

Another hot-gas turbine-alternator power unit uses a solid propellant. It consists essentially of a solid rocket propellant, an impulse turbine, a p.m. alternator, and an electromagnetic control system able to withstand long term storage and insensitive to vibration, shock, and all air-borne environmental conditions. The unit is a light weight source of electric energy.

A 1 KW, 6-pole p.m. generator in a truck refrigeration unit is another interesting application, where the rotor becomes the engine flywheel and it in turn drives the refrigeration compressor by a semiflexible coupling. The generator supplies a 3-phase induction motor-driven evaporator blowers in large semitrailers and also supplies single-phase power for charging battery. Light weight, short axial length, no brushes, the ability to generate power at any speed are the critical requirements. Positive excitation is necessary since generator failure could result in loss of refrigerated cargo.

A dual motor-generator set consisting of a permanent magnet generator normally driven by an induction motor but with a d.c. motor on the same shaft for emergency service from battery power, is used in microwave relay stations, where a

maintenance free power unit that will transfer from normal to the standby power with perfect voltage continuity and negligible change in frequency is required. D.C. field is partially excited and motor brushes are continuously energized but they are held off the commutator by solenoids to prevent wear. When transferring to d.c. power, the brushes are dropped and the field increased to normal. The rotor inertia prevents an objectionable drop in speed that may be there during the transfer from one source to another. If necessary, flywheel also may be added to the rotor.

...CHAPTER - 9...EXPERIMENTAL DETAILS9.1. PRACTICAL DETAILS...

This chapter deals with the experimental study of the behaviour of a small salient pole single phase permanent magnet generator of the U.S. Army Signal Corps available in the Electrical Engineering Department, University of Roorkee, Roorkee. The generator was originally coupled to a gasoline engine designed to run at a speed of 3600 r.p.m. so as to generate alternating voltage at a frequency of 60 cycles per second. The gasoline engine was replaced by a D.C. motor and the coupling was provided through belt and pulley arrangement. The generator was run at a speed of 3000 r.p.m. so that it generated a.c. at 50 c.p.s. Specifications of the set are:

(i) A.C. GENERATOR

| | |
|-------------------|--------------------------------|
| Output | .. 300 watts |
| Voltage | .. 240 volts |
| Full load current | . 1.25 amps. |
| frequency | .. 60 c.p.s. |
| speed | .. 3600 r.p.m. |
| Rotor | .. Permanent Magnet |
| Stator | wound for single phase supply. |

(ii) D.C. MOTOR (SHUNT)

| | |
|---------|----------------|
| Output | .. 5 H.P. |
| Voltage | .. 220 Volts |
| Current | .. 20 amps. |
| Speed | .. 1450 r.p.m. |

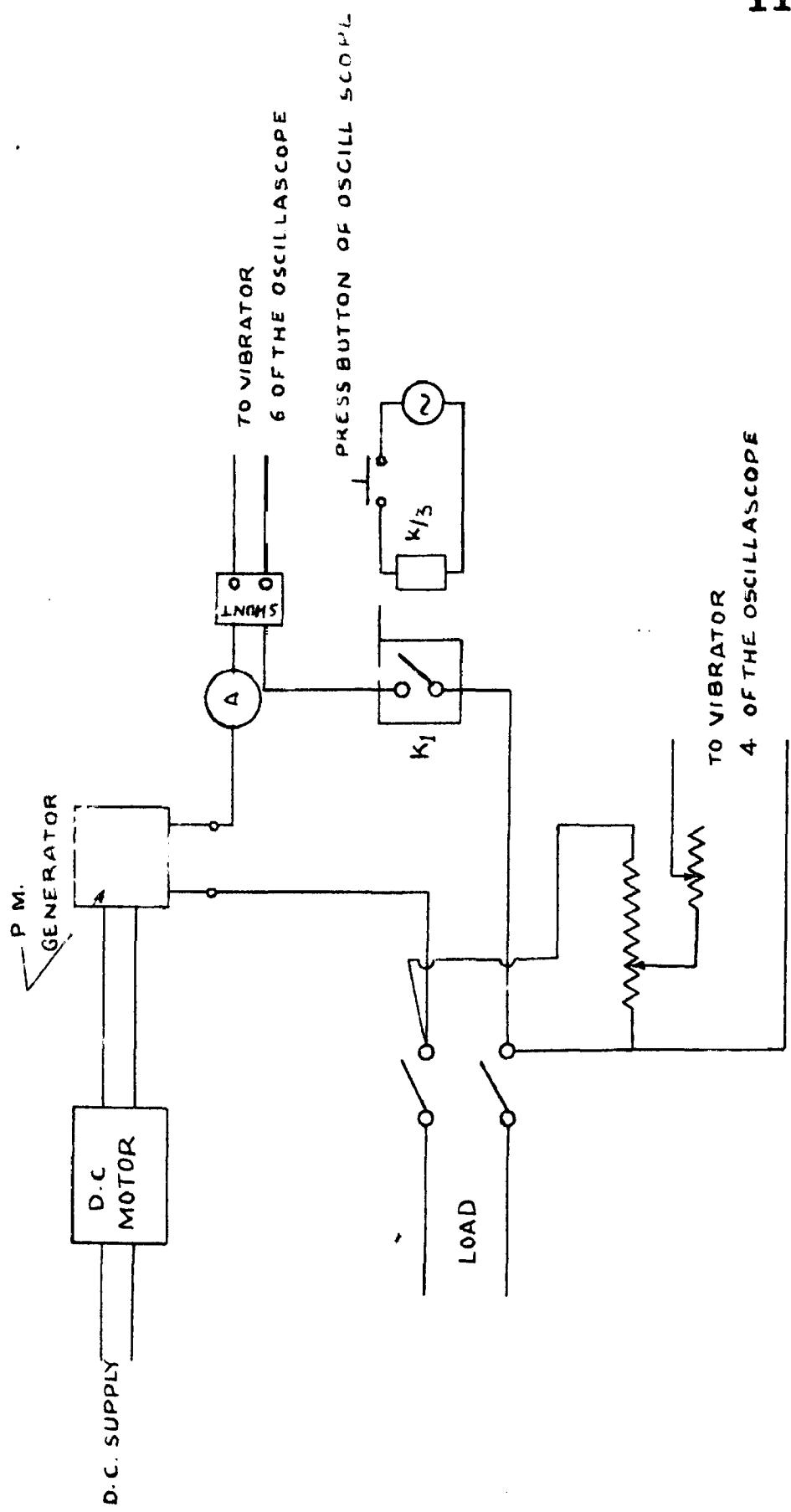
(111) COUPLING Belt and Pully

Fig. 9.11 shows the arrangement of the experimental set.

In addition to the other instruments the cambridge 6-element oscillograph was used for recording the transients. The essential parts of the oscillograph are:

1. Electromagnetic Vibrator
2. Optical system
3. Commutator
4. Drum Camera
5. Motor and Control rheostat

Center or opening section controls simultaneously the operation of the relay and the opening of the shutter. The position of the center segment in relation to the camera driving plate is determined by the setting of the speed scale which should be adjusted to the camera speed being used. This scale is ^{so} calibrated that at all speeds the Camera may be retarded in relation to the opening segment by an amount which ensures that leading edge of the film arrives at the shutter aperture just as the shutter opens. When the expose button is pressed, the commutator takes the control and energises the open magnet at the correct instant and the relay operates. The shutter moves up into its open or middle position where it stays during the recording period. The Commutator then energises the close magnet and shutter moves up in to its closed or upper position. The mechanism is adjusted to work from 40 r.p.m. to 1500 r.p.m.



Current and voltage signals were fed respectively to vibrator 6 and 4. For 'switching in' transient records and sudden short circuit on the generator, the circuit was closed through a contact relay 'K', and the commutator adjusted for 120° . 'Switching off' transient records were taken, by opening the circuit manually and commutator was adjusted for 360° . This had to be done because the opening time of the relay and that of the shutter were not in correspondence.

9.2. EXPERIMENTAL TEST RESULTS...

The following tests were performed to study the behaviour of the p.m. generator:

1. Regulation on different power factor loads,
2. Determination of the machine constants X_d and X_q .
3. Behaviour of the generator when full load is suddenly 'switched in' or 'switched off'.
4. Sudden short circuit on the generator.

Circuit diagram for the test is shown in figure 9.1.

9.2.1. REGULATION ON DIFFERENT POWER FACTOR LOADS...

| <u>AT ZERO P.F. (LAGGING) LOAD</u> | |
|------------------------------------|------------------------|
| <u>Current (Amps)</u> | <u>Voltage (Volts)</u> |
| 0 | 212 |
| 0.4 | 195 |
| 0.88 | 177 |
| 1.00 | 168 |
| 1.10 | 161 |
| 1.20 | 158 |
| 1.25 | 155 |

Contd...

ZERO P.F. (LAGGING)LOAD ..Contd..

| Current (Amps.) | Voltage (Volts) |
|--------------------|--------------------|
| 1.36 | 150 |
| 1.40 | 148 |
| 1.50 | 140 |

UNITY POWER FACTOR LOAD

| Current (Amps) | Voltage (Volts) |
|-------------------|--------------------|
| 0 | 212 |
| 0.6 | 201 |
| 1.08 | 189 |
| 1.25 | 184 |
| 1.36 | 182 |
| 1.48 | 179 |
| 1.66 | 175 |
| 1.85 | 170 |

ZERO POWER FACTOR (LEADING) LOAD

| Current (Amps) | Voltage (Volts) |
|-------------------|--------------------|
| 0 | 212 |
| 0.24 | 224 |
| 0.51 | 239 |
| 1.05 | 265 |
| 1.13 | 267 |
| 1.33 | 277 |

The regulation curves are shown in figure 9.2. Regulation of the generator is not good.

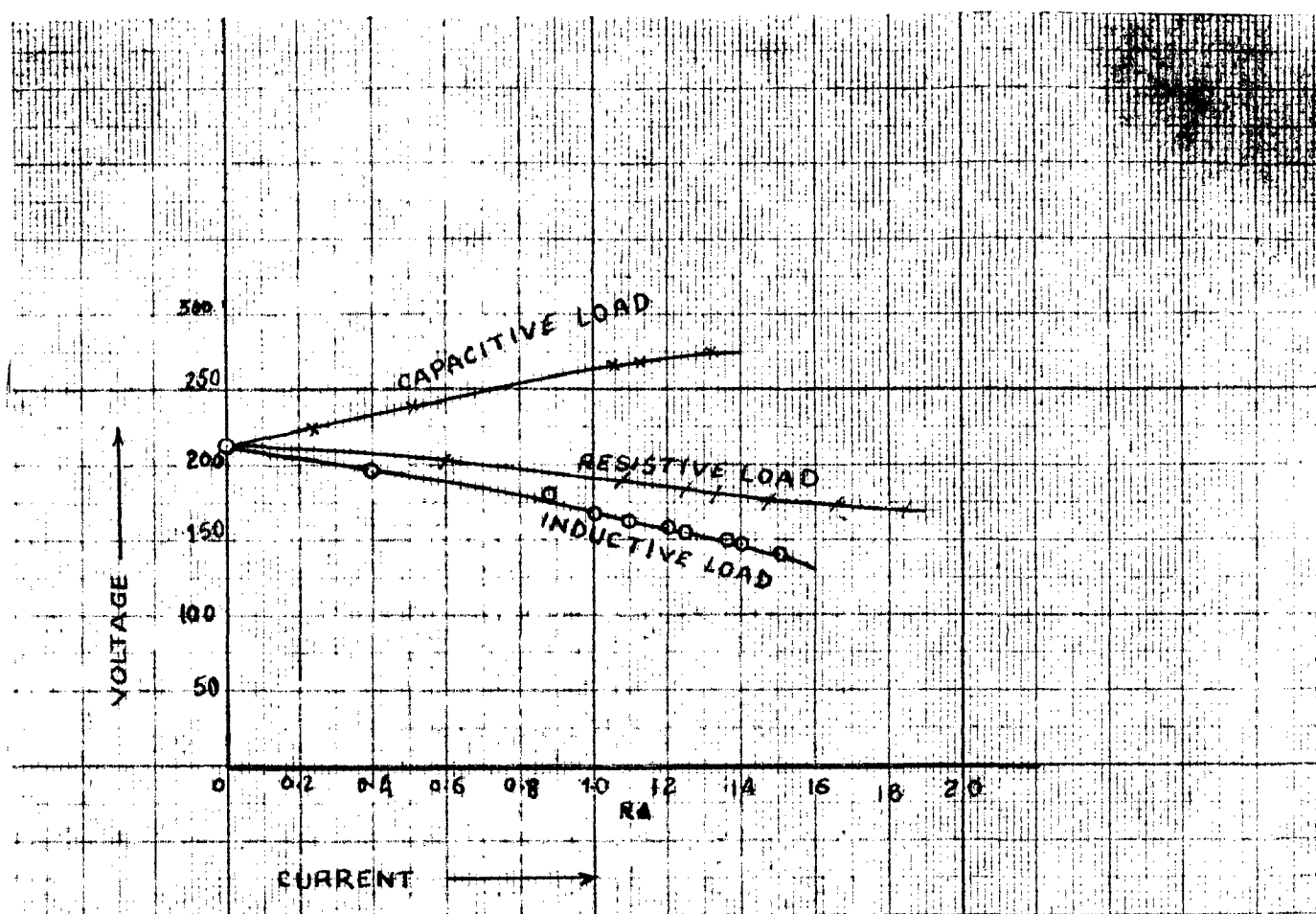


FIG. 9.2. REGULATION CURVES FOR DIFFERENT P.F. LOAD.

It was observed that when the zero p.f. lagging load was removed, the open circuit voltage was 209 instead of 212, and when the capacitive load was removed, the open circuit voltage was found to be 214, instead of 212. This is due to the fact, that armature reaction due to highly lagging load has a strong demagnetizing effect and the permanent magnet is demagnetized to some extent. The armature reaction due to highly leading load has the magnetizing effect and the generator is thus magnetized. Further, it seems that the type of material used as permanent magnet in this generator is not of high quality because a good material would not change its magnetic strength in such a short time. This point is further supported by the fact that when the generator was tested by the author, it generated 220 volts on open circuit at 50 c.p.s. in the beginning and later on the open circuit voltage dropped down to 212 volts.

9.2.2. DETERMINATION OF X_d and X_q ...

It was shown in Chapter 4 equation 4.5, that the p.m., generator excitation increases with the armature reaction thus changing the induced voltage E_0 . This peculiarity of the p.m. generator may be taken into account by either of the following method^{10,15}.

1. The reactance of armature reaction (X_{ad}) is defined as that for an electromagnetic machine and E_0 is the true excitation voltage, the no load voltage corresponding to the main field m.m.f. and is as given by equation 4.5.
2. The excitation voltage E_0 is taken to be the no load

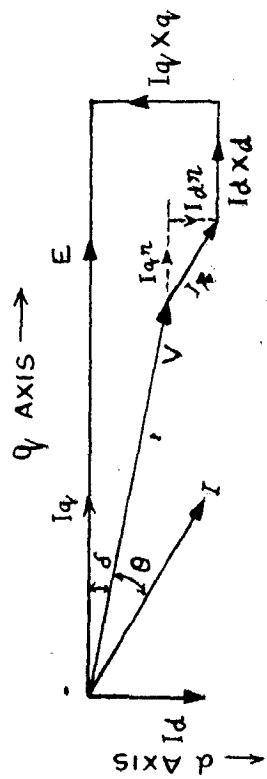


FIG. 9.3

Phasor diagram for synchronous generator.

voltage E_{NL} , and the reactance of the armature reaction is reduced below that value, calculated as if the machine were electromagnetically excited by a factor involving the magnetic circuit constants.

The former concept was used while deriving expressions for various reactances, from equivalent magnetic circuit of the p.m. generator discussed in Chapter 4. The latter method has the advantage that for a particular stabilisation, E_0 is independent of load¹⁰, and had, therefore, been used in the experimental determination of the constants X_d and X_q .

Most of the tests that are normally applied to conventional wound field generators were not applicable to p.m. generator because its field could not be switched off or varied. Steady state short circuit test was the only conventional test that could be applied at full excitation. X_d and X_q were determined by steady state load test. X_d was also determined by steady state short circuit test.

Figure 9.3 shows the Blondel - two reaction diagram for a synchronous generator. It can be seen from the diagram,

$$\begin{aligned} X_d &= \frac{E - V_q - I_q r}{I_q} \\ X_q &= \frac{V_d + r I_d}{I_q} \end{aligned} \quad \begin{array}{c} | \\ 0 \\ | \end{array} \quad \dots 9.1.$$

where suffixes d and q stand for direct and quadrature axis and r is the resistance of the armature.

In order to reduce the cross-saturation effects, the load phase angle was adjusted so that part of the current was in the required axis. Thus for measuring X_d , zero p.f.

(lagging) load was used and for measuring X_q , u.p.f. load was used. The shift between the no load voltage and terminal voltage of the generator when delivering full load current at required power factors was seen on a C.R.O. This shift is a measure of the load angle . From figure 9.3,

$$\begin{aligned} V_q &= V \cos \delta \\ V_d &= V \sin \delta \\ I_q &= I \cos (\delta + \theta) \\ I_d &= I \sin (\delta + \theta) \end{aligned} \quad \begin{array}{c} \text{I} \\ \text{I} \\ \text{I} \\ \text{I} \end{array} \quad \dots 9.2$$

where θ = load p.f. angle

Using equations 9.1 and 9.2, X_d and X_q can be determined.

STEADY STATE LOAD TEST

Resistance of the generator was found to be 9 ohms.

U.P.F. LOAD

$$E = 212 \text{ Volts}$$

$$V = 184 \text{ Volts}$$

$$I = 1.25 \text{ Amps}$$

$$= 32.4^\circ$$

$$\theta = 0$$

$$V_d = 184 \sin 32.4^\circ = 98.4 \text{ volts}$$

$$I_d = 1.25 \sin 32.4^\circ = 0.674 \text{ Amps.}$$

$$I_q = 1.25 \cos 32.4^\circ = 1.05 \text{ Amps.}$$

$$\therefore X_q = \frac{9.84 + 6.04}{1.05} = \underline{\underline{99 \text{ ohms}}}$$

ZERO P.F. (LAGGING) LOAD

The angle in this case was so small that it could not be measured. In this case, however, the numerical difference $E - V$ could be taken as the IZ drop, so that X_d

could be calculated from Z.

$$E = 212 \text{ volts}$$

$$V = 155 \text{ volts}$$

$$I = 1.25 \text{ Amps.}$$

$$IZ = 57 \text{ Volts}$$

$$Z = \frac{57}{1.25} = 45.5 \text{ ohms.}$$

$$X_d = \sqrt{45.5^2 - 9^2} = \underline{\underline{44.4 \text{ ohms}}}$$

STEADY STATE SHORT CIRCUIT TEST

$$E = 212 \text{ Volts}$$

$$I_{sc} = 4.9 \text{ amps.}$$

$$Z = \frac{212}{4.9} = 43.4 \text{ ohms.}$$

$$X_d = \sqrt{Z^2 - r^2} = \underline{\underline{42.6 \text{ ohms}}}$$

The results are tabulated in table 9.1.

TABLE 9.1

MACHINE PARAMETERS

| Machine constant | Method | Numerical value (ohms) | p.u. values on the basis of O.C. Volts (212) |
|---------------------|---------------------------------------|---------------------------|--|
| Armature resistance | Ohm's law | 9 | 0.0538 |
| X_d | Steady state load test | 44.4 | 0.264 |
| | Steady state short circuit test | 42.6 | 0.252 |
| X_q | Steady state load test | 99 ohms | 0.583 |

9.2.3. SWITCHING TRANSIENTS...

Cambridge electromagnetic oscilloscope was used for recording the switching transients.

Figure 9.4 shows the voltage (I) and Current (II) wave forms when full load at unity power factor was suddenly switched on. The voltage signal applied to the vibrator of the oscilloscope was taken from the load terminals. The voltage across the load becomes steady almost instantly. Current becomes steady in 0.029 seconds. The maximum value of the current reached during the transient period is 2.26 times the r.m.s. value of the steady state current (1.25 Amps.)

Figure 9.5 shows the voltage (I) and Current (II) wave forms when full load at zero p.f. (lagging) was suddenly applied and the vibrator was given voltage signal from generator terminals. Voltage becomes steady in 0.01 seconds and the maximum value during the transient period is only 1.70 times the r.m.s. value of the steady state voltage. The current becomes steady in 0.052 seconds and maximum value of the current during the transient period is 2.69 times the r.m.s. value of the steady state current (1.25 Amps.).

Figures 9.6 and 9.7 are the voltage and current wave forms for suddenly applied load respectively at u.p.f. and zero p.f. (lagging), but the vibrator was now excited from the generator terminals. The records reveal the following information:

Figure 9.6 (u.p.f.): voltage becomes steady gradually to the new value in 0.01 seconds and current attains its

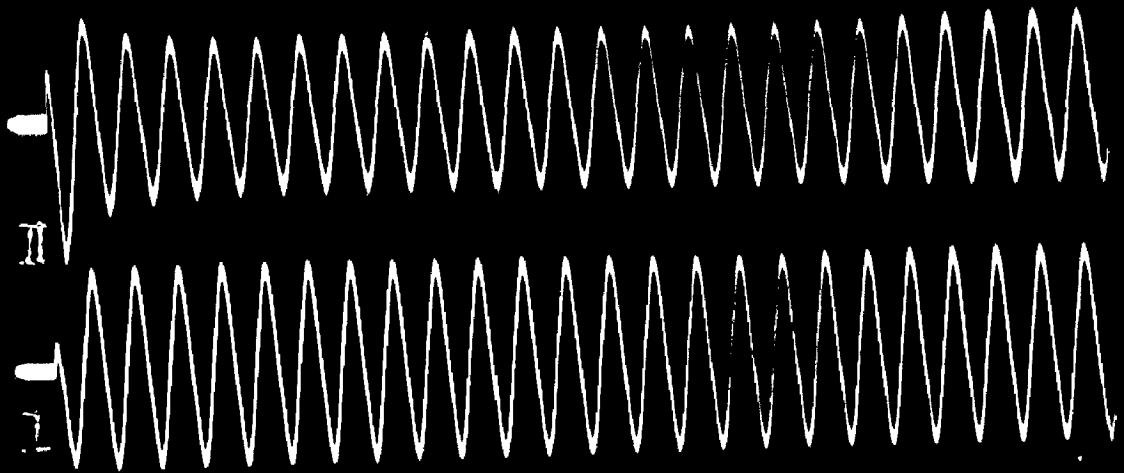


Fig. 9.4(top)

Voltage (I) and current (II) wave forms when full load at u.p.f. is suddenly switched on. (Voltage signal from load terminals).

Fig. 9.5(bottom)

Voltage (I) and current (II) wave forms when full load at zero p.f. (lag) is suddenly switched on. (Voltage signal from load terminals)

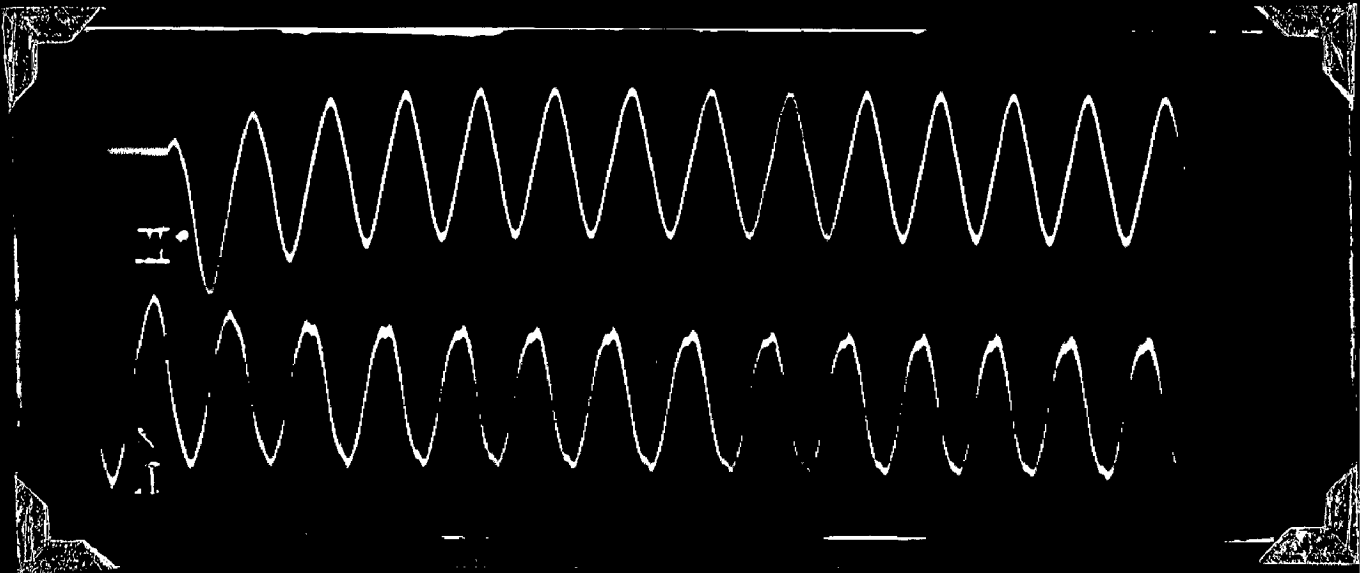
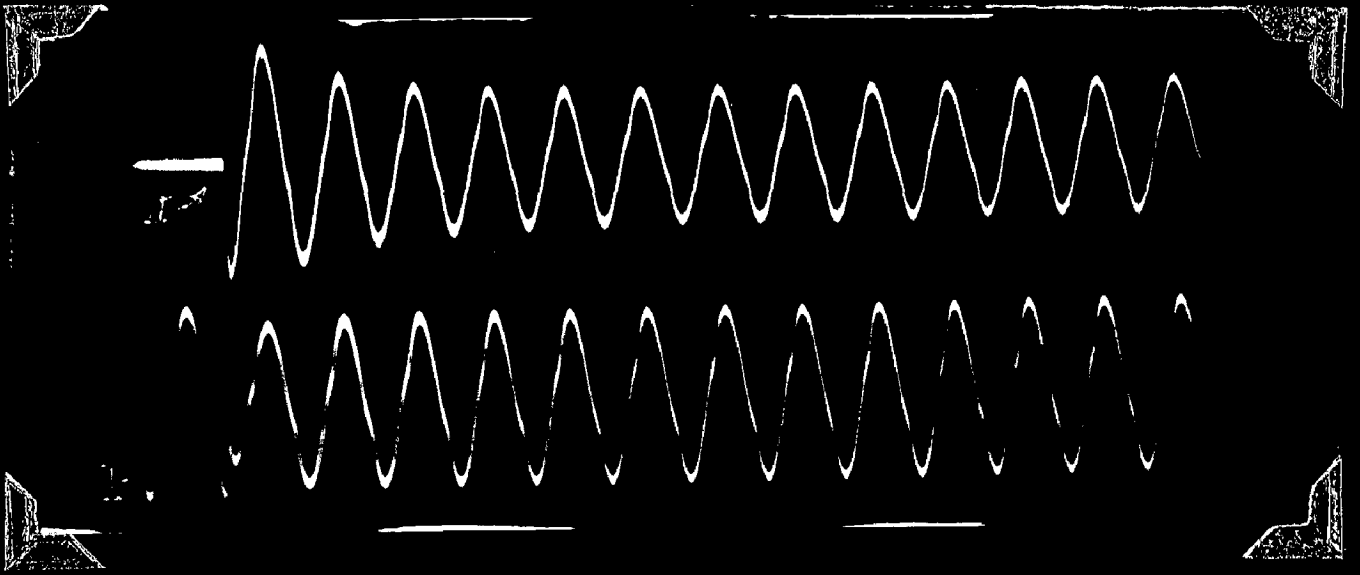


Fig.9.6(top)

Voltage (I) and current (II) wave forms when full load at u.p.f. is suddenly switched on. (Voltage signal from generator terminals).

Fig.9.7(bottom)

Voltage (I) and current (II) wave forms when full load at zero p.f. (lag) is suddenly switched on. (Voltage signal from generator terminals).

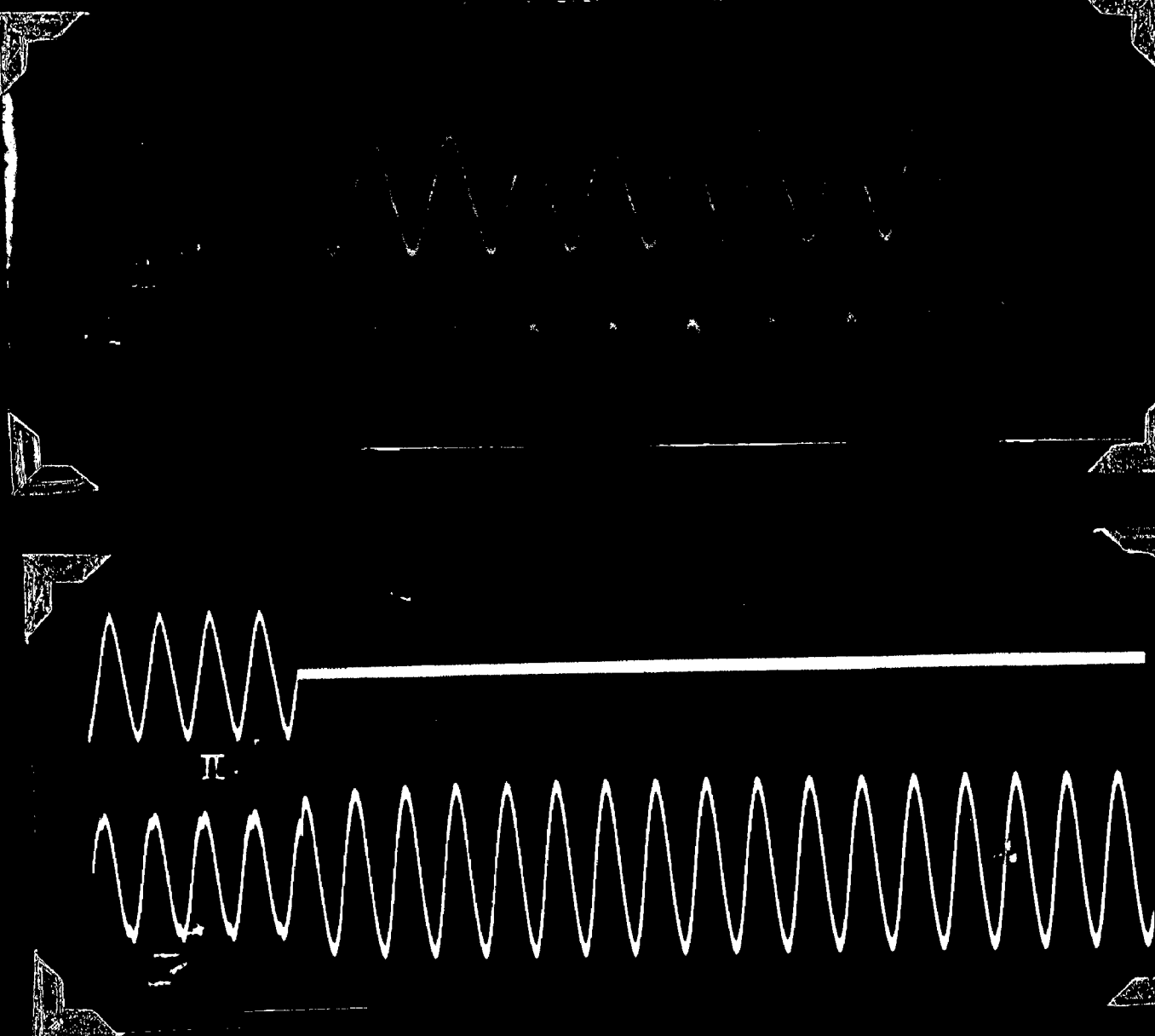


Fig. 9.8(top)

Voltage (I) and current (II) wave forms when full load at u.p.f. is suddenly thrown off. (Voltage signal from generator terminals).

Fig. 9.9(bottom)

Voltage (I) and current (II) wave forms when full load at zero p.f. (lag) is suddenly thrown off. (Voltage signal from generator terminals).

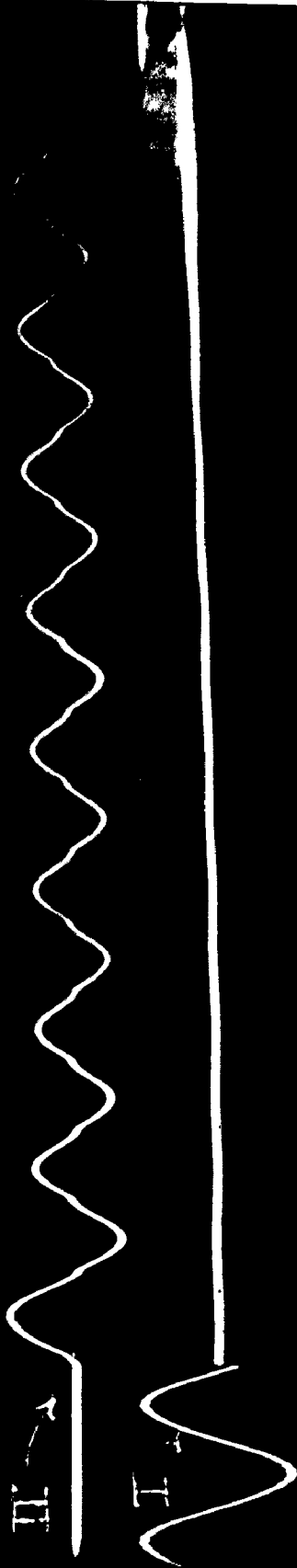


Fig. 9.10

Voltage (I) and current (II) wave forms when the generator is suddenly short circuited.

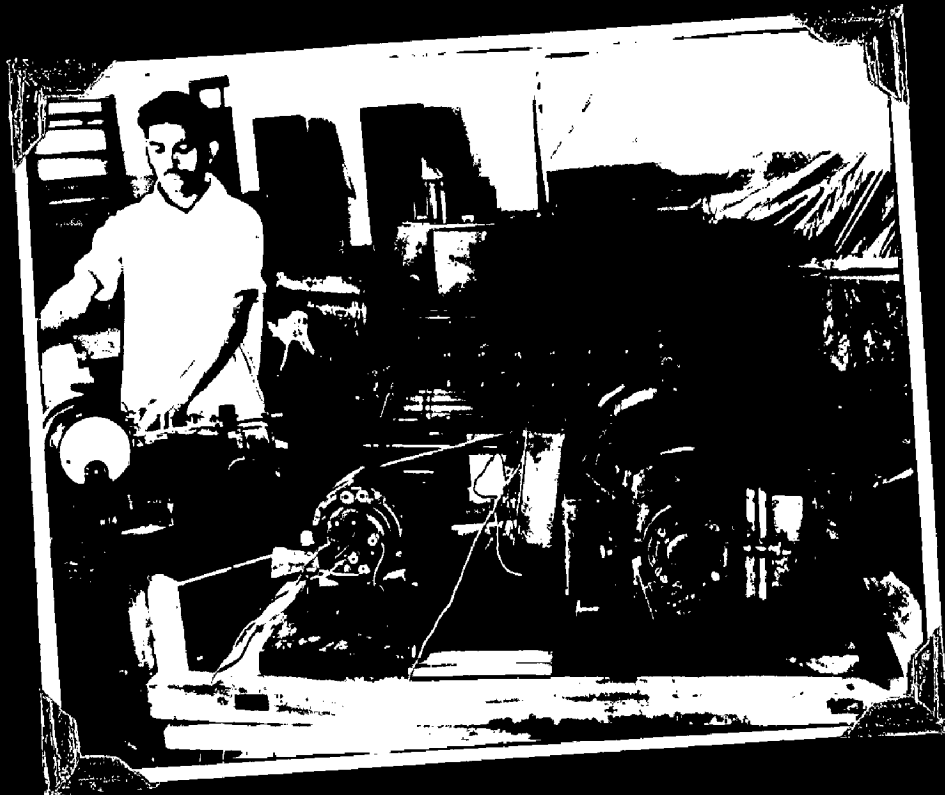


Fig.9.11

Arrangement of the experimental set.

steady state value (r.m.s.) in 0.0423 seconds with maximum value equal to 2.47 times the steady state r.m.s. value.

Figure 2.7 (zero p.f. lagging): Voltage becomes steady gradually to the new value in 0.02 seconds and current attains its steady state r.m.s. value in 0.021 seconds with max. value during transient equal to 2.67 times the steady state r.m.s. value. It can be seen from the aforesaid results that time taken by the current to reach steady state value for either u.p.f. load or zero p.f. load for the two cases (Voltage signal obtained from load terminals and generator terminals) is different. This is due to the fact that load was probably not switched on the same instant.

Figures 9.8 and 9.9 are the oscillograms for the loads having been suddenly thrown off at u.p.f. and zero p.f.(lagging) respectively. In both the cases the current dies instantly. The voltage is steady to the open circuit value in 0.01 seconds.

9.2.4. SUDDEN SHORT CIRCUIT...

Application of sudden short circuit to the machine makes the current short initially to 2.4 times the r.m.s. steady state short circuit current (4.9 Amps.). The short circuit current becomes steady in 0.03 seconds (Fig.9.10).

...CHAPTER - 10...

..CONCLUSIONS..

Permanent magnet generators are assuming an important role for the portable and air craft applications, as they offer a substantial reduction in weight and space and are more efficient and reliable than conventional synchronous generators. Originally the use of p.m. generators was limited only to small sized units but with the development of dispersion-hardening alloys typified by the Alnico group, higher KVA units of the order of 75-100 KVA have been made.

Permanent magnet generators operate on minor hysteresis loop that can approximately be replaced by a straight line, called the recoil line, so that the generator characteristics remains fixed, the permanent magnet must operate on a particular line of return. To obtain this objective, the magnet should be stabilized for certain demagnetizing m.m.f. Application of a demagnetizing m.m.f. smaller than the stabilizing m.m.f., will not demagnetize the magnet further.

The permanent magnets can be stabilized either by taking the rotor 'out of assembly' (air stabilization) or by keeping the rotor 'in assembly' and subjecting it to the expected maximum demagnetizing force. Air stabilization is used in applications where rotor may have to be taken out of assembly very frequently. Modern machines are short circuit stabilized because air stabilization offers a weight penalty, as explained in Chapter 2.

The rotor can be magnetized by coils around the poles,

direct current in the armature, leading power factor loads or magnetizing jig. To assure complete saturation, the magnetizing m.m.f. should be approximately five times the product of H_c and magnet length.

Design of the field system of the generator depends upon the type of stabilization to be used. The general output equation of a conventional synchronous generator is applicable also to the p.m. generator. The air gap in the machine is kept as small as possible. Short circuit ratio of the p.m. generator is high and ranges between 1.5 to 2.5.

To shield the permanent magnet against transient demagnetizing forces, the poles should either be cast in aluminium or copper plated. This reduces also the negative sequence reactance.

Perfect voltage control of p.m. generators can not be obtained as the excitation of the system can not be varied. The generators can be designed to have good inherent voltage regulation but improvements can be made by the use of a toroidal back winding in the stator.

An analysis of a p.m. generator can be made in the same way as that in a conventional wound field generator, the permanent magnet field being replaced by an equivalent electromagnetic field with a constant fictitious field current. The operation of the p.m. generator can also be represented by equivalent magnetic circuit having either a constant m.m.f. source F_0 or constant flux source ϕ_0 . The equivalent magnetic circuit is helpful in deriving the expressions for machine

reactances X_d , X_d' and X_d'' . Appendix II gives values of machine parameters for p.m. generator for different capacities and that for synchronous generators.

Methods for determining X_q , normally applicable to conventional wound field generators are not applicable to p.m. generators. Both X_d and X_q can be determined from the direct load test in which the load angle δ is measured. The calculations are done with the help of Blondel's diagram. X_d can also be determined from steady state short circuit test. The test results on the experimental p.m. generator show that the values of X_d obtained from both the methods agree with each other. The discrepancy in the two results is due to the fact that the angle δ , in the former method, could not be measured accurately when the generator was loaded for zero p.f. loads. X_d is found to be lower than X_q . This is due to the fact that the recoil permeability of the permanent magnet materials is quite low.

Transient records on the experimental p.m. generator show that the steady state conditions are obtained quickly and this in fact is a desirable feature for machines like p.m. generators that are used in control systems, where deviation of signals even for fraction of a second is undesirable. When full load at unity power factor was switched on the experimental generator, the current became steady in 0.029 seconds with the peak value during the transient equal to 2.26 times the r.m.s. value of the steady state current. Similarly for the zero p.f. loads, the time taken was 0.052 seconds and the max. value of current reached was 2.69 times the r.m.s. value of the steady state current. Voltage across the load became steady almost instantly. Switching in

transients were recorded again with the voltage signal taken from generator terminals. Voltage became steady to the new value in 0.01 seconds in case of p.f. load and in 0.02 seconds in case of zero p.f. load. A discrepancy in time taken by the current to become steady and the max. value of the current in the two cases (signal voltage taken from load and generator terminals) was observed. This may be due to the fact that the switching was, probably, not done at the same instant. When the load is thrown off, the current dies almost instantly and the voltage gradually rises to the new value in 0.01 seconds. When the machine was suddenly short circuited, the steady state short circuit current was attained in 0.03 seconds and the maximum value of the current during the transient period was 2.4 times the r.m.s. value of the steady state short circuit current.

A thorough analysis of the p.m. generator in transient state has yet to be done. It is felt that investigation of better permanent magnet materials and better voltage control methods can make the machine comparable with large power units of the wound field type.

Equation for λ (defined by equation 3.23), case A...

Using figure 3.5 the abscissa values F_2 and F_3 of the inter-section points 2, between the straight lines R_0 and m_2 , and 3. between the straight line R_0 and the main demagnetization curve M_{30} , can be calculated as functions of the shape factor S and parameter K . After simplifications and introduction of the terms

$$Z = (S/S_0)/K$$

$$b = \mu_a H_c/B_r \quad \dots \quad \dots \text{I.1}$$

μ_a is always a negative value, therefore b is always negative. The final relation for F_2/F_3 reads

$$= \frac{Z - b/k}{2Z(Z-b)} \left(1 + Z + \sqrt{(1+Z)^2 - 4aZ} \right)$$

Equation for λ , Case B...

Using figure 3.6, the abscissa values F_2 and F_3 of the intersection points 2, between the straight lines R_{t_a} and m_3 , and 3, between the shifting auxiliary line R_a , connecting points 2 and 0, and the main demagnetization curve M_{30} , can be calculated as functions of the shape factor S and C . After simplifications and introduction of the term b , according to equation I-1 the final relation for $\lambda = \frac{F_2}{F_3}$ reads

$$= \frac{1}{2\left(\frac{S}{S_0} - b\right)} \left[\frac{C(1+b) + (1-b)\frac{S_2}{S_0}\left(1 + \frac{S}{S_0}\right) + \sqrt{C(1+b) + (1-b)\frac{S_2}{S_0}\left(1 + \frac{S}{S_0}\right)^2}}{4ab \left[C + (a-b)\frac{S_2}{S} \right] \left[C - \left(1 - \frac{S}{bS_0}\right) \right]} \right] \dots \text{I.2}$$

...APPENDIX - II...

24

...DATA FOR P.M. GENERATORS FOR DIFFERENT CAPACITIES...

| Kw'phases' | p.f. | F | r.p.m. | Weight (lbs.) | Single bearing | Two bearings | d | g | perma- | ISC | 'E.N.L. | 'X _d | 'X _d ' |
|------------|------|--------|--------|---------------|----------------|--------------|----------|----------|----------|--------|---------|-----------------|-------------------|
| | | 'c/s' | | | 'inches' | 'inches' | 'inches' | 'inches' | 'nent | 'Amps' | 'Volts | p.u. | p.u. |
| | | | | | | | | | 'magnet' | | | | |
| 30 | 3 | 0.81ag | 400 | 1714 | 302 | 389 | 15.281 | 0.040 | Alnico V | 350 | 246 | 0.353 | 0.237 |
| 60 | 3 | 0.81ag | 400 | 1714 | 582 | 669 | 15.281 | 0.040 | -Do- | 663 | 230 | 0.348 | 0.237 |
| 2 1/2 | 3 | 0.81ag | 400 | 3428 | 47.71 | - | 8.50 | 0.025 | -Do- | 82 | 133 | 0.204 | 0.24 |
| 1 | 1 | 1.0 | 400 | 1714 | - | 37 | 8.0 | 0.020 | -Do- | 46 | 132 | 0.198 | 0.177 |

Typical per-unit values of reactances for 25 synchronous machines with wound field system. (Machine KVA rating as base). ²⁵

| | Water-wheel generators | Turbo-generators |
|----------------|------------------------|------------------|
| X _d | 0.60 (min.) | 1.15 |
| | 1.00 (average) | |
| | 1.25 (max.) | |
| X _q | 0.40 (min.) | 1.00 |
| | 0.65 (average) | |
| | 0.80 (max.) | |

...R E F E R E N C E S...

- | <u>Sl. No.</u> | <u>Author</u> | <u>Title etc.</u> |
|----------------|-------------------------------------|--|
| 1. | Spreadbury, F.G. | Permanent Magnets (Pitman, 1949) Chapter 1 and 6. |
| 2. | Desmund, D.J. | The economic utilization of modern permanent magnets JIEE Vol.90, 1945 pp.229-52. |
| 3. | Evershed, S. | Permanent magnets in theory and practice JIEE Vol.58, 1920, pp.780-837. |
| 4. | Saunders, F. | Synchronous machines with rotating permanent magnet fields Pt.(I) Trans. AIEE 1952 pp.670-6 |
| 5. | Strauss, F. | Synchronous machines with rotating permanent magnet fields Pt.(II). Trans. AIEE 1952 pp.887-93. |
| 6. | Bozorth, R.M. | Ferromagnetism, (D.Van. Nostrand, 1956) Chapter 9 Co.,Inc. |
| 7. | Brailsford, F. | Magnetic materials (Wiley, 1951) Chapter 7 |
| 8. | Dawes, C. | A course in Electrical engineering Vol.I (Mc Graw-Hill, 1952) Chapter 6. |
| 9. | Hornfeck A.J., and Edgar, R.F. | The output and optimum design of permanent magnets subjected to demagnetizing forces. Trans. AIEE 1940 Vol.59, pp.1017-24. |
| 10. | Hanrahan, D.J. and Toffolo, D.S. | Permanent magnet generator Pt.I(Theory) Trans.AIEE 1957 Pt.(III) pp.1098-1103. |
| 11. | Hanrahan, D.J. and Toffolo, D.S. | Permanent magnet generator (II) optimum design Trans. I.E.E.E. Power App.& System, April 1963 No.65 pp.68-74. |
| 12. | Roters, H.C. | Electromagnetic devices. (Wiley, 1941) pp.116-50. |
| 13. | Say, M.G. | Performance & design of A.C. machines (Pitman, 1958) pp.551. |
| 14. | Ginsberg, D. | Design calculations for A.C. generators Trans.AIEE Vol.50 1951 pp.201-14. |
| 15. | Walshaw, M.H. and Lynn, J.W. | An analytical study of a permanent magnet alternator including its intersection with another synchronous machine. Royal aircraft establishment(Farnborough) Report No.EL.1491, Sept.1960 |

- | <u>No.</u> | <u>Author</u> | <u>Title etc.</u> |
|------------|------------------------------------|--|
| 16. | Pudor, A.T. and Strauss, Fritz. | Salient pole p.m. alternators for high speed drive. <i>Trans. AIEE, 1957, Pt. II, pp. 333-38.</i> |
| 17. | Saunders, R.M. and Weakly, R.H. | Design of P.M. Alternators Trans. A.I.E.E. Vol.70 Pt.II 1961 pp.1678-81. |
| 18. | Kulhman, J.H. | Design of Electrical Apparatus. (Wiley, 3rd en.) pp.226. |
| 19. | Adkins, B. | The general theory of electrical machines. (Chapman & Hall, 1959), Chapter II. |
| 20. | Concordia, C. | Synchronous machines. |
| 21. | Gibbs, W.J. | Tensors in electrical machines. |
| 22. | Ziegler, H.K. | New method for the optimum design of permanent Magnets subjected to demagnetizing effects. <i>Trans. AIEE, 1953(I), pp.253-62</i> |
| 23. | Underhill, E.M.U. | Designing stabilized permanent magnets Electronics, New York, N.Y. Vol.17, Jan.1944, pp.1540-42. |
| 24. | Ginsberg and Misenheimer | Design calculations for P.M.generators Trans. AIES(III) 1953 pp 96-102 |
| 25. | Fitcherald, J.and Kingaloy | Electric machinery |
| 26. | Liwshitz-Garik- Whipple. | Electric Machinery Vol.II A.C.machines 8th edition, pp.336-38. |
| 27. | Goss | Evolution of P.M. fractional h.p.size generators and motors. |
| 28. | Cioffi, P.P. | Stabilized Permanent magnets, A.I.E.E. 1948, Vol.67, pp.1540-43. |
| 29. | - | Test code of synchronous machines (AIES). |